UNIVERSITÀ DEGLI STUDI DI MESSINA

Dottorato di Ricerca in Biologia Applicata e Medicina Sperimentale

CURRICULUM IN SCIENZE BIOLOGICHE ED AMBIENTALI

XXXI CICLO

Study of intracellular signaling network triggered by HSV- 1 and graphene based nanomaterials: their use as potential tools in gene therapy.

Candidata:

DOTT.SSA ROSAMARIA PENNISI

Tutor: **Ch.ma Prof.ssa Maria Teresa Sciortino**

Coordinatore:

Ch.ma Prof.ssa Maria Assunta Lo Gullo

ANNO ACCADEMICO 2016-2018

A mio nonno:
esempio di tenacia e di passione
Grazie

Publications

Mandalari G., Bisignano C., Smeriglio A., Denaro M., Pizzo M.M., **Pennisi R**., Ferro S., Trombetta D., Monforte A., Sciortino M.T., De Luca L. (2018) Simulated human digestion of N1-aryl-2-arylthioacetamidobenzimidazoles and their activity against Herpes-simplex virus 1 in vitro *PLOS ONE*. Under Revision PONE-D-18-15387.

Assunta Venuti, Maria Musarra-Pizzo, **Rosamaria Pennisi**, Stoyan Tankov, Maria Antonietta Medici, Antonio Mastino Mastino, Ana Rebane, Maria Teresa Sciortino. (2018) HSV-1 stimulates miR-146a expression in an NF-κB-dependent manner in monocytic THP-1 cells: enrolment of an HSV-1\EGFP mutant virus. Under Revision. *Scientific Reports* -18-28955

Anna Piperno, Angela Scala, Antonino Mazzaglia, Giulia Neri, **Rosamaria Pennisi**, Maria Teresa Sciortino, Giovanni Grassi. (2018) Cellular Signaling Pathways Activated by Functional Graphene Nanomaterials. *International Journal of Molecular Sciences*. Under Revision ijms-341581

Anna Piperno Roberto Zagami Annalaura Cordaro, **Rosamaria Pennisi**, Maria Musarra-Pizzo, Angela Scala, Maria Teresa Sciortino, Antonino Mazzaglia. Exploring the entrapment of antiviral agents in hyaluronic acid cyclodextrin conjugates. (2018) *Journal of Inclusion Phenomena and Macrocyclic Chemistry*. doi:10.1007/s10847-018-0829-6.

Venuti A, Pastori C, Siracusano G, **Pennisi R**, Riva A, Tommasino M, Sciortino MT, Lopalco L. (2018). The abrogation of phosphorylation plays a relevant role in the CCR5 signalosome formation with natural antibodies to CCR5. *Viruses*, 10, p.1-14, doi:10.3390/v10010009

Antonino Mazzaglia, Angela Scala, Giuseppe Sortino, Roberto Zagami, Yanqui Zhuc, Maria Teresa Sciortino, **Rosamaria Pennisi**, Maria Musarra Pizzo, Giulia Neri, Giovanni Grassi, AnnaPiperno. (2018) Intracellular trafficking and therapeutic outcome of multiwalled carbon nanotubes modified with cyclodextrins and polyethylenimine. *Colloids and Surfaces B: Biointerfaces*, 163, 55-63. doi: 10.1016/j.colsurfb.2017.12.028

Antonino Mazzaglia, Norberto Micali, Valentina Villari, Roberto Zagami, **Rosamaria Pennisi,** Carmen Ortiz Mellet, José Manuel Garcia Fernández, Maria Teresa Sciortino, Luigi Monsù Scolaro.A novel potential nanophototherapeutic based on the assembly of an amphiphilic cationic β-cyclodextrin and an anionic porphyrin. *J. Porphyrins Phthalocyanines* 21, 398 (2017). doi: 10.1142/S108842461750033X

Carlo Bisignano, Giuseppina Mandalari, Antonella Smeriglio, Domenico Trombetta, Maria Musarra Pizzo, **Rosamaria Pennisi**, Maria Teresa Sciortino. Almond skin extracts exhibited antiviral activity against Herpes Simplex Virus type 1. *Viruses* (2017), *9*(7), 178; doi:10.3390/v9070178

Colao Ivana, **Pennisi Rosamaria**, Venuti Assunta, Nygårdas Michaela, Heikkilä Outi, Hukkanen Vejio, Sciortino Maria Teresa (2017). The ERK-1 function is required for HSV-1-mediated G1/S progression in HEP-2 cells and contributes to virus growth. *Scientific Reports* 7, 1-13, doi:10.1038/s41598-017-09529-y [**Co-first author**]

Claudia Conte, Angela Scala, Gabriel Siracusano, Giuseppe Sortino, **Rosamaria Pennisi**, Anna Piperno, Agnese Miro, Francesca Ungaro, Maria Teresa Sciortino, Fabiana Quaglia, Antonino Mazzaglia. Nanoassemblies based on Non-ionic Amphiphilic Cyclodextrin hosting Zn (II)-Phthalocyanine and Docetaxel: Design, Physicochemical Properties and Intracellular Effects. *Colloids Surf B Biointerfaces*. (2016); 146:590-7. doi :10.1016/j.colsurfb.2016.06.047.

Assunta Venuti, Claudia Pastori, **Rosamaria Pennisi**, Agostino Riva, Maria Teresa Sciortino , Lucia Lopalco. Class B β-arrestin2 dependent CCR5 signalosome retention with natural antibodies to CCR5. *Scientific Reports* (2016) Dec 23; 6:39382. doi :10.1038/srep39382

Mobility period during PhD

- HOSTING INSTITUTE: Department of Virology , University of Turku, Finland
  Title of project: HSV-1 infection and regulation of cell cycle.
  Supervisor: Professor Vejio Hukkanen. (January 2016- February 2016)

- HOSTING INSTITUTE: International Institute for Biomedical Research, Shenzhen, China
  Title of project: Signalosome complex activation by new Nanotherapeutic agents in viral and cancer treatment.
  Supervisor: Professor Grace Zhou (August 2017-December 2017)

- HOSTING INSTITUTE: International Agency for Research on Cancer World HealthOrganization (IARC) Lyon , France
  Title of project: Regulation of protein kinase R during HSV-1 replication associated to development of pathologic processes
  Supervisor: Dr. Tommasino Massimo (May 2018-June 2018)

ABSTRACT

Under physiological conditions, cells communicate with one another by activating receptors on the cell surface, which convey the signals enrolling proteins located in the cytoplasm and subsequently, activating transcription factors in the nucleus. The stimulation of this thick network of signaling is responsible for the control of expression of genes that mediate the cellular response. The aberrant production of growth factors and the broken communication cell to cell triggers an uncontrolled cellular transformation interfering with the normal functions of tissues.

The concept of gene delivery is based on the introduction of genetic material into the cells to compensate the abnormal genes and restore the function of misfolded proteins. The intracellular delivery needs genetically engineered carriers, commonly called vectors, which facilitate gene transfer to targeted cells without degradation of the delivered gene. To date, it is possible to refer to two principals families of vectors, viral and non-viral, used in clinical and research studies, responsible for the success of gene therapy in the treatment and prevention of several diseases. In the following chapters, viral and non-viral vectors will be described highlighting the advantages and disadvantages correlated to the use of the ones or the others one for the treatment of cancer diseases. In addition, an overview of the mechanisms and of the improvements of the vectors in several years will be reported, emphasizing that the acquired scientific knowledge on the use of several types of viral and non-viral vectors was helpful to improve target efficiency, cellular bioavailability and to limit the cytotoxicity effect preferentially to tumor environment. Therefore, the aim of this work was to analyze several cellular pathways, which are influenced, manipulated and controlled by a potential engineered HSV-viral and non-viral vectors. The success of gene therapy realized with viral and non-viral vectors, depends on a variety of factors including the interactions between host and vector. The viral model used in this thesis is Herpes Simplex Virus type 1 (HSV-1), whereas, the non-viral vector is represented by graphene-based platforms. The HSV-1 genome is around 150 kilobases (kbp) in length and encodes for about 84 genes. Many genes are not essential for its productive growth and for this reason is possible to manipulate the HSV-1 genome without critically damaging the ability of the virus to replicate. The efficient viral replication depends on delicate balance between host immune surveillance and production of viral proteins, which occurs with an accurate program of gene transcription. In this regard, and in order to create oncolytic HSVs (oHSVs), it is important to analyze cellular signals, including innate immune response, activated by HSV-1 and by involved viral proteins.

The fundamental mission of all viruses is to replicate and spread to persist in the host environment. In order to perform these functions, is essential to confiscate the protein synthetic machinery and reduce the host immune response. An important mechanism, that regulate translation initiation, involves phosphorylation of the alpha subunit of eukaryotic initiation factor-2 (eIF2α) mediated by protein kinase R (PKR). The modulation of PKR was analyzed after infection with HSV-1 and mutant HSV-1-viruses, deleted in tegument proteins closely connected with immunological escape. The model "host shut off" adopted by VHS protein of HSV-1, represents an immune evasion mechanism, which affects the activation of PKR. However, to date, the real mechanism used by the viral protein VHS to block PKR is not perfectly clear. Several years ago, it was proposed a new mechanism based on potential engagement of the mitogen-activated extracellular signal-regulated kinase (MEK), normally involved in the cell survival, in the PKR control. Indeed, Sciortino M.T. and collegues 2013[1] have demonstrated that, in HSV-1 infected cells, MEK protein, a well-characterized kinase in the cancer pathway, blocks phospho-PKR accumulation. Otherwise, in VHS, mutant virus (ΔVHS) infected cells, MEK protein is not able to control phospho-PKR accumulation. This finding highlights the important involvement of VHS tegument protein of HSV-1 in the regulation of PKR phosphorylation and led to investigate the role of additional teguments proteins Ser/Thr kinases US3 and UL13 on VHS/PKR control.

The study of viral proteins and their contribution in PKR regulation could contribute to develop new HSV-1-based vector for cancer therapy. Based on this, infection and transfection experiments were performed on several tumor cell lines to evaluate the expression of PKR active form and the transcriptional levels of PKR after HSV-1 (F) wild-type virus, R2621 (ΔVHS), R7356 (ΔUL13) or R7041 (ΔUS3) mutant viruses infection and after pVHS, pUS3 and pUL13 plasmids transfection. In addition, PKR-/- cell lines have been used to analyze the role of PKR in the HSV-1 replication, in the spread cell to cell, in the regulation of transcriptional and translational levels of the viral proteins. Finally, preliminary results have been obtained by comparing the quantitative expression of p53 in HEp-2 and PKR-/- cells after infection with HSV-1 and all mutant virus considered. The tumor suppressor p53 protein supports a transcriptional response involved in cell cycle arrest or apoptosis and its gene mutation is most frequent in human cancer diseases. Further studies are necessary to analyze the signaling network linking HSV-1 to p53 and PKR and the associated molecular mechanisms.

In the second part of this thesis work, two potential non-viral vectors have been used as a platform to delivery anticancer and antiviral drugs, plasmid DNA and miRNAs.

Carbon nanotubes (CNTs) and graphene are two representative carbon-based nanomaterials used as a platform in this work. The first used carbon-based nanovector, nanotube namely MWCNT, was modified with branched polyethylenimine to form a MWCNT-CD-PEI platform consequently conjugated with Rhodamine (MWCNT-CD-PEI-Rhod) to track *in vitro* the nanocarrier and to elucidate the mechanisms of cellular uptake. In order to explore the potentiality of the nanoplatform as drug delivery system, the cytotoxicity of the platform was evaluated at different concentrations on Vero cell line (kidney epithelial cells extracted from an African green monkey). To investigate the mechanisms involved in the cellular internalization, clathrin-dependent and caveole-dependent endocytosis inhibitors have been used. In addition, the endocytic compartmentation of MWCNT-CD-PEI-Rhod was studied by Cell Light lysosomes-GFP. Finally, the antiviral drug, cidofovir, was assembled with MWCNT-CD-PEI-Rhod platform, with or without pCMS-EGFP to investigate the drug and gene delivery by inhibition of plaque formation assay and expression of the green fluorescent protein, respectively.

The obtained results, published by Mazzaglia A. and collaborators 2018[2], have shown the high drug delivery efficiency mediated by nanotubes but inefficient delivery of nucleic acids. For this reason, further studies were performed by using another type of graphene-based platform and all experiments were carried out by comparing HEp-2 tumor cell lines with Vero non-tumor cell lines. The Graphene-based vector was modified with cationic cyclodextrins producing a G-CD platform which, in combination with a fluorescent probe, such as rhodamine, (G-CD@ADA-Rhod) was used for cellular internalization study. In a first phase, the biological evaluation has been carried out on G-CD platform assembled with the anticancer drug, doxorubicin, G-CD@Doxo, in order to evaluate the regulation of proteins, which, by acting as transcriptional factors, are involved in the control of cell cycle and tumor suppression. The communication cell to cell is guaranteed by molecular signals involved in the formation of signalosome complex. Signalosome consists in a set of several proteins able to respond to extracellular signals activating an intracellular signalling network in order to trigger an appropriate response. Therefore, the protein expression levels of p53 and its downstream and upstream regulators, transcription factor E2F and nuclear kinase Wee-1 have been investigated by western blot analysis. In the second phases, the regulation of autophagy pathway was explored as a response to the activation of intracellular signals driven by G-CD@Doxo.

To monitor autophagy flux, transfection experiments were performed by using the tandem monomeric RFP-GFP-tagged LC3. The GFP signal is sensitive to the acidic and/or proteolytic conditions of the lysosome lumen, whereas mRFP is more stable; therefore, colocalization of both GFP and RFP fluorescence indicates a compartment that has not fused with a lysosome, such as the phagophore or an autophagosome; in contrast, an mRFP signal without GFP, corresponds to autolysosome. In addition, the regulation of autophagy was evaluated by western blot analysis of expression of LC3 and p62, key proteins of autophagy process. Finally, G-CD platform was assembled with miRNA-15a, involved in tumorigenesis, and its delivery was analyzed by studing the expression levels of BCL-2 target.

This thesis work, underlines the importance of molecular research in the design of biological vectors. The study of HSV-1 viral proteins and of the interplay between viral teguments proteins and host immune response could be useful to define new retargeting approaches in the HSV-1 oncolytic virus.

CHAPTER I

Viral and non-viral vectors in gene therapy

Gene therapy is an experimental technique that uses genes to treat or prevent diseases. It introduces genetic material into cells to compensate the abnormal genes and restore the function of misfolded proteins. Gene delivery can be used for different purposes: gene functional studies, correction of genetic defects, expression of therapeutic proteins, and immunization against tumors and infectious agents[3].

The concept of gene delivery was developed in 1963 and represents an important approach to treat acquired and genetic disorders such as cancer, cystic fibrosis, hemophilia, vascular, infectious diseases, and many others. The completion of the Human Genome Project enabled the possibility of treatment of genetic diseases by introducing non-mutated gene or promoting immune response against infectious diseases by administering genes encoding specific antigens[4]. A gene that is inserted directly into a cell usually does not function. Naked DNA molecules do not enter into the cells efficiently because of their large size and hydrophilic nature due to negatively charged phosphate groups. In addition, they are very susceptible to nuclease-mediated degradation. Therefore, the primary challenge for gene therapy is to develop carriers, commonly called vectors, genetically engineered, that facilitate the gene transfer to targeted cells without degradation of the delivered gene. Two major vectors, viral and non-viral, are used in clinical and research studies. The viral vectors can have natural selectivity for tumor cells, can be genetically manipulated and work as vaccine vectors. Finally, the viral vectors are genetically attenuated so not to cause diseases[5]. The non-viral vectors represent an optimal alternative to viral vectors due to low immunogenicity, low toxicity and tissue specificity.

1.1. Cancer gene therapy.

The gene therapy contributes to correction of genetic defects, expression of therapeutic proteins, and inhibition of the synthesis of malignant proteins. The majority of gene therapy clinical trials have addressed cancer, cardiovascular and inherited monogenic diseases (Fig.1)[6].

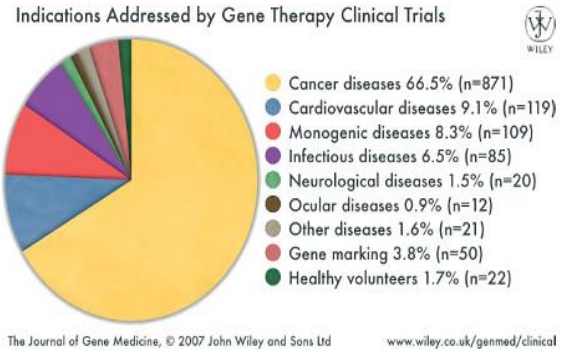

Table 1. Conditions for which human gene transfer trials have been approved

Monogenic disorders	**Cancer**
Cystic fibrosis	**Gynaecological**
Severe combined immunodeficiency (SCID)	- breast, ovary, cervix
Alpha-1 antitrypsin deficiency	**Nervous system**
Haemophilia A and B	- glioblastoma, leptomeningeal carcinomatosis, glioma, astrocytoma, neuroblastoma
Hurler syndrome	**Gastrointestinal**
Hunter syndrome	- colon, colorectal, liver metastases, post-hepatitis liver cancer, pancreas
Huntington's chorea	**Genitourinary**
Duchenne muscular dystrophy	- prostate, renal
Becker muscular dystrophy	**Skin**
Canavan disease	- melanoma
Chronic granulomatous disease (CGD)	**Head and neck**
Familial hypercholesterolaemia	- nasopharyngeal carcinoma
Gaucher disease	**Lung**
Fanconi's anaemia	- adenocarcinoma, small cell, non small cell
Purine nucleoside phosphorylase deficiency	**Mesothelioma**
Ornithine transcarbamylase deficiency	**Haematological**
Leukocyte adherence deficiency	- leukaemia, lymphoma, multiple myeloma
Gyrate atrophy	**Sarcoma**
Fabry disease	**Germ cell**
Familial amyotrophic lateral sclerosis	
Junctional epidermolysis bullosa	**Neurological diseases**
Wiskott-Aldrich syndrome	Alzheimer's disease
Lipoprotein lipase deficiency	Carpal tunnel syndrome
Late infantile neuronal ceroid lipofuscinosis	Cubital tunnel syndrome
RPE65 mutation (retinal disease)	Diabetic neuropathy
Mucopolysaccharidosis	Epilepsy
	Multiple sclerosis
Cardiovascular disease	Myasthenia gravis
Peripheral vascular disease	Parkinson's disease
Intermittent claudication	Peripheral neuropathy
Critical limb ischaemia	
Myocardial ischaemia	**Ocular diseases**
Coronary artery stenosis	Age-related macular degeneration
Stable and unstable angina	Diabetic macular edema
Venous ulcers	Glaucoma
Vascular complications of diabetes	Retinitis pigmentosa
Pulmonary hypertension	Superficial corneal opacity
Heart failure	
	Other diseases
Infectious disease	Inflammatory bowel disease
HIV/AIDS	Rheumatoid arthritis
Tetanus	Chronic renal disease
Epstein-Barr virus	Fractures
Cytomegalovirus infection	Erectile disfunction
Adenovirus infection	Anaemia of end stage renal disease
Japanese encephalitis	Parotid salivary hypofunction
Hepatitis C	Type I diabetes
Hepatitis B	Detrusor overactivity
Influenza	Graft versus host disease

J Gene Med 2007; **9**: 833–842.
DOI: 10.1002/jgm

Figure 1: Clinical target for gene therapy: Conditions for which human gene transfer trials have been approved by *M.L. Edelstein et al. 2007*. The graphical representation of several diseases targeted by gene therapy shows that most of the clinical trials in gene therapy have been aimed to treatment of wide range of cancer disease.

Many different cancer diseases have been targeted, including lung, gynecological, skin, urological, neurological and gastrointestinal tumors, as well as hematological malignancies and pediatric tumors. Under physiological conditions, cells communicate with one another by activating intracellular signals that mediate the cellular response. The broken communication cell to cell triggers an uncontrolled cellular transformation interfering with the normal functions of tissues.

The cancerous signals allow the cells to escape from the regulatory mechanisms and replicate continuously. A range of different strategies has been applied to cancer gene therapy, from inserting tumor-suppressor genes, to immunotherapy, to gene-directed enzyme prodrug therapy (GDEPT). All therapeutic strategies that have been developed in the treatment of cancer ultimately aim to destroy cancerous cells to avoid the spread of the cancer cells and at the same time, protect the normal cells.

To prevent the uncontrolled growth of the cells is essential to check the mutations in specific genes that normally control and regulate the cell cycle. The TP53 gene mutations are frequents in human cancer diseases[7,8] and frequently consist of missense mutations, leading to substitution of a single amino acid in the p53 protein, or frameshift or nonsense mutations resulting in the loss of p53 protein expression. The majority of missense mutations occur within the DNA-binding domain of p53, impairing its sequence-specific interaction with target gene promoters. These mutations generally lead to a loss or diminution of the wild-type activity of p53, and because p53 normally acts as a tetramer, these mutant proteins may function as dominant negative inhibitors over any remaining wild-type p53. Dittmer and collaborators (1993) demonstrated for the first time that the introduction of mutant p53 into p53 null cells give rise to a new phenotype suggesting that the mutant p53 may show a neomorphic gain of function[9].

In vivo experiments, consistently showed that mice expressing mutant p53 display a tumor profile that is more aggressive and metastatic than p53 null or p53 wild-type mice[,10,11,12,13]. The loss of p53-transcriptional activity affects its oncosuppressive responses and is closely link to enhanced invasion and motility and to the increment of the growth factor receptors expression[14]. Therapeutic strategies to restore wild-type activity of p53 provoke the death of the cancer cell and include the use of small molecules that bind to a site in p53 mutant, stabilizing the structure and increasing the level of the wild-type conformation and activity of p53. Alternative strategies promote the mutant p53 degradation by activating the proteasome degradation, ubiquitin ligase MDM2-mediated or chaperone mediated[15,16]. The autophagy process also plays a role in mutant p53 degradation. Normally, the activation of autophagy

allows to lysosomal degradation of intracellular waste materials such as damaged organelles and at the same time guarantee the production of energy from recycling intracellular contents[17].

Alternatively, to insert tumor-suppressor genes, the immunotherapy stimulates directly the immune response against cancer[18]. Cancer immunotherapy aims to promote the tumor-specific T cells activity to fight cancer. Normally, T cell functions include the ability to infiltrate tissues and to produce specific cytokines, chemokines and cytotoxic molecules[6]. The major obstacle in antitumor immunity is due to the deletion of tumor-reactive T cells during T cell development in the thymus and the instauration of anergy condition of T cells.

Borst and collegues reviewed the capability of $CD4^+$ T cells to enhance the B cell response, to help fully the CTL to target and to eliminate tumor cells overcoming the obstacles that typically hamper antitumor immunity. The $CD4^+$ T cells can target tumor cells either directly through cytolytic mechanisms or indirectly by modulating the tumor environmental. In particular, the $CD4^+$ T cells promote the production of co-stimulatory signals to CD8 T cell, responsible for clonal expansion and differentiation into an effector or memory T cells.

Recently, it has been reviewed an immunotherapy strategy mediated by immune checkpoint inhibitor, an important part of the immune system involved in the discrimination of normal and tumor cells. The stimulated immune system attacks the foreign cells and to do that, it activates or inactivates some host molecules during the immune response. Some tumors evade host immunity by dysregulating the immune checkpoints. For this reason, the administration of drugs that target these checkpoints upregulates host antitumor immunity and represents a good strategy for the multiple cancer types treatment[19]. In addition, a suicide gene therapy approach called Gene-directed enzyme prodrug therapy (GDEPT) offers immense therapeutic potential with more tumor specificity and less systemic toxicity. GDEPT is a two-step gene therapy approach because requires a transgene encoding to non-endogenous enzyme and a prodrug injected in the inactive form. The gene is cloned into a vector and delivered to target tissues with or without carriers, is expressed intracellularly and converts the prodrug in an activated cytotoxic metabolite inside cancer cells[20].

One of the most commonly used experimental and clinical models for gene therapy involves the transfection of the thymidine kinase (*tk*) gene of Herpes Simplex Virus into tumor cells, followed by treatment with the prodrug ganciclovir (GCV). The viral thymidine kinase converts the non-toxic pro-drug ganciclovir into the monophosphate form, which is then converted into a toxic triphosphate form by cellular endokinases. The ganciclovir triphosphate is an analogous to 2'deoxyguanosine triphosphate (dGTP) and causes the failure of the replication by inhibiting DNA polymerase. In vivo studies have been demonstrated the antitumor activity of the HSV-TK/GCV system in several animal tumor models [21].

Moreover, the limited clinical usefulness is due to lower concentrations released in target tissue and its high diffusion on non-target tissues responsible for adverse effects. To improve the efficacy of GDEPT, several new delivery systems have been investigated. Viral vector, nanoparticles, liposomes are excellent candidates to optimize the enzyme gene expression on target tissue.

1.2. Viral Vectors: strategies to increase the oncolytic virus efficiency.

The literature told for several years about the use of virus to insert and express cancer-suppressing genes to kill cancer cells[6]. Although the mechanisms of action of oncolytic viruses (OV) is still incompletely understood, it seems that the infection of tumor tissues with an oncolytic virus activates a positive feedback because the oncolytic virus infects a single tumor cell, replicates and kill it releasing virions in the tumor site, which in turn infect, replicate and kill other cells.

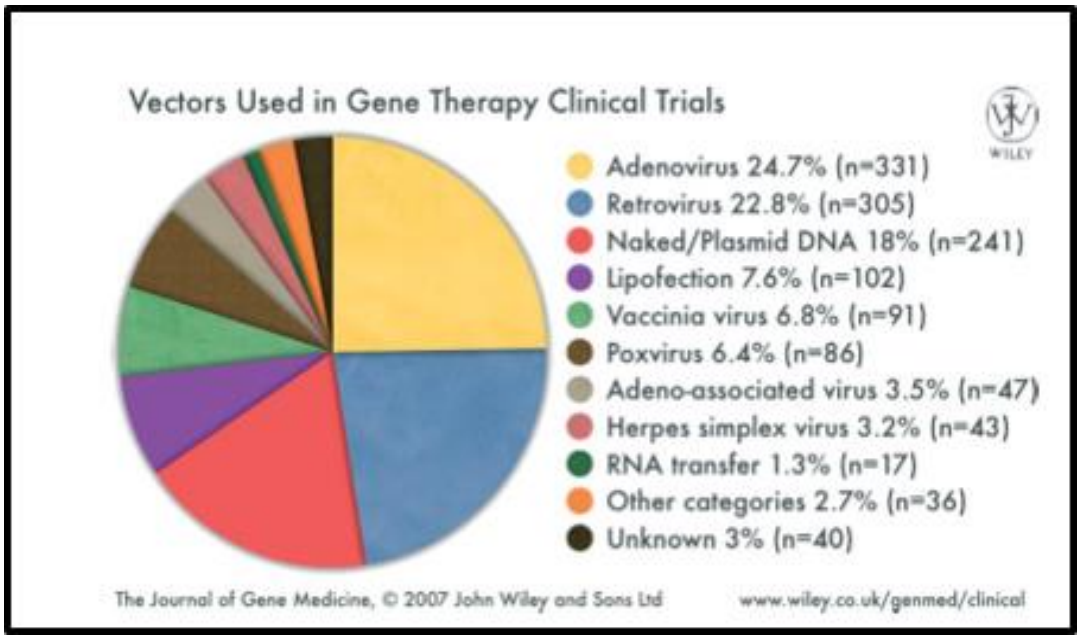

Figure 2: Gene therapy vectors used in clinical trials by *M.L. Edelstein et al. 2007*. Many viruses such as retrovirus, adenovirus, herpes simplex virus, adeno-associated virus and poxvirus have been studied in preclinical and clinical trials and modified to eliminate their toxicity and maintain their high gene transfer capability

Roland Scollay has performed an analysis of the past, present, and future conditions about the combination between gene therapy and oncolytic viruses from 1990s [22]. It was highlighted that, at the beginning, the gene therapy was a bankruptcy approach because it has provoked the first death case. Later years, the acquired knowledge on vectors, on diseases and on biological molecular processes associated to disorders, was responsible for little successes in the gene therapy. The development of genetic engineering in the 1990s made it possible to manipulate viral genomes to improve selectivity and decrease toxicity[23]. Oncolytic viruses by definition have a natural attraction to cancer cells, known as tropism.

Many viruses such as retrovirus, adenovirus, herpes simplex virus, adeno-associated virus and poxvirus have been studied in preclinical and clinical trials and modified to eliminate their toxicity and maintain their high gene transfer capability (Fig. 2). The major advantage of live vectors is that they produce antigens in native conformation, which is important for generating neutralizing antibodies[24]. An interesting review by Choi A.H. and collegues[25] explained two different viral genome modification strategies involved in the enhancement of the tumor selectivity by oncolytic viruses. Indeed, it is possible to use the adaptor molecules to facilitate binding of viral attachment proteins to specific receptors of target cells in order to improve the targeting selectivity. On the other hand, it is also possible to control and limit the viral replication in cancer cells through the viral genes inactivation.

It has been reported that the deletion of thymidine kinase of HSV-1, necessary for the DNA and RNA synthesis, leads the virus to dependent totally on cellular enzyme activity, which is more expressed in cancer cells rather than normal cells. In addition, it is possible to provoke the death of cancer cells by activating death mechanisms, including apoptosis, pyroptosis (caspase-1-dependent cell death), autophagy processes and necrosis[26,27]. The several death mechanisms release cytokines, tumor-associated antigens and other danger signals, which trigger a host adaptive immune response mediated by interferons and interleukins and sometimes an innate immune response mediated by stimulated Natural Killer.

An important role in the viral pathogenesis is carried out by neutrophils that, once activated following released apoptotic signals, produce reactive specie of oxygen (ROS) which can contribute to the oncolytic effect. Alternatively, is possible to use viral constructs engineered with suicide genes such as pro-apoptotic molecules'. Hirvinen M. and collaborators [28]generated a chimeric oncolytic adenovirus expressing the human tumor necrosis factor alpha (TNF-α), Ad5/3-D24-hTNF-α, with an increased cancer-eradicating potency.

In addition, Zhu W., and colleagues [29]armed an oncolytic adenovirus with the tumor necrosis factor-related apoptosis inducing ligand (TRAIL) which was administrated in vivo and they found the reduction of orthotropic breast tumor growth suggesting an increased antitumor activity of engineered adenovector. Often, in solid tissues the viral vectors are not able to infect neighbored tumor cells because the fibrillar collagen proteins and other components of extracellular matrix, which behave as a barrier to viral distribution.

To increment viral penetration into target tissue McKee T.D. and collaborators used a human melanoma oncolytic recombinant HSV vector, MGH2, with collagenase able to cut the peptide bonds in the collagen with a consequence increased distribution of viral particle in the tumor envirolment[30]. The same result has been reached by using matrix metalloproteinases or alternatively by arming oncolytic virus with fusogenic membrane glycoproteins that allow the formation of syncytia responsible for the propagation of viral infection.

In addition, a modern approach is represented by combined therapy of CAR-T cells and oncolytic viruses in order to facilitate the oncolytic virus delivery to tumor site limiting the cytotoxicity effect to tumor environment. Nishio N. and colleagues have performed *in vivo* experiments on murine models with neuroblastoma by using a combined therapy with CAR-T cells and oncolytic adenovirus Ad5D24 armed with RANTES and IL-15. Chemokines and growth factors sustain the growth and survival of chimeric antigen receptor (CAR)-modified T cells increasing their trafficking and their persistence on the tumor site[31]. To maximize the therapeutic effect is necessary that the oncolytic virus persists for a long time and stimulates a persistent adaptive antitumor immunity in target site. However, viruses naturally trigger the host immune responses inducing their clearance before to realize the therapeutic effect. A mechanism involved in the reduction of viral vector clearance is the transient suppression of early immune response through low dose of chemotherapy or TGF-ß treatment or alternatively pretreating with immunosuppressive chemotherapeutics such as cyclophosphamide during HSV-1 based oncolytic virus therapy in murine models of glioma. The depletion of antiviral antibody enhances oncolytic activity, improves viral delivery and promotes the viral replication[32].

1.2.1. Viral Vectors used for the gene therapy.

The major aim in gene therapy is to develop efficient, nontoxic gene carriers that can encapsulate and deliver foreign genetic material into specific cell types, influencing the cancer environment. Many viruses such as retroviruses, adenoviruses, herpes simplex viruses, adeno-associated viruses and poxviruses have been modified to eliminate their toxicity and maintain their high gene delivery capability. Retroviral vectors were the first vectors used in gene therapy as vector able to integrate stably into the chromosome of the cells. The retroviral vectors consist of proviral sequences in which some parts of the original viral genome have been eliminated in order to have more space available to insert a therapeutic gene.

In addition, they are responsible for a low immunogenicity and long-time expression of the delivered gene, but are unable to infect non-dividing cells. For this reason and for their lower transduction efficiency, the Adenoviral vector are the most commonly used vector rather than retrovirus. Adenoviral vectors are derived from Adenoviruses (AdV), DNA viruses with a linear double-stranded genome (36 kbp), replicate in the nucleus and release viral progenies by cell lysis[3,33]. Adenoviruses can carry a larger exogenous DNA, have a high efficiency of transduction, induce high level of transgene expression and are able to infect dividing and quiescent cells. Nevertheless, they have E1A and E1B genes, respectively encoding for proteins essential for viral replication and for the inhibition of host cell apoptosis, deleted and replaced by an expression cassette. The *in vivo* administration provokes the high immunogenicity, inflammation processes and the clearance of AdV-transduced cells. To overcome this problem, several generation vectors succeeded in recent years. Most Ad vectors are genetically modified and lack of the E3 genes, preventing the elimination by immune system, and E4 region encoding for double strand DNA repair functions.

These E1A, E1B, E3, and E4 deleted vectors are much more efficient and are known as replication-defective vectors. Several clinical data have been obtained by using Advexin, an Adeno vector expressing p53 from the CMV promoter in the deleted E1 region, in a phase III trial in the head and neck squamous cell carcinoma treatment. In addition, Gendicine is the first well tolerated and with a certificate anti-tumoral activity approved for commercial use. Besides to replication-defective vectors, another category of adenovectors, called replication-competent, are being studied intensely as therapeutics for cancer. The replication-competent vectors are able to lyse cancer cells, produce viral progeny and spread their activity to neighboring tumor cells. Essentially, all oncolytic Ad vectors replicate efficiently and specifically in cancer cells rather than normal cells, because the proteins expression pattern in a cancer cell is ready to use[33].

Gene delivery vectors based on adeno-associated virus (AAV) have been utilized in a large number of gene therapy clinical trials due to their long-term gene delivery efficacy and lack of pathogenicity and immunotoxicity. AAV is a single-stranded DNA parvovirus with a 4.7 kb genome that contains the *rep* gene encoding for non-structural proteins and *cap* gene coding for structural proteins.

AAVs can incorporate their genome into both dividing and non-dividing cells and the replication occurs in the presence of a helper virus. In the absence of a helper, however, AAV genomes can establish latency and persist as episomes or in some cases integrate into the host chromosomal DNA. Recombinant AAV vectors can be generated by replacing the rep and cap regions with an expression cassette consisting of a promoter that drives the expression of the transgene. Numerous AAV serotypes have been discovered, with a different expression of capsid proteins, which influence the tissue-specific tropism and transduction efficiency[34]. In the cancer field, AAV vectors can transduce a wide variety of cancer primary cells and can promote the activation of suicide genes, immunostimulatory genes and posttranscriptional regulatory proteins. The AAV capsid has been rationally engineered in several ways [35]. Zhong L. and collaborators have demonstrated that site-directed mutagenesis of AAV2 vectors on surface-exposed tyrosinic residues reduces the proteasomal degradation and leads to production of vectors that transduce more efficiently. In addition, modifications of AVV2 capsid proteins, by adding for example glycoproteins highly expressed in tumor cells, increases the affinity of viral vector towards tumor site[36]. Finally, the AAV vectors are highly versatile and can be produced to high titers, well tolerated at very high doses and, unlike Ad vectors, they are poorly immunogenic [37]. The limited packaging capacity represents an important disadvantage of AAVs. The acquired knowledge about herpes simplex virus's genome and host-virus interaction laid the foundations to engine herpes simplex virus as an oncolytic vector and overcome the limitations related to AAVs-based gene therapy.

Oncolytic herpes simplex virus (oHSV) was one of the first genetically-engineered oncolytic viruses considered in the past excellent vectors due to wide cellular tropism, capability to eliminate part of viral genome, reducing the cytotoxic properties and increasing the space available to carry up to 50 Kbp heterologous DNA. The gene therapy represents a promising approach to treated several diseases characterized by abnormalities of cellular components. The success of gene therapy depends on a variety of factors such as vector used for delivery, the vector delivery efficiency to the target, the administrated dose and the interactions between the host and the vector that can limit the efficiency of transfection[38].

1.3. Oncolytic herpes simplex virus: impact of immunological response on the oncolytic HSV-1 vector therapy.

The oncolytic viruses (OVs) are a class of cancer therapeutics targeting selectively cancer cells inducing cytotoxicity effect coupled to stimulation of anti-tumor immunity response. The first virus genetically engineered used as an oncolytic virus is Herpes simplex virus type 1 (HSV-1) in 2005. Talimogene laherparepvec (T-VEC), a genetically engineered HSV-based OV was approved for the treatment of melanoma representing the first oncolytic virus to be approved by the US Food and Drug Administration (FDA) as an anticancer therapy. The expression of immune-stimulating molecules seem to be an important mechanism to enhance antitumor responses mediated by OV. The T-VEC is the most studied OV expressing GM-CSF, the cytokine that promotes APC maturation and stimulates cytotoxic T lymphocytes (CTL) against tumors[39]. However, the stimulation of anticancer immunity processes interferes with the tumor environmental; on the other hand, a prolonged immune response could preclude the efficiency of oncolytic virus. Therefore, the characterization of the complex virus-host relationship is essential in order to augment the selectivity and the efficacy of the oncolytic viruses against cancer cells and counteract the cellular antiviral strategies limiting the oncolytic role of HSV-1. The HSV-1 genome is around 150 kilobases in length and encodes for about 84 genes. Many genes are not essential for its productive growth and for this reason is possible to manipulate the HSV-1 genome without critically damaging the ability of the virus to replicate.

Once HSV enters into tumor cells, it replicates, kills the tumor cells, and subsequently propagates within the tumor microenvironment. During this process, HSV activates multiple transduction signals, including nuclear factor kappa B (NF-κB), IFN regulatory factors (IRFs) and mitogen-activated protein kinase (MAPK) pathways, resulting in the induction of cytokines in infected cells. Cytokines and chemokines derived from oHSV-infected tumor cells or cells of the tumor microenvironment limit the oHSV replication and the spread within the tumor because recruit the innate immune cells (macrophages, NK, T cells) to the site of HSV infection (Fig. 3). The stimulation of the innate immune response coordinates the activation of adaptive immune responses mediated by DCs cells, which pick up the presence of HSV-1, process antigens and activate HSV-specific $CD4^+$ and $CD8^+$ T-cells.

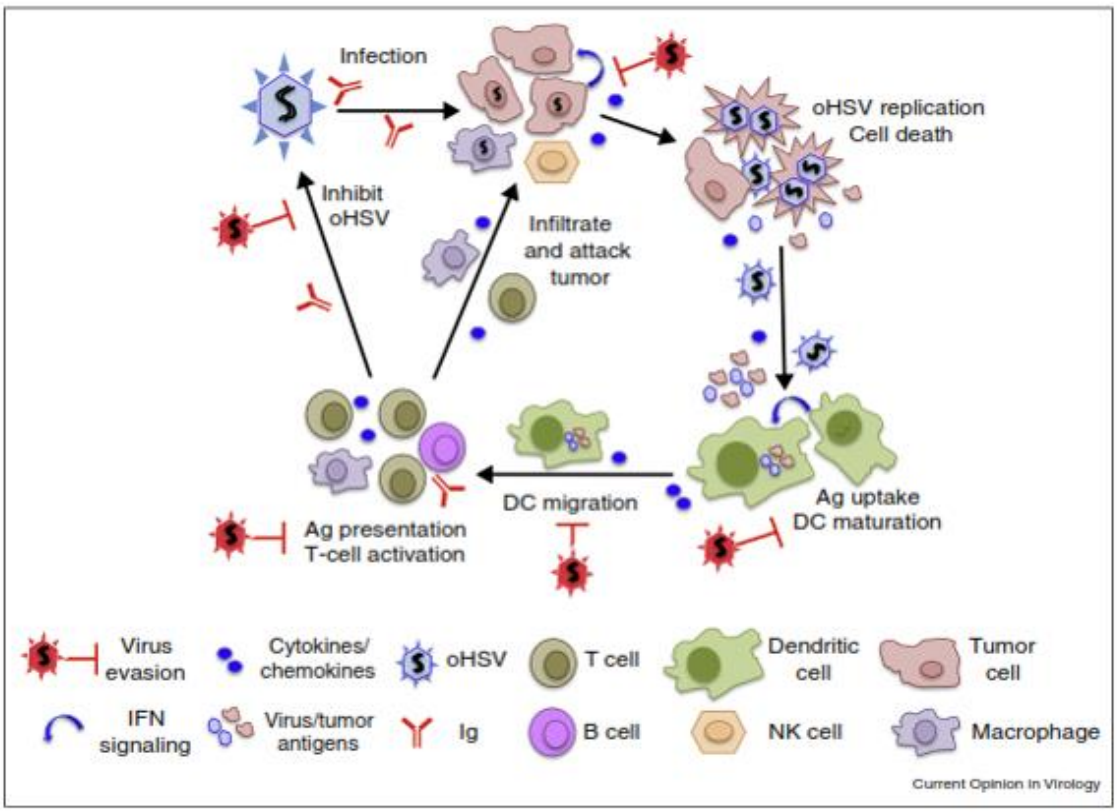

Figure 3: Graphic representation of HSV-host immune interactions by *Saha et al. 2016.* The oncolytic virus induces an anti-tumor immunity through the stimulation of serum factors, cytokines and chemokines production, recruitment of cells involved in the innate and adaptive immune response. The immunological signals, triggered by oncolytic viruses, affect the tumor environmental.

While HSV induces anti-viral innate and adaptive immune responses, it expresses proteins that inhibit both the induction and activity of those responses, allowing the virus to evade the host anti-viral immune surveillance mechanisms and establish both a productive and latent infection. The HSV-1 virion is composed of an envelope, a tegument, and a viral capsid core (Fig 4A). The envelope is studded with viral glycoproteins responsible for the attachment, entry and membrane fusion. The tegument is made up of multiple HSV-1 proteins, including ICP0, ICP4, and Us11, which prepare the cell to virus replication. The capsid is transported to the nuclear compartment for viral replication. The efficient viral replication depends on delicate balance between host immune surveillance and production of viral proteins, which occurs with an accurate program of gene transcription.

All genes are expressed sequentially starting with the immediate early (IE) gene group (ICP0, ICP4, ICP22, ICP27, and ICP47) responsible for gene regulation, followed by the early (E) gene group, involved in the replication of the virus's DNA genome, and finally the late (L) group, including structural proteins required for the progeny viral particles (Fig. 4B).

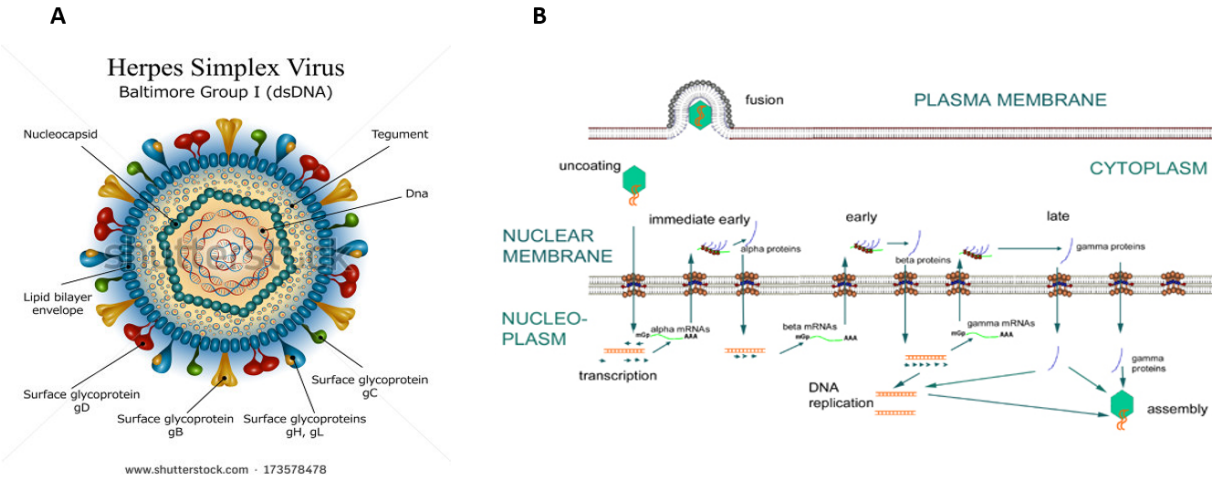

Figure 4: Viral structure and expression of immediate early, early and late genes of herpesviruses:
A) The virion of HSV-1 consists of the envelope; the tegument; the capsid; a core containing the viral genome. B) The productive cycle begins with the expression of the immediate-early genes encoding for viral regulatory proteins involved in transcriptional control of the early genes. The products of the viral early genes regulate the replication of the viral genome and finally, following viral DNA replication, late viral genes encode structural proteins necessary for the assembly and release of infectious particles.

The first response in the HSV-infected cell is the inflammatory reaction that includes secretion of antiviral substances, such as defensins and nitric oxid, and the production of cytokines, including IFNs and chemokines. The aim of the initial innate immune response is to limit spread of the infection[40]. Therefore, the HSV-1 envelope proteins act by binding and inactivating complement proteins in order to avoid the virus neutralization mechanism. The antiviral immune system mediated by IFN pathway is negatively regulated. The signals mediated by TLR3 and TLR2 to TRAF6 are inhibited by Us3 viral HSV-1 protein[41,42]. The MyD88 protein and the p50 and p65 subunits of NF-κB are inhibited by ICP0 HSV-1 viral protein[43]. US11viral protein binds to RIG-I and MDA-5 and inhibits their downstream signaling pathway, preventing the production of IFN-β[44].

The capability of HSV-1 to stimulate and downregulate at the same time the host immunological surveillance allows to deeper understand the host-virus interaction and make HSV as good candidate vector for gene transfer. Most immediate-early genes, which activate and regulate the gene expression cascade during viral replication and block several host defenses, have been removed from the vector in order to reduce cytotoxic activity and host immune response. Considering this, HSV vectors persist longer minimizing pathogenicity effect and ensuring tumor selectivity.

1.3.1. Oncolytic HSV constructs.

Herpes virus vectors mainly derive from HSV type-1, a neurotropic large DNA virus (152 kbp, double-stranded DNA) that incluses more than 80 genes divided in essential and non-essential genes according to their requirement for viral replication. Removal of non-essential genes makes room for up to 50 kb heterologous DNA thus making the HSV vector the largest carrier among the viral vectors[3]. The genetic complexity of the virus genome has allowed different types of attenuated vectors, possessing oncolytic activity, selectively replicating in and killing cancer cells, or able to invade and persist lifelong in neurons from where the transgenes can be strongly and persistently expressed[45].

HSV-1 possesses numerous advantages for *in vivo* gene therapy: to infect a wide variety of both dividing and non-dividing cell types; to be propagated to high titers on complementing cell lines; a large genome able to delivery therapeutic gene sequences (>35 kb); and the long-term persistence of the viral genome in a latent state during infection. Since the virus does not disrupt host cell but stimulates steadily the immune response, therefore, the HSV-1 vector-based therapy can be used to induce a persistent and controlled immunological surveillance in a tumor environmental.

HSV-1 holds several genes involved in nucleotide metabolism, which limit the virus replication to non-dividing cells. Mutations in these genes confer specificity for dividing cells[46]. A thymidine kinase-negative mutant of herpes simplex virus-1, Dlsptk, was the first genetically-engineered oncolytic virus tested, completely lacking *tk* activity as result of the 360-base pair deletion within the *tk* gene. Martuza R.L. and colleagues[47] have demonstrated for the first time that HSV-1 recombinant virus without *tk* activity was able to destroy in *vivo* and in *vitro* human glioblastoma cells opening the doors to a new concept in which genetic alterations on the virus could be used to increase the specificity against tumor cell. To date, this new concept is called “RETARGETING” and is a strategy that refine the target affinity of HSV-1-based vectors in the gene therapy. Retargeting approach can be used to either expand the host range to unlimited cell type or restrict the tropism of viruses to specific cell type.

Different mechanisms have been used to improve the retargeting and include the vector modifications with glycoproteins from other viruses which have different host-range, modification of viral glycoproteins to improve the binding between ligand and receptor and employing soluble adapters that recognize both the virus and a specific receptor on the target cell (Fig.5)[48,49]. Enhanced understanding of HSV entry, allowed to develop a first generation of fully retargeted HSV vectors without or with mutated viral glycoproteins. HSV-1 encodes 12 different glycoproteins among which the B, C, D, E, H, K, L glycoproteins and I are necessary for entry and cell-to-cell spread within the host.

Therefore, these glycoproteins contribute to define the viral tropism and can be used to produce a retargeted HSV-1. The canonical HSV internalization is mediated by attachment between viral glycoprotein and host cell surface receptors[50]. The initial binding of virus to the cells is mediated by interaction of viral glycoprotein(s) gB and/or gC with heparan sulfate proteoglycans (HSPG) on the cell surface. Although gC is not required for entry. The fusion of the viral envelope with the plasmatic membrane is a pH-independent process that requires gB, gD, gH and gL, along with cellular receptors for gD, such as nectin-1, herpes virus entry mediator (HVEM) or 3-O-sulfated HS (3-OS HS)[51,52]. The binding of gD to one of its receptors triggers a conformational change in this glycoprotein's structure that drives the recruitment of a fusion complex including glycoproteins gB, gH and gL. The fusion complex merges with the lipid bilayers and the viral nucleocapsid and tegument proteins are released into the host cytoplasm.

Several years ago, HSV-1 mutant virus was deleted for glycoprotein C (gC) and the heparan sulfate binding domain of gB and was engineered to encode different chimeric proteins composed of N- terminally truncated forms of gC and the full-length erythropoietin hormone (EPO)[53]. Thus, the HSV-1 tropism was expanded and the viral vector acquired the capability to interact, bind and infect other cell type.

In the same way, the Campadelli-Fiume'group has designed two o-HSVs with modifications in gD in N-terminal and core region which affect the interaction with natural receptor[54]. In both viruses, the deleted sequences are replaced with sequences encoding single-chain antibodies (scFvs) to HER-2, human epidermal growth factor receptor 2, a member of the epidermal growth factor receptor (EGFR) family of receptors, overexpressed in several type of cancer disease. Preclinical experiments have demonstrated the therapeutic effect of both retargeted o-HSVs against human cancer. Further findings showed that the retargeting of o-HSV in gH sequence improves the virus's tropism towards cancer cells in gD-independent manner[55]. Recently, it has been demonstrated the retargeting approach via gB despite it is a fusogenic protein not directly connected to HSV tropism[56].

In addition, a recombinant virus with enhanced specificity for malignant gliomas was constructed deleting the heparan sulfate binding site in gB and inserting into glycoproteins C and D site interleukin 13 (IL-13) whose receptor is exhibited on the malignant glioma tumor cells surface[57].

In order to achieve full retargeting of HSV, virus interaction with the canonical HSV entry receptors must be eliminated and functionally replaced with alternative ligand-receptor interactions. These approaches could limit the infection to target cell and so, increase the efficiency of oncolytic HSV constructs.

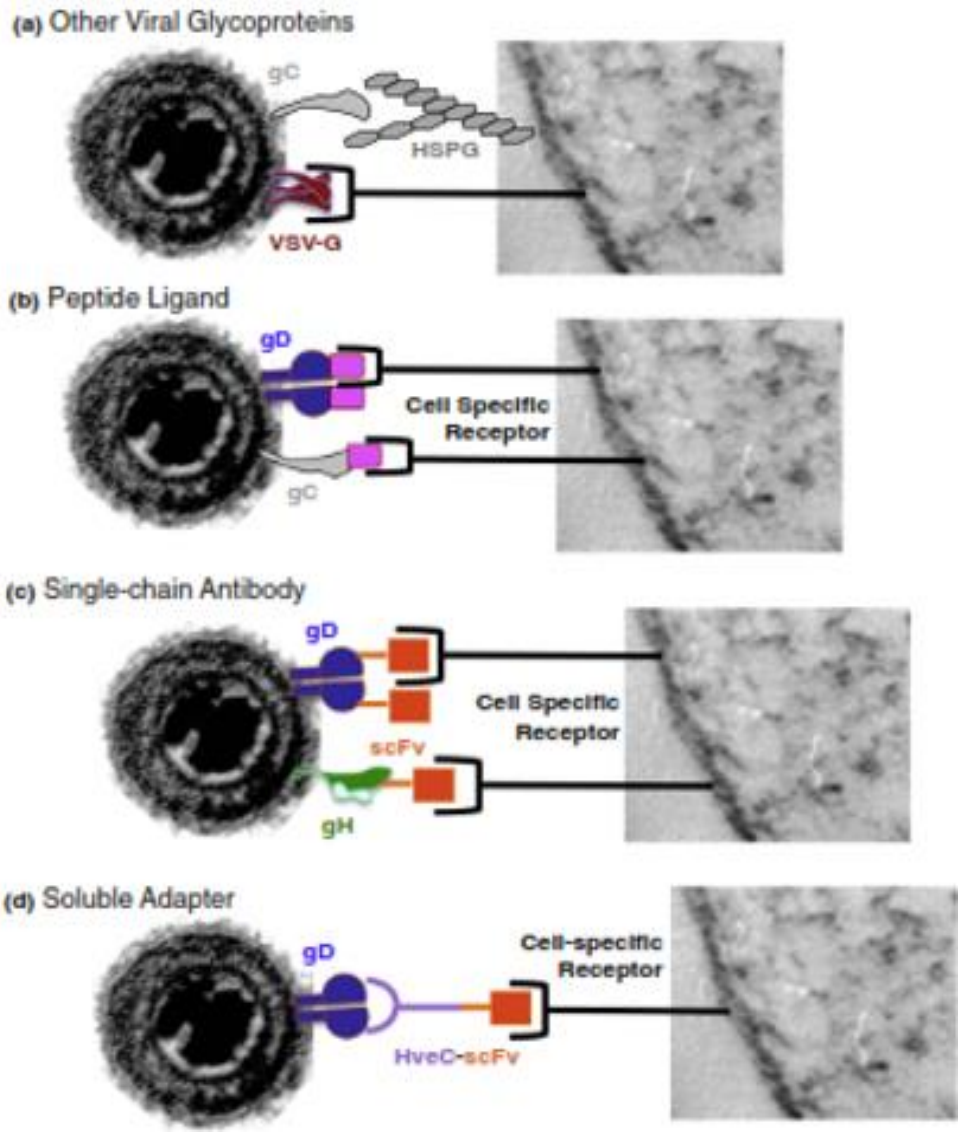

Figure 5: Strategies employed for HSV vector retargeting by *William F Goins et al., 2016.* Multiple strategies have been employed to refine the target affinity of HSV-1-based vectors in the gene therapy (a) Introduction of glycoproteins from Vesicular stomatitis virus (VSV-G) in place of HSV gD or gB glycoproteins. (b) Peptide ligands for naturally occurring receptors have been introduced into HSV gD or gC, in most instances replacing canonical receptor-binding sequences of those glycoproteins. (c) Sequences encoding single-chain antibodies (scFvs) have been introduced into the HSV gD and gH genes to achieve retargeting. (d) Soluble adapter molecules composed of a dual interactive component, one capable of binding to HSV gD and the other to the cell surface receptor target.

1.4. Non-Viral Vectors: advantageous vehicles to gene delivery.

Gene transfer is the technique, which introduces new genetic materials inside the cells in order to study genes function and their regulation, to investigate several diseases characterized by gene inactivation, to acquire DNA-based immunization, and finally, to explore potentials therapeutics applications. The size and the hydrophilic nature of the naked DNA limit the internalization in cellular compartment. In addition, they are very susceptible to nuclease-mediated degradation. Therefore, the primary challenge for gene therapy is to develop carriers able to facilitate gene transfer to targeted cells without degradation of the delivered gene. Alternative vehicles to the popular viral vectors to gene transfer are receiving substantial considerations due to low immunogenicity, low toxicity and tissue specificity[58].

Certainly, viruses mediate efficient gene delivery due to high ability to uptake and intake into the cells. However, several limitations reported in *vitro* and in *vivo* such as low DNA/RNA loading capacity, immunogenicity, toxicity and difficulty in production have encouraged the development of non-viral vectors. From this point of view, non-viral vectors have safe toxicity profiles and it is possible to plan the production in facile and flexible manner. Several cationic polymers, dendrimers, and cationic lipids have been studied to increase the efficient gene delivery. In order to target particular cell types, it is necessary to develop non-viral gene delivery particles whose intracellular circulation times is stabilized.

Cationic lipids are amphiphilic molecules possessing hydrophilic head and hydrophobic tail. These carriers condense DNA/RNA molecules via electrostatic interactions protecting them from enzymatic/non-enzymatic degradation mediated by intracellular components. These lipo-complexes enter into cells via endocytosis followed by destabilization of endosomal membrane and interact with membrane phospholipids allowing to the release of DNA into the cytoplasm[4]. However, disadvantages in the use of non-viral vectors are linked often to biological barriers limiting the intracellular uptake and the efficient gene delivery.

In vivo studies have indicated that the instability of the complexes in the extracellular spaces attenuates the biological response because the vector not specifically interacts with the tissue target and not easily translocate into the nuclear compartment to trigger the biological response. In addition, the insufficient cellular uptake and low endosomal escape, which limits the intracellular release of the vector, represent further problems to overcome in order to improve the gene delivery mediated by non-viral vector[59].

Many cationic polymers are used directly or indirectly as non-viral vectors such as polyethylenimine (PEI, branched/linear), poly-L-lysine (PLL), cationic dendrimers, glycopolymers, poly-amidoamine (PAMAM), and chitosan. Often, they are added to the non-viral vector structures as neutralizing agents to reduce the toxicity and increase half-life in cytoplasm. In addition, the association of PEG to the surface of β-cyclodextrin-containing complexes can increase stability and minimize the non-self interactions. Low endosomal escape represents a limit to use non-viral vector for gene therapy. Lipoplexes and polyplexes can enter into the cells either through interaction with cellular surface proteoglycans or through receptor-mediated endocytosis. The intake evolves in the internalization in endocytic vesicles from which, normally, viruses escape by triggering pH variations.

To overcome the non-viral vector entrapment in the endosomal compartments and to encourage the endosomal escape of non-viral gene delivery systems, viral peptides fuse to non-viral vector bone were developed. Similar findings were reported by using DNA complexes with the cationic polymer PEI that is partially protonated at physiological pH but, upon acidification within the endosome/lysosome, completes the protonation and triggers the destabilization of endosomal vesicles. Once the non-viral carrier escapes from endosomal compartments might reachs the nuclear site and releases the delivered gene to the transcription. To increment the stability and the ability of the non-viral vector in the intracellular trafficking directed to nucleus, is possible to modifying by using the nuclear localization signal peptides assisting transport of genetic material into nucleus[60].

1.4.1. Carbon Nanomaterials: Drug and Gene Delivery Potentials

In recent years, carbon-based nanoparticles have been plenty studied for their capability to drug and gene delivery. These materials, including fullerenes, one-dimensional carbon nanotubes (CNTs), and two-dimensional graphene and show carbon atoms with sp_2 hybridization forming a hexagonal arrangement. Their chemical structure, characterized by a small size and a large surface area, make them efficient platform for the attachment of several drugs and/or ligands. Multiple methodologies have been developed to modify the carbon-based nanoparticles and make them soluble in an aqueous environment, increasing absorption through the gastrointestinal tract but limiting their toxicity.

Fullerenes (C_{60}) are the third allotrope of carbon after diamond and graphite in the nanoscale range with peculiar photoelectrochemical features. However, fullerenes appear to be insoluble in water due to their hydrophobic properties. Therefore, functionalization using amino, carboxyl, or hydroxyl groups enhances the water-soluble properties of fullerene derivatives and results in high biocompatibility. In the cancer therapy, the ability of fullerenes is combined with photodynamic therapy (PDT) able to excite fullerene atoms[61]. The energy excitation is transferred to oxygen atoms and generates singlet oxygen formation, which can counteract tumor growth. Additionally, to the cancer therapy role, functionalized fullerenes can be used as useful nanocarriers for drug and gene delivery because of their optimal sizes and hydrophobic surface, which enable easy crossing of cell membranes and promote a continuously release the drug from the carbon support. Fullerene can act as a porous adsorbent for oral administration to impede degradation by hydrolytic and proteolytic enzymes, and improve low membrane permeability.

In addition to fullerene, many experimental evidences have pointed out that carbon nanotubes (CNTs) endowed with a proper size and degree of functionalization do not exhibit any evident toxic effect and undergo an effective clearance during in *vivo* experiments[62]. Since the discovery of carbon nanotubes in the early 1990s, their development in nanomedicine has emerged as one of the most interesting fields[2]. Mechanisms such as endocytosis, macropynocytosis and phagocytosis, promote their penetration through the membrane. The nature of functionalization of these materials could significantly influence the entry into the cells. Recently, the functionalization of the surfaces of graphene-based materials with diverse functional molecules such as drugs natural compounds, biomolecules and polymers, was reviewed by Piperno A. and collaborators (data not published), highlighting how several functional graphene nanomaterials (FGN) can activate intracellular signaling pathway able to determinate the cellular response and define the cell fate.

The activation of intracellular signaling network affects the cellular environmental through the release of cytokines, growth factors and genes regulatory proteins, which regulate apoptotic, cell cycle-related, inflammatory and metabolic processes responsible for various diseases or disorders. Current emerging therapies for genetic diseases are based on the cellular delivery of foreign nucleic acids, such as DNA, RNA, short interfering RNA (siRNA) and microRNA (miRNA). The delivery of siRNAs mediated by single walled carbon nanotubes (SWCNT) allowed to gene silencing promoting the inhibition of the cancerous cell growth. An efficient delivery system might be equipped of the capability to bind nucleic acids forming stable complexes, the capability to overcome the intracellular barriers and preserve them from the nuclease enzymes.

A stable nanovehicle was created by decoration of CNTs with β-cyclodextrins (CD), which have a hydrophobic inner cavity able to include selectively a large variety of organic molecules.

The Multi-walledcarbon nanotube (MWCNT)/ β-cyclodextrins/polyethyleneimine (PEI) (MWCNT-CD-PEI) platform was conjugated with Rhodamine (Rhod) to track in vitro the nanocarrier and to elucidate the uptake cellular mechanisms, demonstrating that an efficient double covalent functionalization can increase the intracellular intake of the nanocarrier and in this case guarantee the antiviral-mediated response against HSV-1 infection[2]. In addition, in mouse models, PEGylated nanographene sheets have high tumor uptake, which results to the ultra-efficient tumor ablation, without adverse effects[63]. Acid folic-ligand functionalization increases target efficiency. The folate receptors are overexpressed in many malignancies of esophagus, ovary, kidney, lung, breast, and brain, but not in normal tissues. It was developed an efficient nanovector with the folic acid functionalization, able to deliver miR-101 and miR-217 for silencing onco-noncoding RNAs MALAT1, highly expressed in metastatic non-small-cell lung cancer (Fig.6)[64].

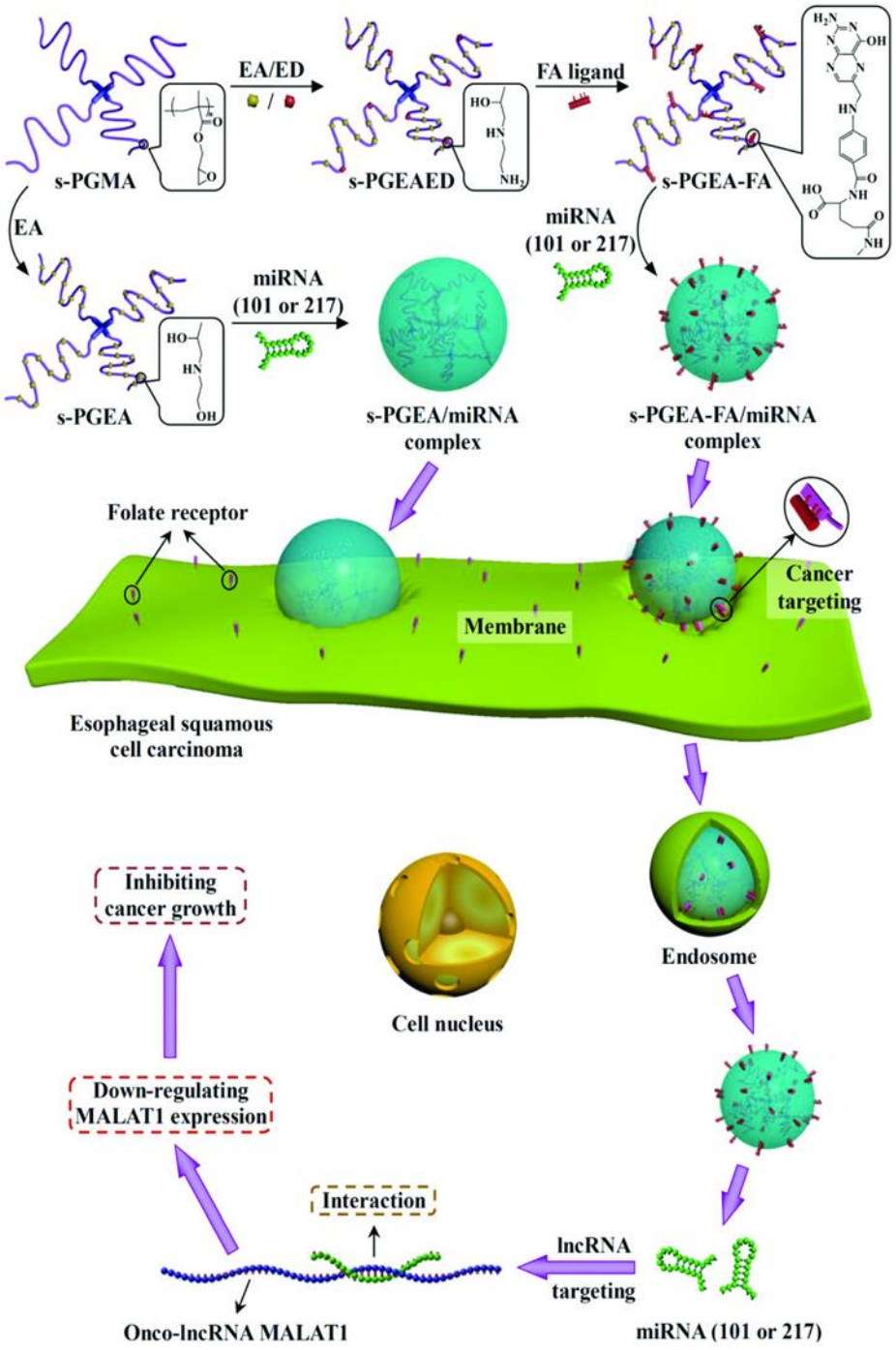

Figure 6: A diagram illustrating the synthesis processes of s-PGEA and s-PGEA-FA and the resultant delivery of miRNAs in esophageal squamous cell carcinoma (ESCC) cells by *Li, et al., 2017*. A poly(glycidyl methacrylate)-based star-like polycations with flanking folic acid (FA) ligands (s-PGEA-FA) was synthesized as an efficient nanovector to deliver miR-101 and miR-217 for silencing onco-lncRNA MALAT1 in differents ESCC cells.

CHAPTER II

Intracellular Signal Transduction Cascades activated by virus infection

The host-virus interaction triggers a complex network of intracellular signaling which rapidly shifts the cell from a stationary to mobile state. The viruses are sensed by pattern recognition receptors (PRRs) which recognize foreigner highly conserved structure known as pathogen-associated molecular patterns (PAMPs), such viral nucleic acids and bacterial components such as LPS or flagellin[65]. Three important classes of PRRs have been discovered and deeply studied, and differ for ligand specificity, cellular localization and activation of specific signaling pathways. Toll-Like Receptors (TLRs) are membrane-associated receptors, Retinoic Acid-Inducible Gene (RIG-I)-Like Receptors (RLRs) and Nucleotide-binding Oligomerization Domain (NOD)-Like Receptors (NLRs) represent cytosolic receptors. Another sensor recently discovered and called DNA-dependent Activator of IRFs (DAI), localizes into the cytosol and recognizes both microbial and host DNA. Viral detection by TLRs, RLRs and DAI leads to recruitment of signal adaptors and promotes the expression of Type I interferons (IFNs) (IFN-α/-β) and pro-inflammatory cytokines. These cytokines are important for recruitment and activation of the immune effector cells (i.e. neutrophiles, B lymphocytes and T lymphocytes) which trigger intracellular network involved in the antiviral response.

All viruses depend on cellular protein synthesis machinery to translate viral messenger RNAs and produce new viral progenies. The coordinated recruitment of host several transcription factor complexes quenches the virus replication and minimizes the viral cells to cells spread. The two main classes of antiviral mediators are proteins belonging to the innate immune system and the adaptive immune system whose defense mechanism results effective if it is able to discriminate self and non-self-particles.

The innate immune response represents a rapid first line of defense: aspecific, activated by the presence of antigens, mediated by physical, physiological, chemical, biological barriers and by several cell types, which secrete high levels of proinflammatory cytokines and chemokines. They play a key role in the initiation and regulation of the immune response. Their release induces the activation and differentiation of the more sophisticated adaptive immune response mediated by T and B cells expressing antigen-specific receptors, which amplify the local inflammatory response and recruite effector cells[66].

The pathogenesis of the viral infection can be acute and often cytolytic, able to destroy the cell or persistent, tolerated from cells. Some viruses establish permanent infections, in which viruses

continually replicate or, alternatively, remain latent within cells and reproduce only periodically. In this way, virus and host live in a dynamic equilibrium in which the immune pathways contribute to stringent control, resulting in viral clearance. Naturally, viruses have evolved strategies to evade the inflammatory and immune responses that their hosts have co-evolved to limit viral impact on reproductive fitness[67,68]. In some cases, cytokine and chemokine homologues are encoded to bind to specific receptors and either trigger signal transduction and biological responses. Alternatively, they are able to occupy receptor-binding sites and prevent binding of host cytokines. They also encode viral proteins with high sequence similarity to the extracellular domains of cellular cytokine receptors neutralizing their activity and enhancing virus dissemination. Noda S. and colleagues[69], compared wild-type MCMV with mutants lacking the *mck* gene, which encodes two forms of viral chemokines and found an increased inflammatory response, which not affect the virus clearance. Whatever used strategy results in the control of the immune response in order to induce virus dissemination.

2.1. Type I interferon-dependent signaling pathway and antiviral actions

Innate immune response against viruses and other pathogens occurs in two waves. Type I IFNs production in response to PAMPs detection by host PRRs constitutes the first wave of genes to be expressed. Type I IFNs expression is responsible for the induction of the second wave of genes, the Interferon-Stimulated Genes (ISGs) that encode antiviral effectors, which allow to the clearance of pathogens[70]. Isaacs and Lindemann discovered interferons in 1957. They are secreted by infected cells and induce an antiviral state able to limit the propagation of the virus. Moreover, it was shown that IFNs have both autocrine and paracrine effects inducing an antiviral state in infected cells and in neighboring non-infected cells.

IFNs are classified in three types: (i) Type I IFNs include IFN-α and IFN-β. They are directly induced in response to viral infection and produced by innate immune cells such as dendritic cells and macrophages but they can also be encountered in fibroblasts. (ii) Type II IFN only comprises IFN-γ member that is produced by NK cells and by activated T cells. (iii) Type III IFNs include IFN-λ1, -λ2, -λ3 also known as IL-29, IL-28A and IL28B, respectively. Type III IFNs are directly produced in response to viral infection. Type I IFNs (IFN-α/-β) play a key role in the activation of the antiviral response[71]. They are responsible for the activation of the Jak/STAT pathway that leads to the expression of ISGs that encode antiviral effectors.

In response to PAMPs, host PRRs also activate NF-κB, AP-1, IRF3. These transcription factors cooperate to induce the expression of type I IFNs. The IFN-α and -β bind to their receptors, the Interferon-Alpha/Beta Receptors (IFNAR) 1 and 2, activate the receptor-associated kinases Jak-1 and Tyk-2 that respectively phosphorylate STAT1 and STAT2 and associate with the protein IRF9. This complex, named interferon-stimulated gene factor 3 (ISGF-3), translocases into the nucleus where it can activate the expression of Interferon-Stimulated Genes (ISGs). Among the ISG proteins, the best characterized are PKR, ISG15, Mx proteins and OAS1. They act by targeting different cellular processes, such as the messenger RNA transcription and the protein translation and in this way, inhibit the assembly of virions and limit the viral spread.

2.2. Role of Protein Kinase R in the regulation of cellular processes

An important mechanism regulating translation initiation in response to environmental stress involves phosphorylation of the alpha subunit of eukaryotic initiation factor-2 (eIF2). Viral infection, starvation for nutrients and ER stress stimulate the activity of one or more members of a family of eIF2 kinases. PKR is one of the four mammalian kinases (the others are GCN2, PERK, and HRI) that phosphorylate eIF-2α at residue S51 in response to stress signals, mainly because of viral infections. As a consequence of dsRNA accumulation in infected cells, PKR-triggered eIF-2α phosphorylation also inhibits translation of viral mRNA.

PKR is a ubiquity expressed Serine/Threonine kinase characterized by two distinct kinase activities: the autophosphorylation at residue Thr446, which induces its activation, and the phosphorylation of eIF-2, which affects eIF-2 activity and inhibits protein synthesis. In addition to its translation regulation function, the PKR protein is also involved in the signal transduction processes and transcription control through the NF-κB pathway[72], and in other biological effects such as differentiation and control of cell growth, apoptosis, deletion of the tumor, and RNA-interference. In particular, it has been demonstrated that PKR interact directly with the C-terminal part of p53 and phosphorylate p53 on the Ser392 residue. Once activated, it supports a transcriptional response involved in cell cycle arrest or apoptosis. Cuddihy A.R. and collaborators [73] highlighted the important of PKR contribution in the p53 activity. *In vitro* experiment performed on PKR-/- MEF cells demonstrated that the ability of p53 to cause cell cycle arrest and regulate transcription of target genes is reduced in absence of PKR. In addition, PKR is an activator for signaling cascades involving stress-activated protein kinases and is described as mediating JNK and p38 activation in response to specific stimuli. By using MEF cells derived from PKR-null mice, it was shown that PKR is required for p38 MAPK activation in response to dsRNA, LPS, and proinflammatory cytokines but not in response to other forms of stress. ATF-3 was identified as a gene that is selectively upregulated by the active PKR enzyme. ATF-3, a 181-amino-acid protein, is a member of the ATF/CREB family of transcription factors, which are expressed at low levels in quiescent cells. ATF-3 acts as a sensor that interacts with and activates p53 under various types of stress by blocking its ubiquitination. Furthermore, ATF-3 overexpression enhances caspase 3 activity.

At the end of 90s was studied the NF-κB activation in response to PKR. The NF-κB family of transcription factors controls the expression of genes involved in immune and inflammatory responses, cell differentiation, and apoptosis. The key mechanism that regulates NF-kB activation is its cytoplasmic retention mediated by interaction with inhibitory molecules of the IκB family. IκB proteins are phosphorylated by the IKK complex in response to a variety of stimuli, which tag them for ubiquitin proteasome-mediated degradation.

This event allows NF-κB translocation to the nucleus, where it regulates transcription. PKR interacts physically with the IKK complex and regulates NF-κB through phosphorylation of its inhibitor, IκB[74]. In human and mouse cells tested to date, seem that the stable activation of NF-κB requires activated PKR. Furthermore, it was also suggested that TRAF3, adapter proteins and signal transducer, is required to activate NF-κB through the physically association with PKR[75]. Additionally, to interferon-induced antiviral defense mechanism, PKR is a potent pro-apoptotic protein involved in the activation of antiviral response that acts by rapidly eliminating infected cells and preventing viral spread[76].

Effector molecules in apoptosis are proteolytic enzymes known as caspases, synthesized as inactive preforms and activated following cleavage. The activation of caspases follows the stimulation of membrane receptor- mediated and mitochondrial-mediated signals, which trigger an extrinsic or intrinsic pathway, respectively. Links between the receptor and the mitochondrial pathway exist at different levels and their activation terminates with activation of caspase-3 able to induce the degradation of DNA and cell death, consequentially. It was demonstrated that PKR induces apoptosis activating both, the extrinsic and the intrinsic routes of caspases activation. The involvement of PKR in interferon-mediated activities, in the induction of apoptosis, in the activation of pro-inflammatory transcription factor NF-κB and in several biological pathways, identify it as an important cellular indicator. A failure in the PKR regulation results in unbalanced and dysregulated cellular condition that could contribute to neurodegeneration, cancer and inflammatory diseases. For this reason, the study of PKR and the increased knowledge about the regulation mediated by host and foreigner proteins, represents a new target for the scientific community.

2.2.1. Structural feature of PKR

PKR is a component in the cellular antiviral defense mechanism composed of tandem copies of conserved double-stranded RNA binding motif (dsRBMs) in its N-terminal domain, with a flexible linker connecting to a C-terminal kinase catalytic domain. The dsRBD of PKR can bind to any RNA containing sufficient A-form helical structure. However, higher concentration of RNAs have an inhibitory effect on the PKR activation. The 20 amino acid linker, between N- terminal and C-terminal domains, has a random coil conformation and probably contributes to wrap around dsRNA to A-form helix structure and facilitate interaction between RNA and dsRBM. Expression of PKR is transcriptionally induced by interferon, and the kinase is activated upon binding to double-stranded RNA (dsRNA).

Human PKR consists of 551 amino acids, with the lobate structure of kinase domain (KD) in the C-terminal half (residues 258-551) of the protein. The kinase domain of PKR contains the conserved protein kinase subdomains that, together to dsRNA-binding regulatory domain, are involved in the regulation of PKR function. The N-terminal regulatory region of PKR consists of two dsRNA binding domains (dsRBDs) labeled dsRBM I and dsRBM II[77]. Several groups have been demonstrated that, although dsRBM1 is more important for dsRNA binding than dsRBM2, both domains cooperate to guarantee an optimal binding (Fig.7).

The binding of dsRNA to the dsRBDs causes a conformational change in PKR and shifts it to active form. It has been hypothesized that PKR exists in a closed conformation in which the dsRBD interacts with the kinase, autoinhibit and blocks the binding of the substrate. Several study support a different model for the activation of PKR based on the presence of equilibrium state between open and closed conformation and dsRBM2 transiently interacts with the kinase on the C-lobe, far from the active site. The autoinhibition model for the PKR activation, reviewed by Cole J.L. [78], indicates that the binding of dsRNA removes dsRBM2 from the kinase domain and exposes the catalytic site for autophosphorylation. It has been demonstrated that the autophosphorylation is an intermolecular mechanism, which involves the dimerization of two monomers of PKR. In addition, seems that PKR can auto-phosphorylates itself in the absence of dsRNA or by non-dsRNA molecules including polyanions such as dextran sulfate, chondroitin sulfate, poly (L-glutamine) and heparin and cellular protein such as PACT, which contains two dsRBMs and heterodimerizes with PKR via the dsRBD.

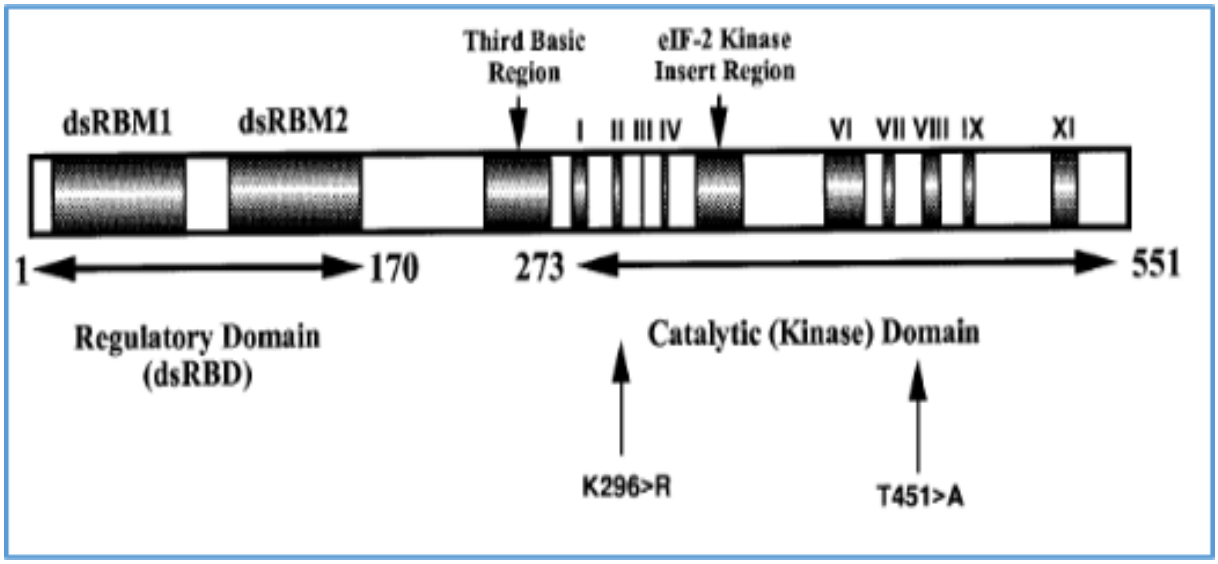

Figure 7: Structural organization of PKR domains by *Williams B. RG, 1998.* PKR is composed of tandem copies of conserved double-stranded RNA binding motif (dsRBMs) in its N-terminal domain, a C-terminal kinase catalytic domain that contains the insert region for translation initiation factor eIF2 and several phosphorylation sites within the activation loop between kinase subdomains VII and VIII.

The autophosphorylation of PKR induces structural rearrangement responsible for the exposition of catalytic site in the C-terminal catalytic domain. Mapping the peptide, it was possible identified several phosphorylation sites, two of which at Thr446 and Thr-451 within the activation loop between kinase subdomains VII and VIII. Substitution of Thr-451 to alanine completely inactivated PKR, while a mutant with a Thr-446 to alanine substitution was partially active. Phosphorylation sites in the third basic region (Thr-258, Ser-242, Thr-255) seem to be important to block PKR in active conformation with the catalytic domain irreversibly uncovered by the regulatory domain. The characteristic "bell curve" of PKR activation based on the optimal concentration of RNA able to activate or inhibit PKR. This mechanism can be used by several viruses to avoid the immune response or in the same time could represent an endogenous cellular control, which regulates PKR in response to stress[79].

As a component of antiviral mechanism, PKR acts by inhibiting protein synthesis initiation and activating the transcription of genes involved in an inflammatory response. The translation initiation factor, eIF2 is a GTP binding protein that, in the first step of translation initiation, delivers the initiator methionyl-tRNA to the small ribosomal subunit. The phosphorylation of eIF2α factor, mediated by PKR, occurs on Ser51 residue and block the protein synthesis. It has been demonstrated that the PKR autophosphorylation on the activation segment residue thr446 enhances recognition of the alpha subunit of eIF2[77].

Indeed, a three-step pathway was proposed for PKR activation in which a specific dimer orientation between the catalytic domains of two PKR molecules promotes autophosphorylation in trans-intradimer fashion exposing more the residue of Thr446 and enhancing PKR catalytic efficiency and the recognition of eIF2α (Fig.8).

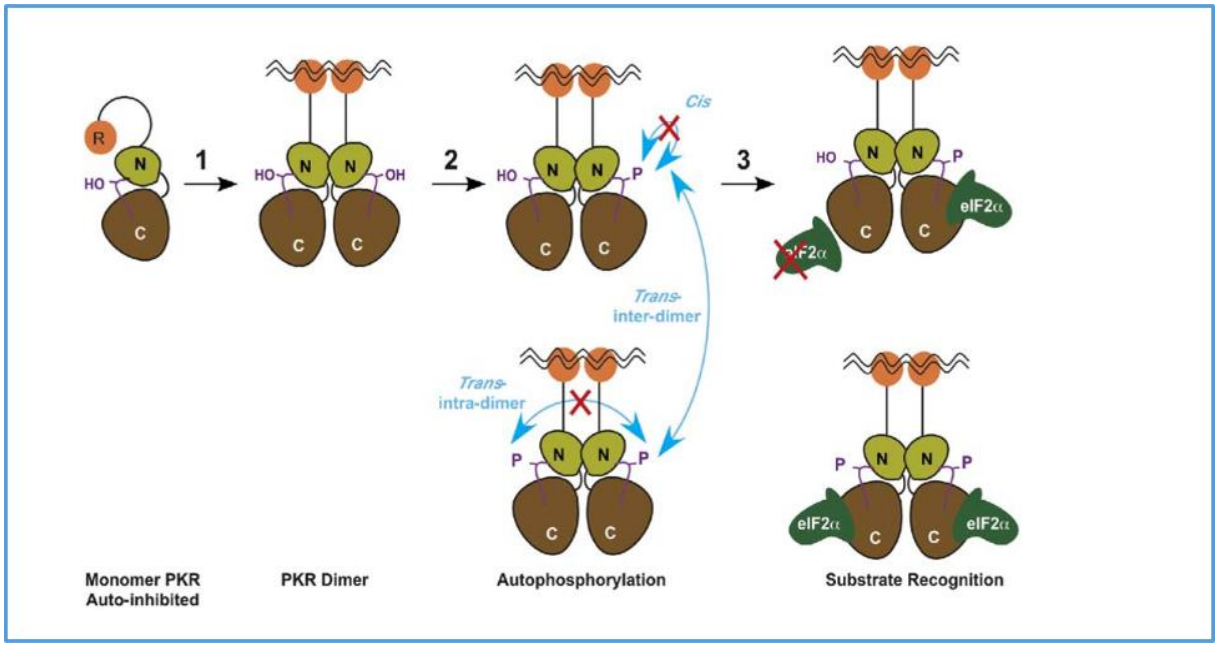

Figure 8: Model of PKR Activation Pathway: Dimerization-Dependent Autophosphorylation and eIF2α Substrate Recognition *by Dey et al 2005*. The closed conformation of PKR (1) make the protein inactivated. The interaction with dsRNA promotes catalytic-domain dimerization (2), the auto phosphorylation between dimers and dimers (trans-interdimer) (3) on Thr446 residues, which improves PKR catalytic activity and the binding with Eif2α protein.

All viruses depend on cellular protein synthesis machinery to translate viral messenger RNAs and produce new viral progenies. For this reason, the control of PKR represents a fundamental strategy to avoid the innate immune response and guarantee viral survival.

2.3. Viral Strategies used to subvert the innate immune response

The fundamental mission of all viruses is to replicate and spread to persist in the host environment. The activation of the innate immune response allows to the activation of several transcription factors such as NF-κB and IRF3, which are key regulators of IFN-β expression. The released IFN-β leads to the activation of the ISGs, which encode antiviral effectors such as the PKR. In this way, the antiviral response is going to establish in the infected cells as in the neighboring non-infected cells preventing them from viral invasion. The importance of antiviral pathway is highlighted by the diverse mechanisms that viruses have evolved to avoid the immune response at every step in their life cycle. Not always, the viral mechanism of immunological escape coincides with the total block of immune host proteins because some of this are vital for the cells and if the host die, the survival of the virus is not guaranteed.

Since IFNs are key players in the activation of antiviral responses, many viruses, including HSV-1, blocks interferon-mediated pathways in certain steps[80]. They can control the synthesis of IFN-α/β, inactive the molecules secreted by IFN or interfere with their activity producing viral homologous proteins. The virion host shutoff protein (VHS) of HSV-1, a viral endoribonuclease encoded by the UL41 gene, has been described to interfere with both type I and type II IFN dependent signaling pathways, accelerating degradation of ISGs mRNAs.
In addition, considering the role PKR plays in the regulation of protein synthesis, many viruses have evolved intricate mechanisms to control its activation. The inhibition of PKR-mediated response represents the immune escape mechanism used to ensure their survival and propagation. Some of viruses, such as adenovirus and Epstein-Barr virus, transcript non-coding RNA that contain structural elements required for binding to dsRBMs of PKR. These fake RNAs bind and prevent autophosphorylation of PKR. The combined activity of Tat protein of HIV and cellular factors, for example, contributes to inhibit the PKR activation. In addition to block the activation of PKR, other viruses use alternative strategies that can either disrupt or occlude the RNA binding site of PKR. Vaccinia virus, Influenza virus, Human herpesvirus 8, and Rotavirus produce viral protein against PKR. Therefore, vaccinia virus produces two proteins responsible for the interferon-resistance phenotype: E3L, a dsRNA-binding protein able interact with dsRNA or directly with PKR via its N-terminal domain and K3L, which act as a competitive inhibitor of PKR because, through its high homology with eIF2α maintains a persistence of protein synthesis[81].

The sigma 3 protein of reovirus is able to prevent the activation of PKR by sequestering dsRNA instead, a similar mechanism is discovered for Rift Valley fever virus and Toscana virus. Both virus codify for viral protein involved in the post-transcriptional proteosomal degradation of PKR with a not perfectly understood mechanism, which could include, for

Toscana virus, the direct interaction between PKR and viral proteins. Instead, vIRF-2 of HHV8 is homolog of interferon regulatory factors able to affect several cellular transcriptional factors and prevents PKR autophosphorylation through direct interaction with PKR. Several proteins involved in this process against PKR have structural function otherwise than other viruses, such as Picornavirus, which codify viral proteases with a gene expression regulatory function, normally[80].

Recent evidences demonstrated that, viral 3C protease of Enterovirus 71 (EV-A71) belong to *Picornaviridae* family, cleaves PKR following direct interaction to facilitate viral replication[82]. Other studies suggested that PKR inhibition occurs with an RNA-independent mechanism but with the formation of complexes between the viral protein and PKR. Indeed, the NS1 protein of Influenza virus contains residues involved in protein–protein interactions capable to promote the interaction with PKR and block it[83]. By mapping HCV RNA genome is discovered that viral nonstructural 5A (NS5A) protein co-localizes with PKR and suppresses its dsRNA-dependent activation[84]. HSV-1 contains a late gene, Us11, which, expressed early, binds to PKR and blocks its activation[85]. This prevents the phosphorylation of eIF-2α and thereby precludes the inhibition of viral transcripts translation. US11 acts as an inhibitor of PKR via both RNA-dependent and RNA-independent interactions. In the first case, it is able to sequester dsRNA or interact with double-stranded RNA binding motifs with high-affinity.

Alternatively, US11 inhibits PKR in RNA-independent manner by binding the protein activator of PKR (PACT). PACT contains three binding domains, two of which bind the PKR binding domain in the N-terminal site of the protein. The third domain interacts with the kinase domain of PKR and promote the conformational switch towards active form. Peters and collaborators showed a model of inhibition of PACT-mediated-PKR activation through the formation of trimeric complex between Us11- PACT and PKR (Fig.9)[86]. When all domains of PACT protein bind to N-terminal and C-terminal site of PKR, trigger a conformational change of PKR mediated by interaction between domain 3 of PACT and kinase domain of PKR. PKR switches towards activated form by exposition of its kinase domain. The inhibition of PKR mediated by US11 viral protein prevents this conformational change and maintains PKR in a closed conformation.

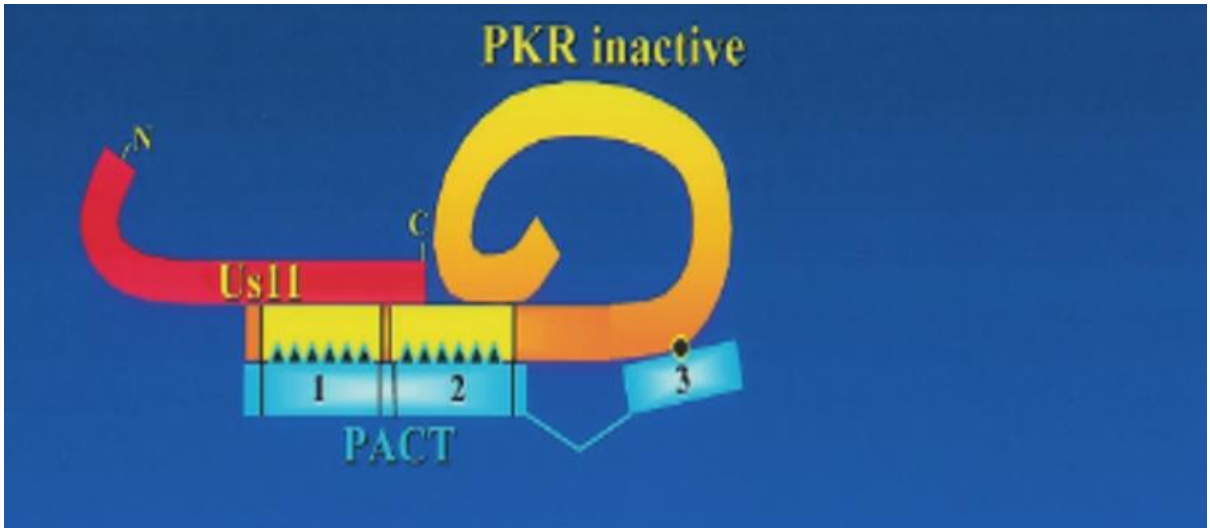

Figure 9: Model of Us11 inhibition of PACT-mediated PKR activation modified by *Peters et al., 2002.* The C-terminal domain of US11 viral protein binds to amino terminus site of PKR preventing the interaction between the domains 1 and 2 of PACT protein with PKR and at the same time, inhibiting the conformational changes, which normally activate PKR.

Instead of blocking its activation, HSV encodes ICP34.5 protein involved in the inhibition of PKR with a different mechanism than proposed before. ICP34.5, known as major determinant of neurovirulence, is detected during the early phase and its expression significantly increases during later phase of the viral infection. The immune evasive mechanism precludes the shutoff of protein synthesis by targeting phosphorylated eIF-2α rather than either PKR or double-stranded RNA. ICP34.5 recruits the phosphatase alpha to dephosphorylate eIF-2α, preserve the viral protein translation and indirectly block the PKR activity downstream its activation[87].

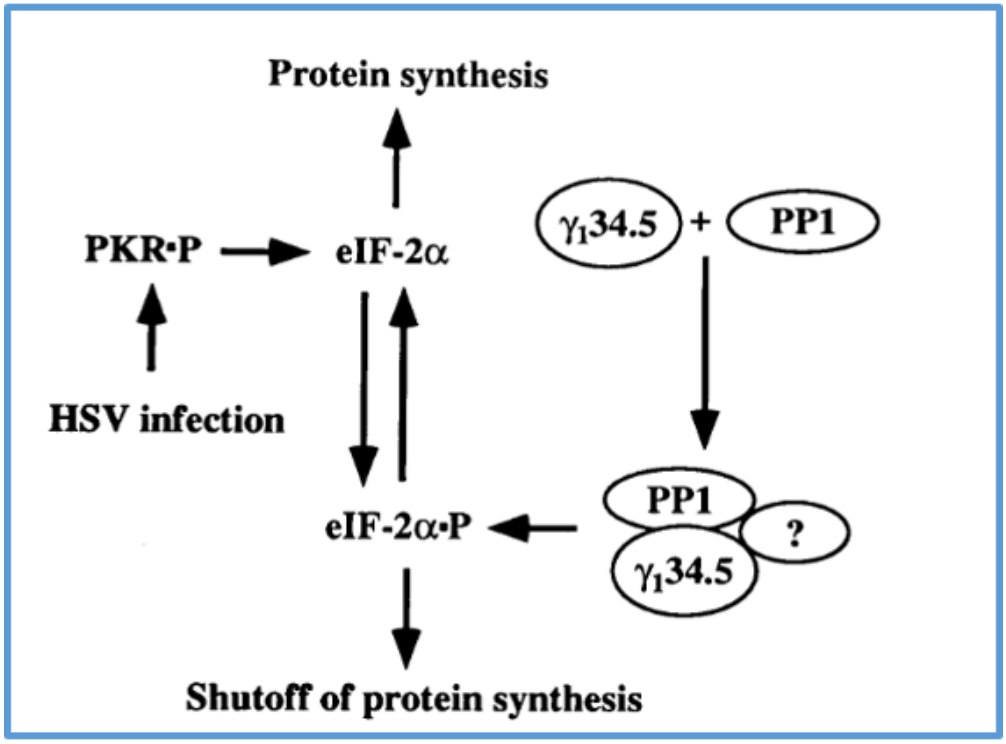

Figure 10: **Schematic representation of the regulation of protein synthesis by γ 34.5 in infected cells by *HE et al., 1997***. PKR is activated by HSV-1 infection and its downstream regulatory mechanism is blocked by γ34.5 viral protein which enrolls a phosphatase alpha enzyme to dephosphorylate eIF-2α and prevents the shut off of protein synthesis.

ICP34.5-mediated dephosphorylation of eIF-2α also leads to the inhibition of autophagy and other cellular stress responses. Lussignol and colleagues[88], demonstrated that both viral proteins, Us11 and ICP34.5, involved in PKR activity block, negatively regulate the autophagy process during the viral life cycle (Fig.10). Therefore, the action of one reinforces that of the other and the resulting shut off PKR signaling response is closely link to inhibition of autophagy induction, which represent a cellular mechanism against HSV-1 infection.

2.4. Regulation of the viral and cellular proteins expression by virion host shut off protein of HSV-1

An important defense against viral infection is represented by the block of proteins synthesis whose activation reduces the possibility to establish a productive infection. During viral infection, several viruses begin to accumulate viral proteins and to reduce the production of host proteins, progressively. This phenomenon, known as "host shutoff", is performed by VHS protein of HSV-1. Many viruses, including HSV-1, have developed many complex mechanisms to inhibit the PKR response, which is upstream of the activation of protein synthesis. Several years ago, it was showed that during HSV-1 infection the cellular protein synthesis is downregulated with a mechanism that involved virion host shutoff (VHS) protein of HSV-1. VHS is packaged to the virus as a tegument protein and released into the cytoplasm of infected cells, where it functions as an endoribonuclease and provokes the instability and degradation mRNA. The degradation mechanism has a dual purpose; on the hand, it served to beat time of sequential expression of viral proteins during HSV-1 cycle by accelerating the turnover of viral mRNAs and the viral proteins endogenous levels step-by-step[89]. Therefore, a sequential and coordinate cascade of events turns off and turns on the expression of three groups of viral proteins, designated as alpha, beta, and gamma proteins[90].

The RNase activity is an event tightly regulated during HSV-1 cycle. In particular, during the late phases of infection, VP16 and VP22 tegument proteins promote the accumulation and the packaging of VHS into virions. Instead, in the early phases of HSV-1 infection, it binds the tegument proteins pUL47 and moves to nuclear compartment. The association of VHS with UL47 in the nuclear compartment seems to preserve viral mRNAs from degradative activity defining the viral regulator mechanism responsible for gene cascade[91]. On the other hand, VHS switches the gene expression machinery to viral processes by degrading host mRNAs. The degradation of cellular mRNA during herpes simplex infection occurs with a selective manner. Esclatine, A. and collaborators[92] demonstrated that RNAs that are subject to VHS degradation contain AU-rich elements in the 3'UTR ends and are frequently found in mRNA that encode proto-oncogenes, nuclear transcription factors, and cytokines[,93,94].

Therefore, VHS mediates the degradation of both viral and cellular mRNAs with a mechanism not perfectly understood and probably based on its capability to working as an RNase or activate cellular enzyme with an RNase activity. In addition, the studies performed on the specific degradative action of VHS on RNAs of cellular proto-oncogenes, demonstrated that in presence of VHS the RNAs not containing ARE sequences are stabilized rather than degraded.

In contrast to stabilization of RNAs, which occurs in the cytoplasmic compartment, it was demonstrated that the AU-rich mRNAs can be degraded by VHS-RNase in either the nucleus or cytoplasm thanks to VHS capability to shuttle between the nucleus and cytoplasm. In addition, it was suggested that the VHS protein could be used in the suicide cancer gene therapy. Preliminary data, obtained by Hossein Bannazadeh Baghi and collaborators[95], showed a strong inhibitory activity in proliferation of HeLa and Human breast adenocarcinoma tumor cells transfected with a eukaryotic expression vector containing VHS. In addition, β2 microglubolin mRNA content, used as an indicator for total mRNA, showed a sharp decrease in both cell lines.

2.4.1. Role of VHS in the innate immune response mediated by PKR.

The model ‘’host shut off’’ adopted by VHS represents an immune evasion mechanism which affects the activation of PKR. However, to date, the real mechanism used by VHS to block PKR is not perfectly clear. Several years ago, it was proposed a new mechanism based on potential engagement of MEK protein, normally involved in the cell survival, in the PKR control. Indeed, by basing on the earlier results performed by Smith and collaborators[96], in which the activation of MEK, following HSV-1, correlated with suppression of activation of PKR, Sciortino and colleagues[1] analyzed the involvement of VHS in this regulatory mechanism (Fig.11)'. The VHS-null (ΔVHS) mutant virus was used to provide the important comparative informations about the regulatory role of VHS protein compared to wild type herpes simplex virus. In addition, the experiments were performed on cell line expressing a dominant-negative form of MEK (dnMEK), overexpressing a constitutively active form of MEK and parental HT1080 human fibrosarcoma cell lines.

The results demonstrated that whereas wild-type HSV-1 virus infection enhanced slightly the activation of PKR in cells expressing dnMEK, the ΔVHS mutant activated PKR in both the parental cell lines and those expressing dnMEK and even in the cells expressing constitutively active MEK.

This finding highlighted that VHS plays a significant role in blocking activation of PKR at early times after infection and associate to earlier results by Pasieka and colleagues[97], showing enhanced levels of phosphorylated eIF2a during ΔVHS infection.

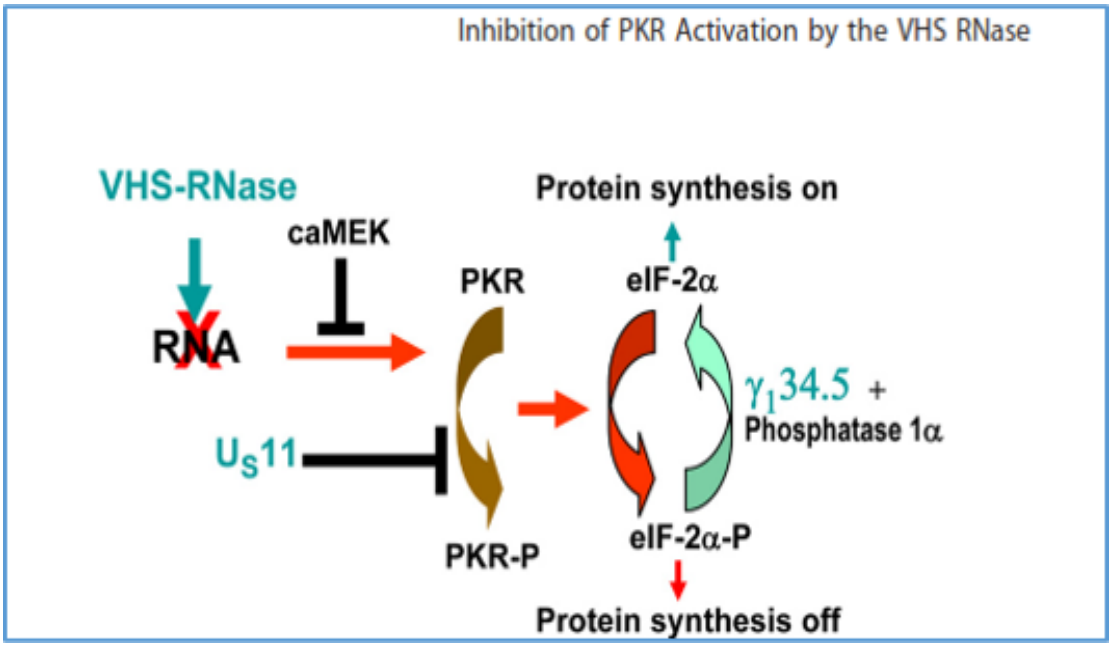

Figure 11: Schematic representations of the viral and cellular pathways that affect activation of protein kinase R (PKR) by *Sciortino et al., 2013*. The combination of different viral strategies induces the block of immunological response mediated by PKR, upstream and downstream of its activation. US11 block the switch of PKR from closed to open conformation, γ34.5 induces indirectly, the inhibition of phosphorylation of eIF-2α protein and VHS degrades the RNAs, which potentially activate PKR. In addition, the activation of MEK cellular protein plays a major role in blocking activation of PKR.

Recent evidences demonstrated that the PKR activation following viral infection is correlated with stress granules (SGs) formation. The SGs consist of aggregates of the translationally stalled mRNAs and associated 40S ribosomal subunits, translation initiation factors, and a variety of RNA binding proteins. They are considered storage depots containing untranslated mRNAs, which can be reintroduced in the protein synthesis circuit rather than degraded.

The functional importance of SGs in host innate responses is unclear and has primarily been examined in response to infection with RNA viruses. The Smiley's group established that PKR is required for SGs formation during infection with ΔVHS virus and that VHS is able to suppress SG assembly with a mechanism not fully understood but that could include the decrease of mRNA levels or alternatively downstream of stress kinase activation. Anyway, the PKR activation is intimately linked to SG formation and in the same time its action is potentiate during HSV-1 infection[98]. Taken together, these results showed that VHS helps HSV to evade host innate targeting mRNAs, triggering a global mRNA destabilization in infected cells and affecting one or more components of the cellular translation initiation machinery. In particular, seem that it directly binds the cellular translation initiation factor, eIF4H, and this interaction

serves to target VHS to sites of translation initiation on mRNAs[99,]. However, it is not perfectly clear if VHS mediates the degradation of both viral and cellular mRNA by working as an RNase or activate cellular enzyme with an RNase activity or if recruits other viral proteins directly or indirectly to improve its activity[100].

2.5. Conventional structural role of the HSV-1 tegument proteins associated to immune response regulation.

The HSV-1 virion structure consists of four elements: The core and capsid are composed of a double-stranded DNA genome and surrounded by an icosahedral capsid; The tegument is a layer between the capsid and the envelope; The envelope is the outer layer of the virion and is composed of viral glycoproteins and is shaped by the alteration of cell membrane[101]. The tegument occupies a significant part of the virion space. All tegument proteins are delivered inside the cell before the viral genome replication. Therefore, they function in the early stages of HSV-1 infection and play crucial roles in viral gene regulatory transcription, viral replication and virulence, viral assembly and even in the interaction of the virus with the host immune system[102]. HSV-1 contains more than 20 tegument proteins.

The most notable proteins include the α-trans-inducing factor (αTIF, VP16), the virion host shutoff (VHS) protein (UL41), and very large protein (VP1–3) proposed as major representative proteins of the tegument material. VP16 defined as a transcription activator to its essential function in viral infection and gene transcriptional regulation. Therefore, additionally its role as a structural component of the tegument compartment, VP16 induce the transcription of viral immediate–early genes as a result of its presence in the cellular environment. In addition, UL36 is associated to the release of the viral genome into the nucleus instead other tegument protein, such as UL31, US3, ICP34.5, UL36, UL37 and UL51 are required for regulating viral nuclear egress. The regulatory role of the tegument proteins in addition to structural function raised interest of several researchers on potential involvement of this protein in the immune response field.

2.5.1. HSV-1 protein kinases US3 and UL13: viral and cellular regulators.

When a viral genomic DNA enters into the nucleus, the VP16 viral protein first promotes the transcription of the immediate early proteins ICP0, ICP4, ICP22, ICP27 and ICP47. Once produced, ICP0 directs to nuclear compartment and provokes the disruption of nuclear matrix domains ND10, stimulating the viral infection and the early gene and late gene transcription activation. About half of the HSV-1 encoding tegument proteins play essential roles in viral transport and maturation. US3 and UL13 viral protein are involved in these processes but in the same time their kinases enzymatic nature makes them multifunctional viral proteins able to modulate the host metabolism and shut down the host antiviral mechanism.

Protein kinases appear to play regulatory roles in primary envelopment as well as development occurring at the outer nuclear membrane or endoplasmic reticulum. Serine/threonine kinase US3 is a multifunctional viral protein with an amino acid sequence highly conserved in the subfamily *Alphaherpesvirinae*. It plays a role in several processes including egress of virus particles from the nucleus, modulation of the actin cytoskeleton to promote the virions spread and inhibition of apoptosis[103]. UL34, ICP22, Us9, UL12, cytokeratin 17, Bad, and Bid have been reported to be putative substrates for US3[104]. Its importance in the structural architecture of the virion depend on its kinase activity through which US3 phosphorylates UL31 and UL34, two critical regulators of capsid budding from nucleus to endoplasmic reticulum, thereby facilitating virion egress. The HSV-1 vdUTPase, encoded by the UL50 gene, is one of the proteins involved in the nucleic acids metabolism targeted by US3. The US3 protein phosphorylates vdUTPase at Ser-187 contributing to efficient HSV-1 replication[105]. US3 has been shown to repress histone deacetyltransferases and enhance viral gene expression via phosphorylating histone deacetylase (HDAC-1) and HDAC-2 thereby reducing viral genome silencing. In addition, US3 phosphorylates the envelope glycoprotein B (gB), probably to direct it to the cell surface and redefines the complete structure of the viral envelope. The identification of other substrates could characterize the mechanisms by which US3 regulates different intracellular processes and highlight its potential and undiscovered functions in viral replication.

The survival of HSV-1 into the cells depends on the capability to overcome and manipulate the immune response. HSV-1 encodes two viral proteins, ICP47 and virion host shutoff protein (VHS) that inhibit the immune response mediated by $CD8^+$ cytotoxic T lymphocytes (CTLs) involved in the clearance of herpesvirus-infected cells.

Normally, the CTLs recognize and present viral antigens on the major histocompatibility complex class I (MHC-I) to start a specific immune response against pathogens. It has been demonstrated that also US3 is involved in the downregulation of cell surface expression of MHC-I molecules[106]. In addition, Wang and collaborators [107] demonstrated that HSV-1 protein kinase US3 inhibits NF-κB activation and decreases the expression of inflammatory chemokine interleukin-8 (IL-8). US3 hyperphosphorylates p65 at serine 75 to inhibit NF-κB activation and then represents an indispensable viral mechanism to abrogate the nuclear translocation of p65.

Recently, US3 protein kinase was proven necessary and sufficient to suppress extracellular signal regulated kinase (ERK) activity and subvert host mitogen-activated protein kinase (MAPK) signaling pathways[108]. The catalytic activity of US3 is tightly regulated by autophosporylation events on Ser-147 residue and by phosphorylations mediated by UL13, another HSV-1-encoded protein kinase. Proteins phosphorylation by protein kinases is one of the most common and effective posttranslational modifications by which viruses auto-regulate and regulate the cellular targets[109]. However, the biological significance of UL13-mediated phosphorylation of US3 for the regulatory activity of US3 has not been determined. One possibility is that phosphorylation of US3 by UL13 plays a partial role in the regulation of the basal US3 protein kinase.

The UL13 protein is a 56 kDa polypeptide with amino acid sequence conserved in the *Herpesviridae* family. It is expressed with late kinetic, but it is packaged into the tegument of virus particles and is thus present from the onset of infection. UL13 is the second known serine/threonine protein kinases of HSV-1, whose kinase activity has been shown to promote viral replication because regulates the expression of viral proteins. Specifically, the HSV-1 UL13 kinase phosphorylates itself and US3 protein kinase, tegument proteins VHS, UL49, VP11/12, glycoproteins I and E, and ICP0, as well as the cellular proteins p60, suppressor of cytokine signaling-3 (SOCS3), and translation elongation factor 1delta. In addition, UL13 kinase has been proposed to play a role in the posttranslational modification of UL42, which encodes the DNA polymerase processivity factor[110].

An important study, performed on both UL13 and US3 kinases in order to examine their complementary involvement in the virus egress, demonstrated that the HSV-1 ΔUS3/ ΔUL13 mutant exhibited defects in assembly and release of virions[111]. However, the failure in the expression of UL13 kinase provoked more profound effects on viral egress in several cell lines than the loss of US3 kinase suggesting an unequal contribution from each of the kinases to viral egress. Nevertheless, combined activity of the HSV-1 protein kinases played an important role in viral replication indicating that both HSV-1 protein kinases act in a cooperative manner to

promote viral replication. In the context of immune response, it has been previously discussing that interferon signaling pathway y is activated by HSV-1 infection in order to inhibit the viral replication in a very early stage, mainly during the transcription of alpha genes. In this regard, Shibaki and collaborators [112]showed that deletion of the UL13 gene enhances the susceptibility to type I IFN proposing an immunological escape mechanism correlated to kinase activity of UL13.

CHAPTER III

Intracellular Signal Transduction Cascades activated by Carbon nanomaterials

Intracellular signaling is an important mechanism by which cells can sense environmental stimuli and trigger several cellular responses, including modification of gene expression, mRNA splicing, expression and modification of proteins. Intracellular signal transduction cascade begins from the stimulation of extracellular receptors and concludes with biological response. Whether the triggered signal is disadvantageous for the cellular equilibrium, a wide variety of cellular events such as cell cycle arrest, apoptosis, inflammation and induction of antioxidant enzymes could be activated in order to reestablish an advantage cell condition. All of these cellular events result from the activation of different cellular pathway and are realized by biological molecules. The aim of this signaling network is to save the cells and spread the specific triggered signal to neighboring cells. In the context of cancer disease or whatever disorder, several intracellular pathways are modified and activated in negative way. In the same time, posttranslational modifications, exposition of phosphorylation sites in the activation loop and the subsequent persistent activation of the proteins, make cell-signaling proteins principal actors in cancer and cellular disorders and target for new therapeutic approaches.

3.1. New findings on intracellular network activated by funzional graphene nanomaterials

Nanomaterials include particles in the nanometer range whose chemical structure make them able to deliver a wide spectrum of therapeutic compounds. Carbon-based nanomaterials are recently discovered and include nanodiamonds, fullerenes, carbon nanotubes, graphene, and carbon nanofibers. In the last years, the graphene-based materials are deeply studied for their application in several fields: electronics, energy, bioremediation, nanomedicine as potential platforms for multifunctional biological applications.

The graphene-based materials include few layer graphene (FLG), graphene oxide (GO), reduced graphene oxide (G-Red) and functionalized graphene (f-G) characterized by high availability of surface functional groups, good biocompatibility and versatile biofunctionality.
The intracellular internalization of graphene-based materials triggers a wide variety of cellular response mediated by activation of intracellular signaling network, which affects the cell environmental, negatively or positively. The expression of cytokines, growth factors and genes regulatory proteins emerges from the ability of nanomaterials to modulate cellular pathway such as apoptosis, cell cycle, inflammation and metabolic processes[113]. Therefore, nanomaterials delivery can potentially provide to interfere with diseases or disorders closely related to defects in specific intracellular pathway[114,115]. The chemical modifications on the graphene-based materials surface enhance their performance in the biomedical application. Some of modifications, such as the functionalization of graphene-based materials with polyethylene glycol (PEG), minimize the immunological response and increase the cellular stability. In another case, for example the functionalization with hyaluronic acid-based polymers, guarantees a controlled delivery multiple therapeutic agents to intracellular target improving the specificity [116,117].
The functionalization with cationic polymer such as polyethylenimine (PEI) increases the transfection efficiency of these novel nanocarriers enhancing their biocompatibility and reducing the cytotoxicity effect. In the context of biological response, the decoration of graphene-based materials influences the cell growth, the ROS release or the secretion of nitric oxide (NO) allowing to the differentiation of cancer cells from normal cells[118,119,120]. On the other hand, the graphene functionalization promotes the drug delivery and increases the tissue specificity in order to enhance the drug bioavailability and overcome multidrug resistance in the conventional cancer therapy[121,122]. The GSH levels reduction, the lipid peroxidation, the alteration of antioxidative enzyme gene expressions (SOD1, SOD2, CAT, GSTA1, and GSTA4)[123] and mitochondrial depolarization[124] are induced by graphene-mediated

overproduction of ROS. Several groups have been demonstrated that the ROS-induced high toxicity depends on the size of graphene-based materials and surface functionalization demonstrating that the reduction of oxygen functional group on grahene surface minimizes the citotoxicity and increases the biocompatibility[125].

The ROS and NO production resulted on the downstream activation of transcriptional factor NF-kb, proinflammatory cytokines (TNF-α, IL-1β, or IFN-γ) and cellular kinases involved in the promotion of cell proliferation. Studies *in vivo* have been demonstrated that G-Red-dextran enhanced immunostimolatory capability of dendritic cells (DCs) triggering the inflammatory cytokines release and the subsequent activation of cytotoxic T cells[126]. The modulation of immune response related to graphene exposition was studied in primary murine and immortalized macrophages. Zhou and collaborators[127] have demonstrated that lower concentrations of pristine graphene increase the transcriptional levels and the expression of cytokines and chemokines which activate proinflammatory signals and shut off their expression to avoid the effects of an over activation related to graphene exposition. The proinflammatory stimuli were activated by upstream interaction between Toll-like receptor (TLR) and graphene sheets, which stimulates NF-kB nuclear translocation and promotes the transcription of proinflammatory gene. The proinflammatory cytokines release influences the neighboring macrophages morphology by inducing an F-actin rearrangement resulting in a limited macrophages adhesion to inflammatory site. In addition, the clearance of infections and the removal of cellular debris is macrophages-mediated. The graphene-exposition limits the phagocytosis ability and opens a new prospective on the use of graphene on the regulation of inflammatory disease and tissue lesions due to unbalanced production of inflammation mediators[127].

Current knowledge has been demonstrated that the graphene nanostructure triggers in vitro a programmed cell death mechanism in dose-dependent manner. During earlier events of apoptosis, the translocation of phosphatidylserine (PS) occurs from inner to outer leaflet of plasmatic membrane. The fluorochrome-labeled Annexin V analysis allow to detecting, through flow cytometry assay, the interaction between Annexin V and the PS exposed on outer surface. Tanveer Tabish and collaborators has been shown that lung cancer cells exposed to lower concentration of graphene exhibit late stage of apoptosis, rather than early stages, with a consequent formation of the apoptotic bodies and damage of cell membrane[128].

Instead, Kang and colleagues performed a comparative analysis between intracellular molecular signaling activated by exposition of GO and G-Red on neuronal cell lines (PC12) showing significant levels of apoptosis induced by higher doses GO rather than G-Red[129]. Probably, the differences related to chemical propriety impact on the molecular mechanism activated by

graphene exposition. In addition, extrinsic or intrinsic death signals stimulate the release and the activation of mediators of apoptosis. In particular, seems that the exposition to graphene increases the mitochondrial membrane permeability provoking the release of apoptosis inducing factor.

Li Y. and collaborators[130] have demonstrated the mitochondrial outer membrane depolarization after graphene exposition and the increment of expression levels of apoptotic effector enzyme such as caspase-3. Graphene treatment promotes the accumulation of cleaved form of nuclear protein PARP, substrate for caspases and biomarker for the activation of cellular death programs. The accumulation of pro-apoptotic proteins, Bax and Bim, the consequent mitochondrial permeabilization, the release of cytochrome c from mitochondrial to cytoplasmic side, and the downstream activation of caspase 3 occurs following pristine graphene induction and according to a mitogen-activated protein kinase (MAPK)-dependent mechanism[130]. The involvement of the MAPK cascade occurs also in the context of cell cycle and among the MAPKs, the ERK protein interacts with a network of downstream kinases and regulate the cellular outcome. Neuronal ERK signaling activation was detected in response to GO in nematode *Caenorhabditis elegans*. In addition, Kang et al. have been demonstrated [129] that GO and G-Red seem to be able to arrest cell cycle progression in tumor neuronal cell lines and shape the ability of the cell to divide normally by decreasing MEK1/2 and ERK phosphorylation state following GO and G-Red treatment.

3.2. Endocytosis mechanisms mediated by nanoparticles.

Generally, nanocarriers interact with the cell membranes and enter into the cells by endocytosis mechanisms. Endocytosis is the major transport-mechanism used to outcome the plasmatic membrane. All type of phagocytic cells (monocytes, macrophages and neutrophils) incorporate large particles through phagocytosis mechanism, instead the rest of cells activates different pinocytosis processes classified according to the proteins involved. Pinocytosis is present in all types of cells in four forms, such as clathrin-dependent endocytosis, caveolae-dependent endocytosis, macropinocytosis, and clathrin- and caveolae-independent endocytosis (Fig.12).

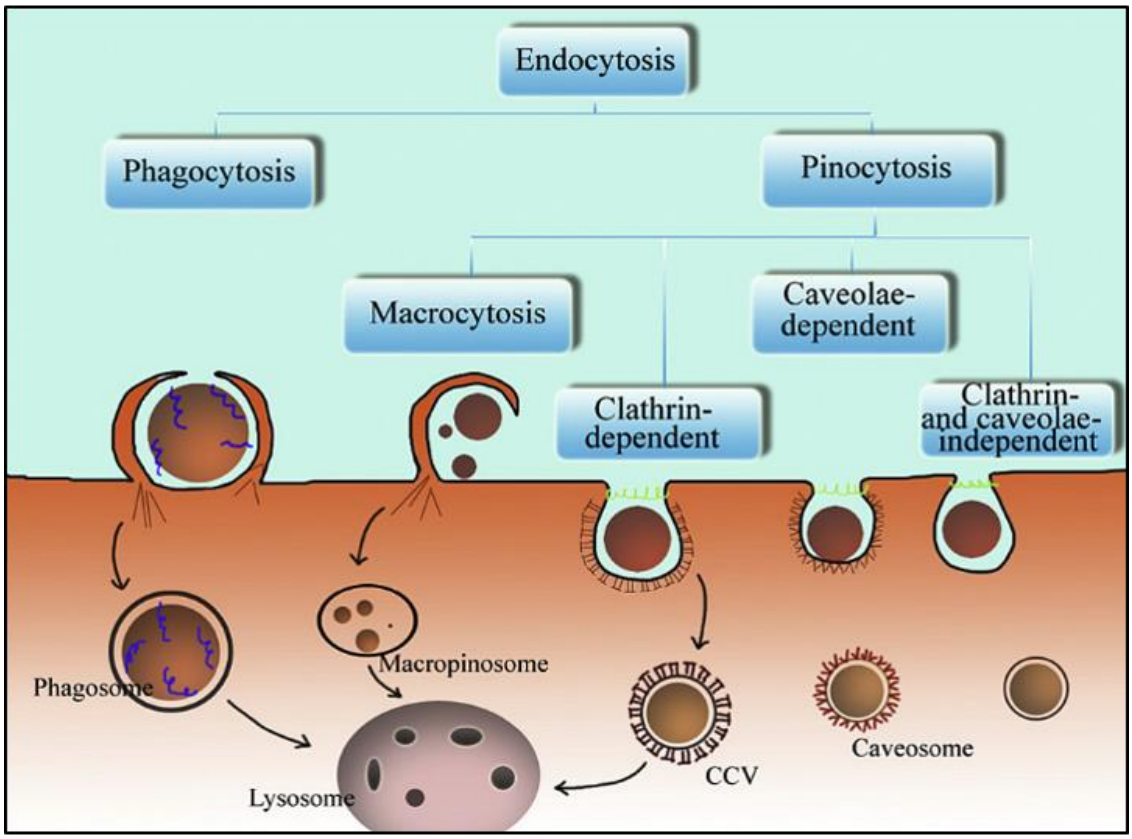

Figure 12: Classification of endocytic mechanisms by *Longfa Kou et al., 2013*. The intracellular trafficking is regulated by specific internalization mechanism of several particles. The size, the surface charge and the shape define the endocytosis mechanism used to cellular uptake. CCV indicates clathrin coated vesicle.

The clathrin-dependent endocytosis and the caveolae-dependent endocytosis represent the most common entry mechanisms used by nanoparticles. In the first condition, the internalization is guaranteed by the interaction between nanomaterials and surface receptors called clathin-1, which wraps the nanoparticle and form a clathrin-coated vesicles[131].

Normally, the destination of vesicles depends on the cellular target, for this reason, the functionalization of surface of nanomaterials with specific ligand facilitates the delivery to target cells and the interaction ligand-receptors necessary to induce a biological response. This type of endocytosis mechanism could be blocked by using inhibitory molecules, such as chlorpromazine, a hypertonic sucrose or potassium depletion.

The chlorpromazine induces the irreversible membrane translocation of clathrins and other adapters proteins to endocytic vesicles. The hypertonic sucrose traps clathrin in microcages and the potassium depletion induces the clathin aggregation[132]. The second endocytosis mechanism is based on the formation of flask-shaped vesicles following interaction between nanoparticles and specific receptors exposed by caveolin proteins. These vesicles move along the microtubules network and fuse with other vesicles to form caveosomes or multivesicular bodies. methylb-cyclodextrin (MbCD), filipin, nystatin and cholesterol oxidase can be used as the inhibitors for caveolae dependent endocytosis.

The use of the inhibitors represents one of the most common approachs to confirm whether clathrin-dependent endocytosis rather than caveolae-dependent endocytosis is employed by the nanomaterials to entry into the cells. In addition, seems that the size, the charge and the shape of nanomaterials can be decisive to activate a specific endocytosis pathway. The size of vesicle involved in clathrin mediated endocytosis is about 100 nm instead around 60-80nm for caveolae-mediated mechanism. Larger particles can be engulfed via macropinocytosis. Another physicochemical characteristic of nanoparticles, which affects the internalization, is the charge on surface responsible for a rapid or slow cellular absorption. In fact, considering that the cellular membrane charge is negative, cationic nanoparticles induce a strong interaction with the cells, which promotes an efficient and rapid internalization. On the contrary, the anionic nanoparticles may be internalized through the interaction with the positive site on the membrane proteins and neutral particles establish hydrogen bond, which in both cases lead to less absorption. In addition, seems that the particles shape can be important in the drug delivery. In general, a proportional shape facilitates the intracellular nanoparticles uptake and promotes an efficient delivery of the cargo.

3.3. Functionalized graphene selects lysosomal compartment

The intracellular uptake of nano-compound triggers the activation of intracellular trafficking mediated by endocytic vesicles showing the compartmental flux and the final destination of internalized materials. Studies on subcellular localization have showed a lysosomal compartmentalization of graphene oxide (GO)-based nano assemblies and functionalized by polyethyleneglycol (PEG). Often, the lysosomal localization is tightly correlated to the autophagy process indeed several studies has been reported the induction of autophagy process in different cell lines such as CT26 colon cancer cells and RAW264.7 macrophage cells. Instead, Li Y. and collaborators, have showed that the distribution of graphene oxide coated with layer-by-layer assembled polyelectrolytes is limited to cytoplasmic environment and in particular to the lysosomal side rather than mitochondria side and not involves the autophagy induction[133]. Contrarily, Jin P. and colleagues have reported high autophagy levels following graphene exposition promoting the degradation of misfolded protein inducing Huntington's disease and not involving a degradation mechanism mediated by ubiquitin-proteasome system[134].

Combined approaches allow discriminating the accumulation of autophagosomes from the activation of autophagy flux as a consequence of graphene-based nanomaterials exposition because the accumulation autophagosomes indicates either increased autophagosome synthesis or decreased autophagosome turnover. The biological marker to identify autophagy is the microtubule associated protein 1A/1B-light chain 3 (LC3). During autophagy, cytosolic LC3-I is converted to LC3-II and associates to the autophagosomal membrane. The increased levels of LC3II protein, the GFP-LC3 dots number and the treatment with chemical autophagy inhibitor indicate that, following graphene treatment, the autophagosome accumulation occurs in HeLa cells. To monitor additionally, the autophagic flux activation, the p62 expression levels, normally reduced during autophagy process, are evaluated demonstrating that following graphene exposition the accumulation of LC3II on the autophagosomal membrane corresponds to the accumulation of p62 protein. Therefore, the autophagy induction mediated by graphene exposition not evolves in the degradation of engulfed contents in the autolysosome vesicles.
Furthermore, Ji X. and collaborators demonstrated that the increased accumulation of autophagosome after graphene oxide quantum dots treatment results by the block of autophagy flux due to low degradative activity of lysosomes[135].

In another case, Lin K.C. and colleagues recently found the non-canonical activation of autophagy[136]. It has been demonstrated, that graphene nanosheets loaded with anticancer drug cisplatin induce the initiation of autophagy, which precede cellular death. In particular, occurs the nuclear translocation of both LC3 autophagy marker and chemiotherapic drug.

This translocation shuts off the late autophagy event and activates the cell death signals. Deep and elaborate studies on the molecular dynamics related to graphene nanomaterials exposition are still necessary in order to understand whether the graphene endosomal trafficking concludes with lysosomal compartmentalization or involve in the recycling of unengulfed materials. The accurate study on molecular pathways triggered by engineered graphene-based nanocarriers is necessary to remark their importance role as an anticancer platform in the biomedicine able to modulate cancer cellular micro-environmental.

Aim of the work

The concept of gene delivery was developed in 1963 and is based on the introduction of genetic materials into the cells to compensate the abnormal genes and restore the function of misfolded proteins[6]. The acquired knowledge after the completion of the Human Genome Project and the support of sophisticated molecular biology techniques allowed to the treatment of genetic diseases by introducing non-mutated gene or by stimulating the immune response directly against cancer cells. To date, the primary challenge for gene therapy is to develop carriers, commonly called vectors, genetically engineered, that facilitate gene transfer to target cells without degradation of the delivered gene. Therefore, clinical and research studies have been performed by using viral and non-viral vectors. The main advantage of the use of the viral vectors is the natural selectivity for tumor cells[3,5,48.] The interaction virus-host triggers a productive immunological response, which often is not limited to tumor environmental. The non-viral vectors represent an optimal alternative to viral vectors due to low immunogenicity and low toxicity but at the same time the size, the surface charge and the instability of the complexes in the extracellular spaces attenuate the biological response and can restrict their use in cancer therapy[58,60].

The knowledge of the intracellular signaling pathways triggered by interaction host-vector could be helpful to design efficient viral and non-viral vectors for the cancer treatment. The success of the oncolytic herpes simplex virus-based therapy requires deep knowledge about the interaction between virus and host. The oncolytic virus induces an anti-tumor immunity through the stimulation of serum factors, cytokines and chemokines production, recruitment of cells involved in the innate and adaptive immune response[40]. Once HSV enters into tumor cells, it replicates, kills the tumor cells, and subsequently propagates within the tumor microenvironment triggering immunological signals, which amplify the death signal. At the same time, it expresses proteins that inhibit both the induction and activity of the immunological responses, allowing the virus to evade the host anti-viral immune surveillance mechanisms[66].

In the context of cancer disease, the activation of immune-evasion signals should shut down the immunological response within tumor environmental. Based on this, a deep molecular research on the interaction between host proteins, regulators of immunity, and viral proteins, responsible for the immunity escape, could drive in the future, to design an oncolytic virus able to manipulate immune response rather than to be manipulated.

An important molecular pathway, activated during HSV-1 infection and involved in the regulation of antiviral response, is mediated by PKR protein. PKR is a potent pro-apoptotic protein implicated in the activation of antiviral response that acts by rapidly eliminating infected cells to prevent viral spread. It phosphorylates the alpha subunit of eukaryotic initiation factor-2 (eIF2) and blocks the protein synthesis upon viral infection[77,78,79].

PKR is activated by dsRNA originated by RNA viruses, or by dsRNA replicative forms that represent obligatory intermediates for the synthesis of new genomic RNA copies[79]. As an alternative, the DNA viruses produce overlapping mRNA transcripts that can mimic dsRNA which are responsible for PKR activation in infected cells. During viral infection, several viruses begin to accumulate viral proteins and to reduce the production of host proteins, progressively. This phenomenon, known as "host shutoff", is performed by VHS protein of HSV-1[137]. VHS is packaged to the virus as a tegument protein and released into the cytoplasm of infected cells, where it functions as an endoribonuclease and provokes the instability and degradation mRNAs[99,100]. Original data obtained by Sciortino *et al.,* (2013)[1] showed an accumulation of p-PKR on HT1080 cell lines infected with deleted virus for VHS protein suggesting that VHS is involved in the regulation of PKR with a mechanism not yet understood but that could be related to its endoribonuclease function.

This thesis work tries to complement and extend first; the studies reported by Sciortino et al, and in particular tries to analyze the involvement of additional tegument proteins in the regulation of PKR. About half of the HSV-1 encoding tegument proteins play essential roles in viral transport and maturation. US3 and UL13 viral proteins are involved in these processes but at the same time, their kinases enzymatic nature makes them multifunctional viral proteins able to modulate the host metabolism and shut down the antiviral mechanism[109,111]. For this reason, it has been investigated the role of US3 and UL13 tegument viral proteinsin the regulation of PKR transcripts and in the control of p-PKR expression levels. In general, protein kinases are tightly regulated by phosphorylation events and, at the same time, phosphorylate other proteins by inducing posttranslational modifications. US3 and UL13 of HSV-1 induce the phosphorylation of viral and cellular proteins and the identification of further substrates could be helpful to understand the molecular pathways in which they are involved. To date, there is a lack of information on how these viral protein kinases are co-regulated during HSV-1 infection. For this reason, it has been investigated the interplay between the examined viral tegument proteins by evaluating the proteins expression and the transcripts levels of VHS, US3 and UL13 during HSV-1 replication.

It has been used a combined approach of infection and transfection experiments performed through, respectively, deleted virus for the *vhs*, *us3* and *ul13* genes and plasmid DNA encoding for VHS, US3 and UL13 proteins in order to verify whether they regulate with each other and consequently, control the PKR activation. In addition, in *vivo* studies with PKR-/- .compared to parental cell lines have been performed to analyze the role of PKR during HSV-1 replication by evaluating the expression of cascade of immediate-early (α), early (β), and late (γ) genes, the quantification of viral DNA and the viral titers.

The acquired knowledge about the cellular proteins target of PKR highlight the its multiple roles in the signal transduction processes. Additionally, to its translation regulation function, the PKR protein is also involved in differentiation and control of cell growth, apoptosis, deletion of the tumor, and RNA-interference. In particular, it has been demonstrated that PKR interacts directly with the C-terminal part of p53 and phosphorylate p53 on the Ser392 residue. The p53 protein responds to a wide range of stress factors through regulation of a variety of cellular pathways, such as apoptosis, cell cycle, cellular senescence, DNA repair, autophagy, and innate immune control[138]. Viral infection represents a type of cellular stress and in the context of HSV-1 infection, it has been demonstrated that p53 plays as positive and negative regulator in HSV-1 replication[139]. Previous studies have demonstrated that p53 promotes the HSV-1 replication and that, at the same time, downregulates the ICP0 expression. It seems that viruses had developed regulatory mechanisms to utilize one or more of p53's functions to regulate some cell components for efficient viral replication. Based on these data, the transcripts levels of p53 have been analyzed during HSV-1 infection in PKR-/- and parental cell lines and infection with mutant viruses for VHS, US3 and UL13, have been performed to determinate the tegument viral proteins contribution in this cellular pathway. The PKR control mediated by viral proteins of HSV-1 and the potential role of PKR as a target in cancer therapy, remarks the importance to develop HSV-1-based vectors, able to regulate positively or negatively PKR and modulate the cancerous cellular environmental.

The intracellular delivery needs genetically engineered carriers, which facilitate gene transfer to targeted cells without degradation of the delivered gene. To date, it is possible to accost to viral vectors the chemical platforms, engineered to facilitate the safe and specific drug and gene delivery. Cationic lipids, possessing hydrophilic head and hydrophobic tail, can condense DNA/RNA molecules via electrostatic interactions protecting them from enzymatic/non-enzymatic degradation mediated by intracellular components[58,59]. Functionalized fullerenes can be used as useful nanocarriers for drug and gene delivery because of their optimal sizes and hydrophobic surface, which enable easy crossing of cell membranes and release the drug into the cells[61].

In *vivo* studies have showed that PEGylated nano-graphene sheets have high tumor uptake, which results to the ultra-efficient tumor ablation, without adverse effects[63]. The hardest challenge in the construction of a chemical platform, as potential vector in gene therapy, is to produce a nano-vector able to delivery and release the loaded compound without toxicity effect for the cells. At the same time, it is important to develop a chemical platform able to be conjugated with different compounds, such as drug and genes and ligands, to increase the tissue specificity and the biological response.

In this context, the second part of this thesis work proposes an investigation of intracellular signaling pathway triggered by two types of carbon-based platforms, developed as potentials non-viral vectors. It has been evaluated the intracellular uptake mechanisms, the toxicity and the drug and gene delivery by studying the expression of proteins involved in a wide range of molecular pathways, such as cell cycle regulation and autophagy.

The importance of the interactions between host and vector is defined by thick network of signals, which exchange with each other and that influence the success of gene therapy. Therefore, on the hand, the study of HSV-1 viral proteins and of interplay between viral teguments proteins and host immune response could be useful to define new retargeting approaches in the HSV-1 oncolytic virus. On the other hand, efficient and safe vectors that protect DNA from nuclease degradation and facilitate its uptake with high transfection efficiency could be used to gene therapy in several cancer diseases.

CHAPTER IV

4.1. Materials and Methods

4.1.1. Cell culture.

Cell lines were originally obtained from the American Type Culture Collection (ATCC). Vero cell lines were propagated in Eagle's Minimum Essential Medium (EMEM, Lonza, Belgium), supplemented with 6% fetal bovine serum (FBS) (Euroclone), 100 U/ml penicillin and 100µg/ml streptomycin mixture (Lonza, Belgium). HEp-2 cells (human larynx epidermoid carcinoma cell lines), PKR-/- derived from HEp-2 parental cell lines, were grown in Roswell Park Memorial Institute (RPMI) 1640 medium (Lonza, Belgium) supplemented with 10% of FBS, 100 U/ml penicillin and 100µg/ml streptomycin mixture. 293T (human embryonic kidney cell line) cells were maintained in Dulbecco's Modified Eagle's Medium (DMEM Lonza, Belgium) supplemented with 10% FBS, 100 U/ml penicillin and 100µg/ml streptomycin mixture. SHSY5Y (epithelial neuroblastoma cell lines) cells were grown in MEM medium supplemented with fetal bovine serum to a final concentration of 10%, 100 U/ml penicillin and 100µg/ml streptomycin mixture, 15% of Non-Essential Amino Acid Solution (NEAA) 1X and 20mM of L-Glutamine. All cell lines were grown at 37 °C in a 5% CO_2 incubator.

4.1.2. Viral infection.

HSV-1 strain F is a prototype HSV-1 strain kindly provided by Professor Bernard Roizman (University of Chicago, USA). HSV-1 mutant viruses R2621 (deleted virus for *vhs* gene)[140], R7041 (deleted virus for *us3* gene)[141], R7356 (deleted virus for *ul13* gene)[142] were generous gifts from Professor Bernard Roizman. ΔUL49, deleted virus for *ul49* gene, was generated by Sciortino and colleagues as described elsewhere[143]. Viruses stocks were produced and then titered in Vero cells. The experimental infections were carried out by exposure of all cell lines to the wild type and/or mutant HSV-1 viruses at the multiplicity of infection (MOI) of 1 and/or 10, according to the experimental design. The absorption of the virus was carried out for 1h at 37 °C with gentle shaking. After infection, the supernatant was replaced with fresh culture medium, and then the infected cultures and related controls were incubated at 37 °C, under 5% CO_2, and collected at the established times of the experimental design.

4.1.3. Standard Plaque Assay.

The infected samples were frozen and thawed three times and serial dilutions were prepared. Confluent monolayers of Vero cells were cultured in 12 multiwall plates and were infected with 100µl of each dilution. The plates were incubated for 1 h at 37 °C with gently shaking. Then viral inoculum was removed and monolayers were covered with Dulbecco's modified Eagle's medium containing 0.8% methylcellulose. After 3 days, the cells were fixed, stained with crystal violet, and visualized at 10x magnification with an inverted microscope (Leica DMIL) for plaque detection.

4.1.4. Transient transfection.

293T cells were transfected with the plasmids pVHS, pVHSm, pUS3, pUL13, pUL48 and pUL49, expressing the wild-type VHS, nuclease-defective mutant VHS, US3, UL13, UL48 and UL49 open reading frames (ORFs), respectively, as described elsewhere[144,145,146]. The plasmids pcDNA 3.1 (Invitrogen) and pCMS-EGFP (Clontech) were used as a controls. A total of 5×10^5 cells were seeded in 6-well plates in the presence of DMEM medium supplemented with 10% FBS and 100 U/ml penicillin and 100µg/ml streptomycin mixture. The next day, the medium was replaced with fresh medium without serum and antibiotics. 1.5µg of each DNA plasmids, reported above, was incubated with Reagent Plus (Invitrogen) in OptiMEM separately, for 20 min at RT. Lipofectamine (Invitrogen) was then added to the mixture and the two solutions were incubated at RT for 30 min. The DNA-Lipofectamine mixture obtained was then slowly added to cultured cells and incubated for 4h at 37°C. The medium was then replaced with OptiMEM supplemented with 10% FBS. After 48h/72h, the cells were collected and processed for immunoblot analysis.

4.1.5. Protein extractions and immunoblot.

Immunoblot assay was carried out to evaluate the accumulation of both viral and cellular proteins. Total proteins were extracted by lysing cells in SDS sample buffer 1X (62.5 mM Tris-HCl pH 6.8; DTT 1 M; 10% glycerol; 2% SDS; 0.01% Bromophenol Blue) and analysed for protein determination using a Qubit™ Protein Assay Kit (Invitrogen™). An equal amounts of protein extracts was subjected to Sodium dodecyl sulfate-polyacrylamide gel electrophoresis (SDS-PAGE) and transferred to nitrocellulose membranes (Bio-Rad Life Science Research, Hercules, CA).

The membranes were incubated overnight at 4°C with the appropriate primary antibody and then probed with secondary antibodies at room temperature for 1h. Protein bands were visualized by using Immobilon Classico Western HRP substrate (Merk, Millipore) and Super

Signal West Pico (Thermo Scientific, Rockford, IL) as a chemiluminescent substrates. Quantitative densitometry analysis of immunoblot band intensities was performed by using the TINA software (version 2.10, Raytest, Straubenhardt, Germany).

4.1.6. Antibodies.

Polyclonal antibody against the housekeeping gene GAPDH was purchased from Santa Cruz Biotechnology. Antibodies to the viral proteins ICP0 (sc-56985), UL42 (2H4) (sc53333) and PKR (A12) (sc393038) were purchased from Santa Cruz Biotechnology (Santa Cruz, CA). Anti-PKR (phospho-T446) (ab 32036) was purchased from Abcam (Cambridge, England). Antibodies against the viral proteins Us11, VHS and US3 were kindly provided by Professor Bernard Roizman. Secondary antibodies anti-rabbit and anti-mouse IgG conjugated to peroxidase were purchased from Merck Millipore.

4.1.7. Reagents.

Polyinosinic-Polycytidylic acid [Poly (I:C)]_was used to induce activation of PKR and was provided by Sigma Aldrich (P1530). 293T cells were transfected as described above and 24h post transfection the cells were treated with 10µg/ml of Poly (I: C) diluted in OptiMEM. Samples were then collected at indicated time post transfection to perform immunoblot analysis. Actinomicin D (A9415) and Cycloheximide were purchased from Sigma-Aldrich.

4.1.8. RNA extraction and Reverse Transcription.

Total RNA was extracted using TRIzol® (Life Technologies) according to the manufacturer's instructions. Total RNA was DNase-treated before cDNA transcription as follows: 20-50µg of RNA were incubated at 37 °C for 2h with 5µl 10X DNase I Buffer, 2µl Recombinant RNase-free DNase I (10U) (2270A TaKaRa, Dalian, China) and RNase inhibitor (20U) (N251A Promega). Heat treatment was performed to inactivate the recombinant DNase I treating samples with 2.5µl EDTA 0.5 M for 2 min at 80°C.

Samples were then incubated with 10µl sodium acetate 3 M and 250µl cold ethanol at -80 °C overnight. Next, the RNA pellet was precipitated by centrifugation at 12,000 rpm for 10 min at 4 °C. RNA pellet was then washed with 70% cold ethanol, centrifuged at 12,000 rpm for 5 min at 4 °C, air-dried at RT to remove ethanol and dissolved in a suitable amount of DEPC-treated water. Total RNA was reverse transcribed using ReverTra Ace® qPCR RT Master Mix (FSQ-201 Toyobo). The RT reaction was carried out in Biometra TGradient PCR thermocycler under the following conditions: at 37°C for 15 min, followed by 50°C for 5 min and 98°C for 5 min. The cDNA was stored at -80 °C and used for quantitative Real-time PCR.

4.1.9. DNA extraction.

HEp-2 and PKR-knockout cells were infected at MOI 1 and MOI 10 of HSV-1 wild type and HSV-1 mutant R2621, R7041, R7356 viruses, separately. Cells were collected at indicated time post infection and suspended in TRIzol® for DNA extraction, according to the manufacturer's instructions. The DNA extraction was performed as described previously[1]. Briefly, the DNA was precipitated from the interphase and organic phase by adding 100% ethanol and store the samples at room temperature (RT) for 2 to 3 min. Then, the DNA was sedimented by centrifugation at 2,000×*g* for 5 min at 4°C. The DNA pellet was washed twice in a solution containing 0.1 M sodium citrate in 10% ethanol. The DNA pellet was stored in the washing solution for 30 min at room temperature with periodic mixing and centrifuged at 2,000×*g* for 5 min at 4°C. Next, the DNA pellet was suspended in 75% ethanol, stored for 10-20 min at room temperature with periodic mixing, and centrifuged at 2,000 ×*g* for 5 min at 4°C. Finally, the DNA pellet was air-dried by keeping tubes open for 3 to 5 min at RT to remove any residuals of ethanol and dissolved in 8 mM NaOH. The insoluble material was removed by centrifugation at 12,000×*g* for 10 min.

4.1.10. Real-time PCR.

Quantitative Real-time PCR was carried out on a Cepheid Smart Cycler II System (Cepheid Europe, France) using Maxima SYBR Green (Thermo fisher Scientific). The reaction conditions and the analytic primers to Real-time PCR are showed in the table 1. The cDNA copy numbers were normalized to GAPDH[147,148]. Each quantitative Real-time PCR experiments include a minus-reverse transcriptase control.

Absolute quantification using specific TaqMan probe was performed to detect viral DNA as reported in Sciortino *et al.,* 2013[1]. The amplification was carried out in a 25µl reaction mixture containing 1µg of DNA, 1µl each HSV-1 forward and reverse primers 0.5µM, (Fw 5'-CATCACCGACCCGGAGAGGGAC; Rev 5'-GGGCCAGGCGCTTGTTGGTGTA), 1µM TaqMan probe (5'-6FAM-CCGCCGAACTGAGCAGACACCCGCGC-TAMRA, where 6FAM is 6-carboxyfluorescein and TAMRA is 6-carboxytetramethylrhodamine), 0.2µl dNTP mix 100mM, 2.5µl NH4 Reaction Buffer 10X, 1µl $MgCl_2$ 50mM solution and 0.2µl BIOTAQ^{TM} (5U/µL) thermostable DNA polymerase (BIO-21040 Bioline). The following conditions were used for amplification: incubation for 10 min at 95°C, followed by 40 cycles of 30s at 95°C, 30s at 55°C, and 30s at 72°C, with a final cycle of 5 min at 72°C. Each amplification run contains one negative control and 10-fold serially diluted reference DNA obtained from bacterial artificial chromosome (BAC)-HSV in order to generate the standard curve. Viral load was derived from the threshold cycle (*CT*) using the standard curve generated in parallel and the result is expressed as concentration in ng of DNA/µl as described in Kessler *et al.,* 2000[149].

Primes	Forward	Reverse	Conditions
ICP0	TCTGCATCCCGTGCATGAAAAC	CTGATTGCCCGTCCAGATAAAG	95 °C ..15 sec 60 °C 30.. sec.. 40 cycles 72 °C ..20 sec
Us11	GGCTTCAGATGGCTTCGAG	GGGCGACCCAGATGTTTAC	95 °C ..15 sec 60 °C 30.. sec.. 40cycles 72 °C ..20 sec
UL42	CTCCCTCCTGAGCGTGTTTC	CACAAAGCTCGTCAGTTCGC	95 °C ..15 sec 60 °C 30.. sec.. 40 cycles 72 °C ..20 sec
PKR	CCAGGCAAACAAGGTCCCATC	GCGAGTGTGCTGGTCACTAA	95 °C 15 sec 60 °C 30 sec35 cycles 72 °C 20 sec
p53	GATGAAGCTCCCAGAATGCC	CAAGAAGCCCAGACGGAAAC	95 °C 15 sec 60 °C 30 sec35 cycles 72 °C 20 sec
VHS	ACATAACTGCGGTGCTCTTC	CCGAAATTCTAACCCAACAG	95 °C 15 sec 60 °C 30 sec40 cycles 72 °C 45 sec
US3	ACTGGCATGGGCTTTACGATC	GGAGGACCAGACACGTGACCC	95 °C 15 sec 60 °C 30 sec35 cycles 72 °C 45 sec
UL13	GGGATCAGCCACCTGGATATC	GTTATACCCGTGACCCACCAG	95 °C 15 sec 60 °C 30 sec35 cycles 72 °C 45 sec
GAPDH	GAGAAGGCTGGGGCTCAT	TGCTGATGATCTTGAGGCTG	95 °C 15 sec 60 °C 30 sec35 cycles 72 °C 35 sec

Table 1: Primer sequences used for Real-Time PCR.

4.1.11. Statistical analysis.

The statistical studies were performed with One-way analysis of variance (ANOVA) and Student's t-test in order to compare different conditions. Quantitative densitometry analysis of immunoblot bands intensity was performed using T.I.N.A. software (version 2.10, Raytest, Straubenhardt, Germany) or ImageJ. For the data analysis and graphical representations, the GraphPad Prism 6 software (GraphPad Software, San Diego, CA, USA) was used. Each experiment was repeated for at least three times. The results are reported as means ±SD and asterisks (*, ** and ***) indicate the significance of *p*-values less than 0.05, 0.01 and 0.001, respectively.

4.2. RESULTS

4.2.1. The viral protein VHS controls the PKR-phosphorylation levels in different cell lines

As a component of antiviral mechanism, PKR acts by inhibiting protein synthesis initiation and activating the transcription of genes involved in the inflammatory response. For this reason, the control of PKR represents a fundamental strategy to avoid the innate immune response and guarantee viral survival. HSV-1 contains a late gene, Us11, which, expressed early, binds to PKR and blocks its activation. Instead of blocking its activation, HSV encodes ICP34.5 protein, which recruits the phosphatase alpha to dephosphorylate eIF-2α, to preserve the viral protein translation and indirectly to block the PKR activity downstream its activation. Several years ago, it has been proposed a new mechanism based on VHS tegument protein (Sciortino et al., 2013)[1]. The following experiments will highlight the VHS's role in the control of PKR and the potential contribution mediated by other tegument protein.

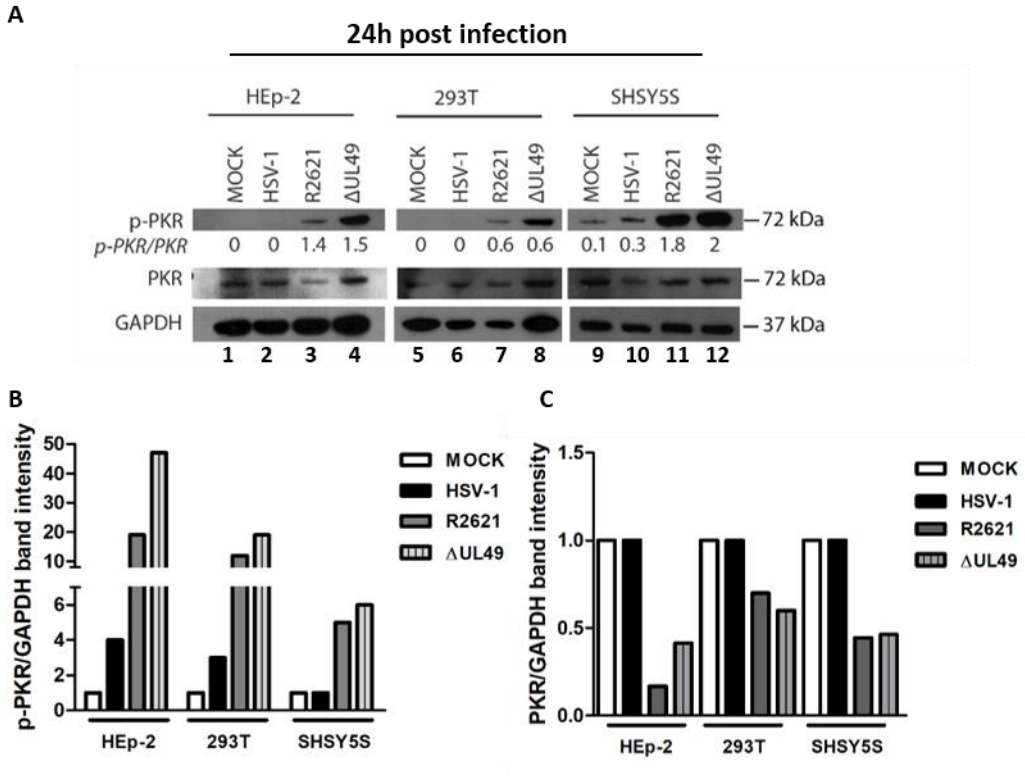

Figure 13: Evaluation of total PKR and phosphorylated PKR in different cell lines infected with HSV-1, R2621 and ΔUL49 mutant viruses. (A) HEp-2, 293T and SH-SY5Y were infected with HSV-1, *vhs*- deleted (R2621) and ΔUL49 mutant viruses at MOI 10 and harvested 24h post infection. The ΔUL49 mutant virus, deleted vp22 gene, exhibits a natural mutation in *vhs* gene, responsible for the RNase activity (Sciortino et al., 2007). The samples were subjected to western blot analysis to p-PKR and PKR expression. GAPDH used as a loading control. (B-C) Quantification of band intensity was determined with T.I.N.A program, the p-PKR and PKR values were normalized to GAPDH protein levels.

Based on previous results obtained by Sciortino *et al.*, 2013[1] that showed the accumulation of phospho-PKR abrogated by VHS protein in HT1080 cells, further experiments were performed to understand whether the modulation of PKR activation, HSV-1 mediated, depends on used cellular model. Therefore, HEp-2, 293T and SH-SY5Y cell lines were mock infected and infected with HSV-1, R2621 and ΔUL49 at MOI 10 and harvested 24 hours post infection. The total cellular extracts were eletrophoretically separated in denaturing polyacrylamide gels, transferred to nitrocellulose membranes and probed with antibodies directed to total and phosphorylated form of PKR (Thr 446). GAPDH used as a loading control. As shown in figure 13 A, the HEp-2, 293T and SHSY5Y cell lines infected with HSV-1 wild-type lack in the accumulation of phosphorylated form of PKR if compared with the uninfected cells (Fig. 13 lanes 2, 6, 10). On the contrary high phosphorylation levels of PKR were observed following both R2621 (Fig.13 lanes 3, 7, 11) and ΔUL49 (Fig.13 lanes 4, 8, 12) infection.

To note the ΔUL49 is genetically deficits in VHS RNAse activity[143]. The obtained results were complemented by quantitative analysis of the band-intensity of phospho-PKR on GAPDH levels (Fig.13 B) and PKR on GAPDH levels (Fig. 13 C). The accumulation of phospho-PKR, following infection with both mutant viruses, coincides with the simultaneous reduction of total form of PKR. In addition, the ratio between p-PKR/PKR, as reported in figure 13A, shows the switch of the total form of PKR on the phospho-PKR, in particular in HEp-2 and SH-SY5Y cells after R2621 and ΔUL49. In cell infected with HSV-1, the expression of phospho-PKR and the total PKR levels remain unchanged compared to the levels of the moc. These finding demonstrate that HSV-1 is capable to control the accumulation of phospho-PKR in different cell lines with a mechanism that involves most likely VHS activity. Indeed, the deletion of *vhs* gene in R2621 and the natural loss of its RNase enzymatic function in ΔUL49 implies the control failure of the PKR-mediated response during HSV-1 replication.

4.2.2. Transient transfection of VHS suppresses the accumulation of phospho-PKR and total PKR

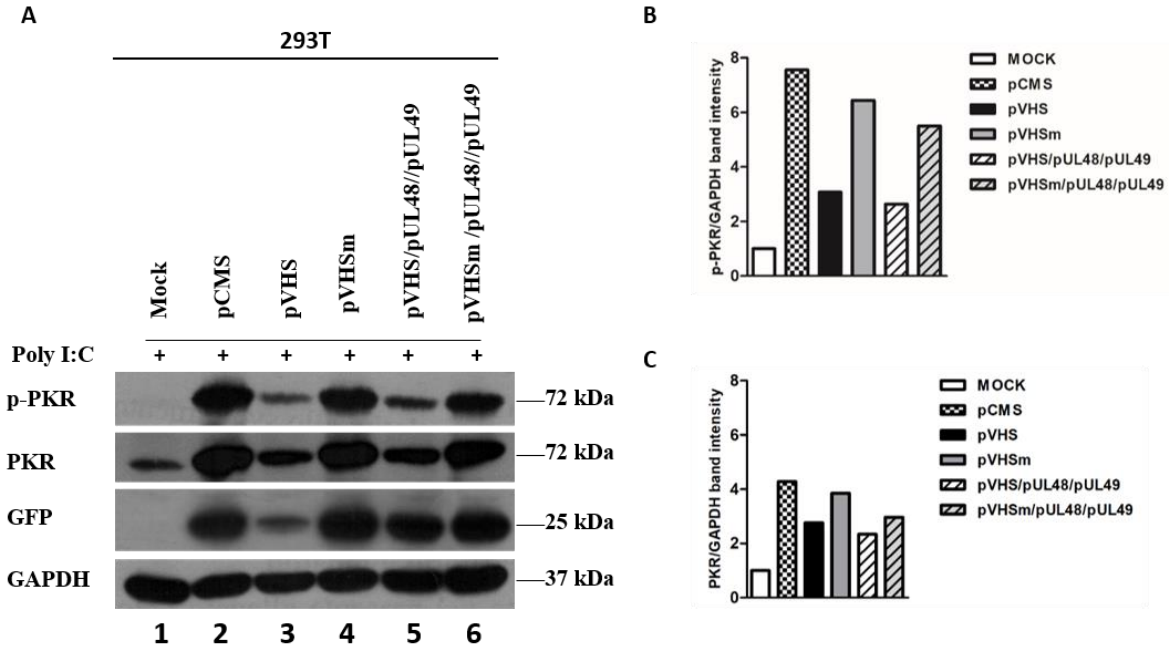

Figure 14: Transient transfection of VHS and mutant VHS plasmids in 293T cells. The cells were transfected with 1 µg of plasmid DNA as described in Methods. 48h post transfection the cells were untreated and treated with Poly I:C (0,01 µg/µl) for additional 24h. (A) Western Blot analysis was carried out to analyze phospho-PKR, PKR, PKR, GFP and GAPDH expression following transfection with pCMS, pVHS, pVHSm, pVHS /pUL48/ pUL49 and pVHSm /pUL48/ pUL49. (B-C) The quantification of band intensity was determined with T.I.N.A program, the phospho-PKR and PKR values were normalized to GAPDH protein levels.

To support the above data on role of VHS on the PKR regulation and to remark the importance of VHS endonuclease activity in the accumulation of phosphorylated form of PKR, transient transfection experiments were performed by using plasmids expressing the wild type VHS and mutant VHS, designed as pVHSm, alone or in triple transfection with pUL48 and pUL49. The pVHSm is characterized by substitutions of three amino acid residues, E192, D194, and D195, which are essential for the nuclease activity[94]. Therefore, the pVHSm encodes for catalytically inactive form of VHS protein. In addition, the UL48 and UL49 plasmids, able to overexpress UL48 and UL49 HSV-1 proteins, were chosen because, according to literature data, they control the expression of VHS[144]. 293T cells were transfected with 1µg of DNA plasmids for 48h and treated with poly I:C for further 24 hours.

It was previously demonstrated that poly I:C, as a synthetic analog of double-stranded RNA (dsRNA), behaves like an inductor of PKR decreasing the activation of pre-existing PKR[150]. The expression of the total and phosphorylated forms of PKR was monitored and compared to cells transfected with pCMS plasmid, used as a control vector. Nejepinska J. and coauthors has been previously reported that the transfection of plasmid DNA, allow the transcription of spurious RNAs which can activates PKR response[151]. Therefore, the simultaneous transfection of pCMS and poly I:C represents a double stimulus to PKR response which allow to better understand the VHS's role.

The figure 14 A shows the reduction of phospho-PKR accumulation in poly I:C treated cells transfected with a VHS plasmid alone and in triple transfection with UL48 and UL49 plasmids, compared to cells transfected with pCMS alone (Fig.14A lanes 3 and 5 vs lane 2). On the contrary, an accumulation of phosphorylated form of PKR was detected in VHSm transfection, alone and in triple transfection with UL48 and UL49 plasmids, if compared to VHS (Fig 14 A lanes 4 and 6 vs 3 and 5). The quantitative analysis of the band intensity related to phospho-PKR expression was graphically reported in figure 14B.

In addition, the transfection experiments have also showed the reduction of the total form of PKR (Fig. 14 C) when the VHS is actived compared to VHSm indicating a pivotal role of the RNase activity of VHS on PKR activation. These observations suggest the importance of VHS in regulating PKR response during HSV replication..

4.2.3. The accumulation of mRNA is responsible for the PKR activation.

Considering the activation mechanism of PKR based on interaction/activation with viral RNAs, experiments were performed in presence of pharmacological inhibitors, which affect to RNAs in different manner in cell infected or not with virus.

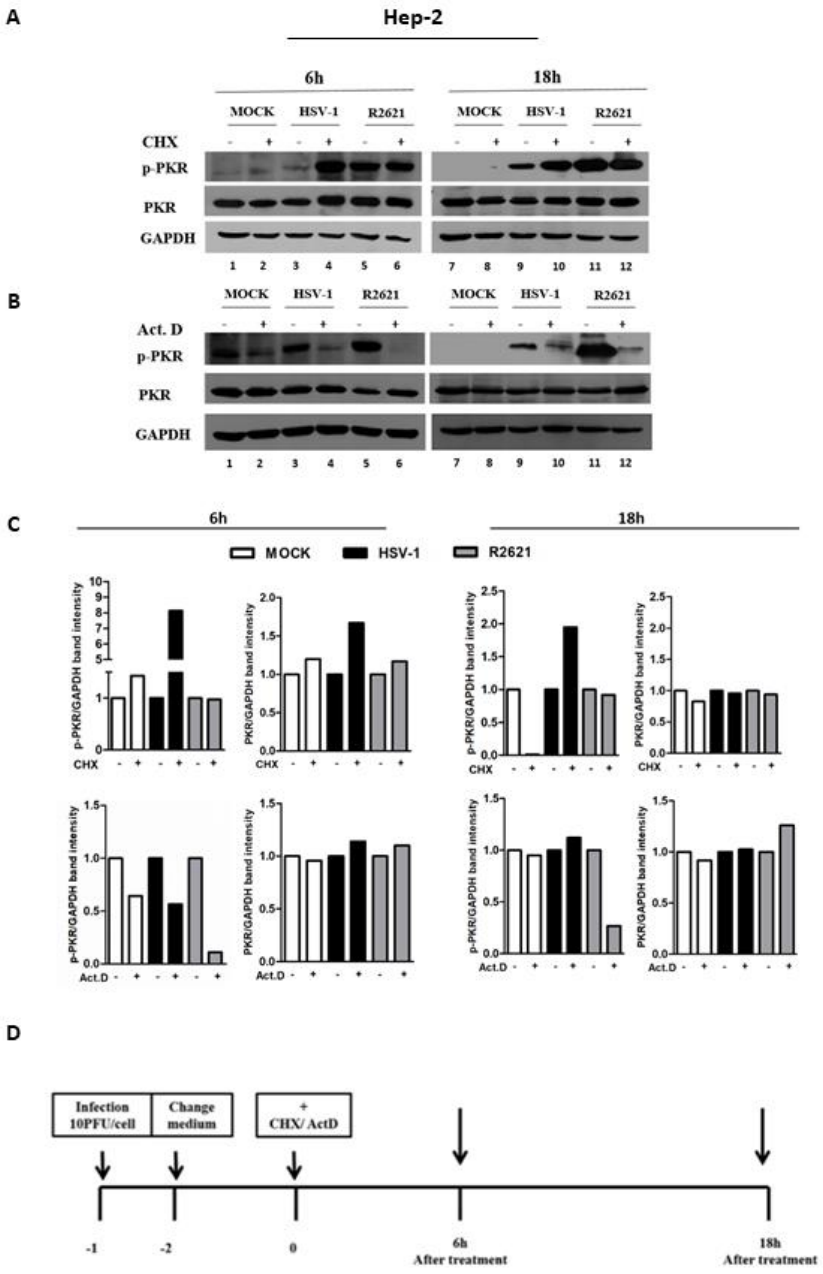

Figure 15: Detection of phosphorylated PKR and total PKR during viral replication in cells treated with protein or mRNA inhibitors. (A-B) HEp-2 cells were mock infected and infected with HSV-1 (F) and R2621 viruses. Three hours post infection, the cells were untreated and treated with Cycloheximide (CHX) (50µg/ml) and with Actinomycin D (Act.D) (10µg/ml) separately, and collected at 6h and 18h of treatment. Western Blot analysis was performed to evaluate p-PKR, PKR and GAPDH expression. (C) Band density was determined with the T.I.N.A. program, and was expressed as fold change over the appropriate housekeeping genes. (D) Graphical representation of the experiment.

.

HEp-2 cells were infected with 10 PFU/cell with HSV-1 (F) wild-type virus or R2621 mutant virus deleted in *vhs* gene. Three hours after infection cells were treated with cycloheximide (CHX) (50µg/ml) and/or with actinomycin D (Act.D) (10µg/ml) separately and then cells were harvested at 6h and 18h of treatment (Fig.15 D).

Equal amount of total proteins was electrophoretically separated, transferred and probed with antibodies directed to phospho-PKR (thr446), total PKR and GAPDH. The CHX treatment was used to inhibit protein synthesis and provokes an overload of mRNAs. It in *vitro* model reproduces the activation of PKR[152]. On the contrary, the Act.D is a transcription inhibitor and provokes a reduction of mRNAs accumulation.

The key features of the results presented in Fig.15 were as follow: i) high accumulation of phospho-PKR was detected in HSV-1, R2621 infected cells treated with CHX if compared to the mock treated cell at all-time considered (Fig. 15 A lanes 2, 4, 6, 8, 10, 12). The results suggested that in examined cellular model, the overload of viral mRNAs triggers the phospho-PKR accumulation. ii) In CHX-untreated cells, the accumulation of phospho-PKR is greater in HEp-2 cells infected with R2621 rather than with HSV-1 (Fig. 15A lanes 3, 5, 9, 11) confirming the role of VHS on the PKR control. iii) phospho-PKR fails to accumulate in infected and Act. D treated cells (Fig.15B lane 4, 6, 10, 18) instead highly accumulates in infected R2621 cells (Fig.15B lanes 3, 5, 9, 11). Besides, in the R2621 infected cells, the accumulation of phospho-PKR is detected with or without an overload of mRNAs (Fig. 15A lanes 5, 6, 11, 12). The quantitative analysis of the band intensity related to phospho-PKR and total PKR expression during HSV-1 replication and following CHX and Act. D treatment was graphically reported in figure 15C. Taken together these data, it is possible to conclude that HSV-1 uses VHS not only as a regulator of viral genes cascade but also to control p-PKR activation. Nevertheless, the finding that VHS protein was incapable to interact physically with PKR (Our unpublished data; Dauber *et al*. 2016[98]), raised the questions if additional mechanisms and additional viral proteins were involved in controlling PKR response during HSV replication

4.2.4. Involvement of viral proteins US3 and UL13 in the accumulation of phospho-PKR

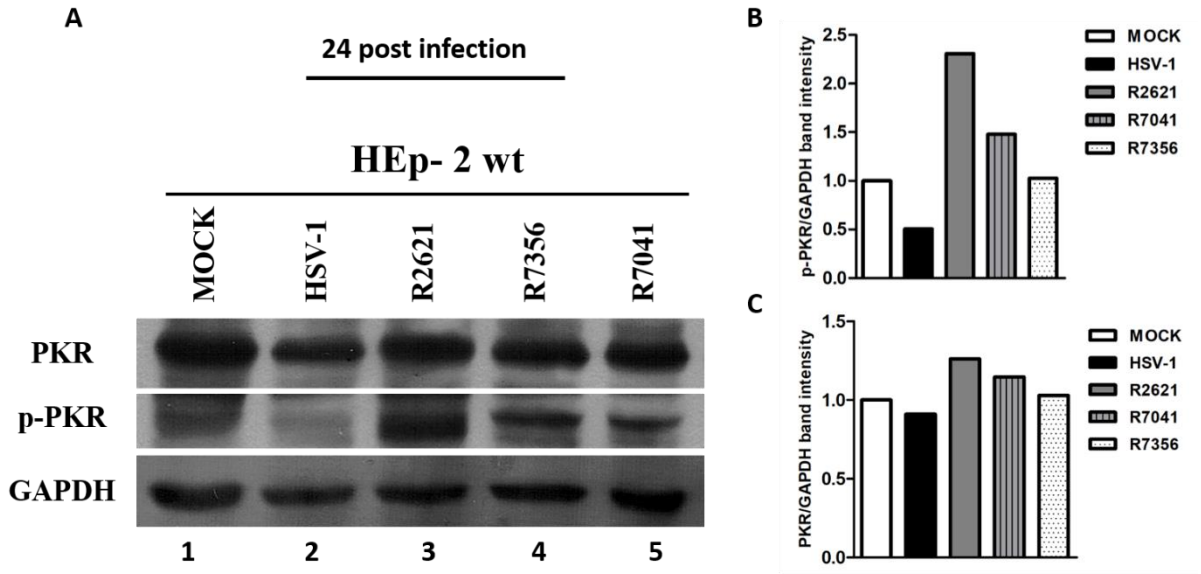

Figure 16: Detection of total PKR and p-PKR in HEp-2 infected with ΔVHS, ΔUS3 and ΔUL13 viruses. (A) HEp-2 cells were mock infected or infected with HSV-1 wild-type virus, R2621 (ΔVHS), R7041 (ΔUS3), R7356 (ΔUL13) mutant viruses at MOI 10 and harvested 24h post infection. Western Blot analysis was performed to detect p-PKR (Thr-446), PKR and GAPDH expression. (B-C) Band density was determined with the T.I.N.A. program, and was expressed as fold change over the appropriate housekeeping genes.

The above data indicate that HSV-1 controls the activation of PKR by acting on mRNAs accumulation and that VHS protein is mainly involved in this regulatory mechanism. It is well known that the viral countermeasures to shut down the PKR-mediated immunological response occur at upstream and downstream of the pathway and depend on multiple viral genes expression. In this context, the tegument proteins are the first viral proteins that interact with the cell and that potentially regulate intracellular pathways.

Therefore, additionally to conventional structural role, the HSV-1 tegument proteins play dual roles during the viral life cycle. Indeed, they are modulators of cellular and viral functions in infected cells and at the same time, they perform different enzymatic activities to improve viral replication. How these are coordinated during infection is largely unknown. Therefore, based on the above considerations, the regulatory role of two HSV-1 tegument proteins, US3 and UL13, in the PKR activation, was investigated in the next experiments. US3 and UL13 are serine / threonine kinases proteins involved in the viral and cellular regulation.

Indeed, it is well documented the role of US3 and UL13 tegument viral proteins in the regulation of cellular PI3K/Akt signaling pathway. Therefore, deleted viruses for *us3* and *ul13* genes and plasmids expressing US3 and UL13 proteins were employed to verify their involvement in the PKR control during HSV-1 replication. First, HEp-2 cells were mock infected and infected with HSV-1 wild-type virus, R2621, R7041 and R7356 mutant viruses, separately, at MOI 10 and harvested 24h post infection. The results, shown in figure 16, demonstrate for the first time that the deleted viruses for *us3* and *ul13* genes accumulate the phospho-PKR. The expression levels of phosho-PKR in HEP-2 infected with R2621, R7041 and R7356 are statistically increased compared to HSV-1 infection (Fig. 16A, lanes 3, 4, 5 vs 2). The quantitative analysis of the band intensity related to phospho-PKR expression was graphically reported in figure 16 B and indicates the accumulation of phospho-PKR following viral infection with R2621, R7041 and R7356 mutant viruses. To confirm these data, transient transfection experiments were carried out in 293T cell lines.

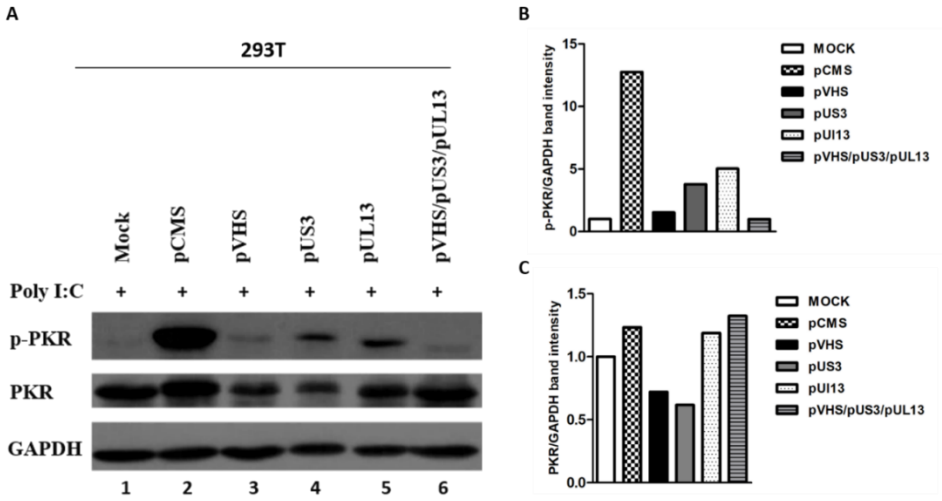

Figure 17: **Detection of total PKR and p-PKR in 293T cell transfected with US3 and UL13 plasmids.** (A) 293T cells were transfected with 1 µg of plasmid DNA according to manufacturer's instructions. 48h post transfection the cells were treated with Poly I:C (0,01 µg/µl) for additional 24h. WesternBlot analysis was carried out to analyze p-PKR, PKR and GAPDH expression. (B-C) Band density was determined with the T.I.N.A. program, and was expressed as fold change over the appropriate housekeeping genes.

The 293T cells were transfected with plasmids encoding the VHS, UL13 and US3 viral proteins and 48h post transfection the cells were treated with Poly I:C (0,01 μg/μl) for additional 24h. Then cells were harvested and subjected to western blot analysis. The expression of both total and phosphorylated forms of PKR was analyzed and compared to cells transfected with pCMS plasmid, used as a control vector. According to the previous results, VHS transfection is able to control the accumulation of phosphorylated form of PKR compared to the control vector (Fig.17A lane 3). Interestingly, low accumulation levels of phosho-PKR were detected after single transfection with pUS3 and pUL13 (Fig.17A lanes 4 and 5). Besides, the triple transient transfection with pVHS, pUS3 and pUL13 shows a clear absence of accumulation of phospho-PKR (Fig.17A lanes 6). The quantitative analysis of the band intensity related to phospho-PKR expression was graphically reported in figure 17B.

It was also noted that, the transfection with viral plasmids encoding for VHS and US3, affects to the expression of total form of PKR compared to the basal levels in mock sample (Fig. 17 lanes 3, 4 vs 1). The quantitative analysis of the band intensity related to total PKR expression was graphically reported in figure 17C. These findings, associated to results obtained in the infected cells (Fig. 16), demonstrated for the first time the involvement of additional HSV-1 structural proteins in the regulation of PKR expression.

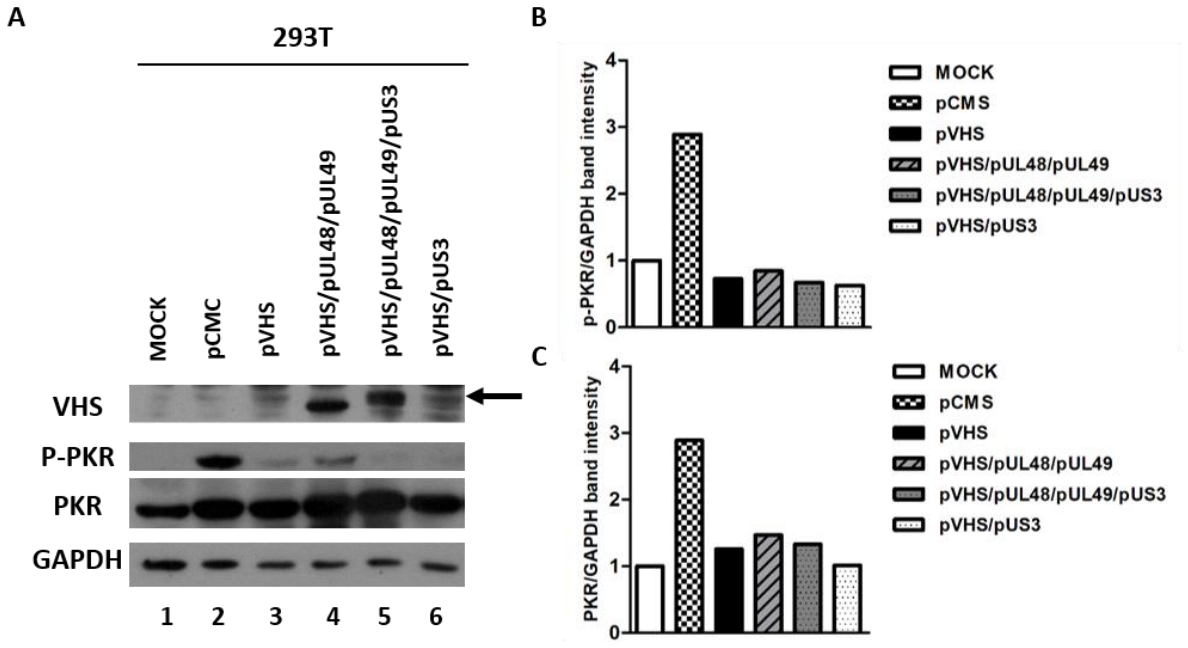

Figure 18: **Detection of VHS in 293T cell transfected with VHS, UL48, UL49, US3 and UL13 plasmids. (A)** 293T cells were transfected with a combined plasmids encoding for VHS , UL48, UL49, and US3 viral proteins. The pCMS plasmid was used as a control vector. After 72h cells were harvested and the expression of VHS, pPKR and PKR proteins was detected by western blot analysis. The row indicates the high molecular weight of VHS in presence of Us3 protein. (B-C) Band density was determined with the T.I.N.A. program, and was expressed as fold change over the appropriate housekeeping genes.

The results showed in figure 14 and in figure 17 highlight two mains points: i) VHS affects to expression levels of phospho-PKR and total PKR mainly dependent on the RNase activity, mainly; ii) US3 and UL13 collaborate to control the accumulation of phospho-PKR and total PKR. To analyze the potential regulatory mechanism mediated by US3 in phospho-PKR expression and the implication of VHS protein, single, double, triple and quadruple transient transfections were performed on 293T cells. Studies on UL13 protein remain not still feasible because a specific antibody for detection of this protein was not available in our lab. The results, shown in Figure 18, demonstrate that: i) VHS protein accumulates in presence of UL48 and UL49 viral proteins as demonstrated by Taddeo and collaborators[144](Fig. 18A lane 4). ii) VHS protein accumulates in presence UL48, UL49 and US3 at high molecular weight, demonstrating a higher state of phosphorylation mediated by Us3 (Fig. 18A lane 5). iii) VHS protein fails to accumulate in presence of US3 at low molecular weight (Fig.18A lane 6). In this contest, the expression levels of phospho-PKR, as graphically reported in figure 18B, were lower following triple transfection with pVHS , pUL48 and pUL49 (Fig 18A lanes 4) , single transfection with pVHS (Fig. 18A lane 3), double transfection with pVHS/pUS3(Fig. 18A lane 6) and quadruple transfection with the pVHS/pUL48/pUL49/pUS3 transfection (Fig. 18A lane 5).

Based on the above data, it is plausible to hypothesize that the hyperphosphorylation of VHS, mediated by Us3 protein, greatly controls the accumulation of phospho-PKR.. Taken together the above data, US3 regulates the accumulation of phospho-PKR with or without the presence of its regulatory proteins UL48 and UL49.

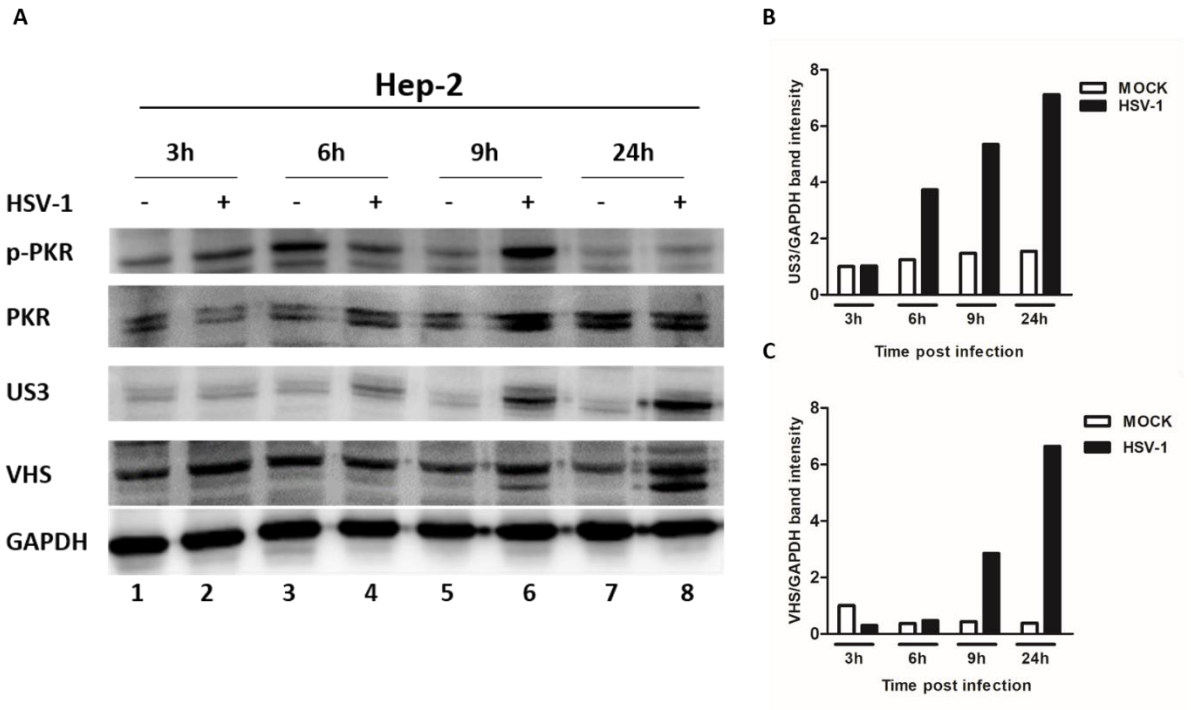

Figure 19: Temporal expression of US3 and VHS in HEp-2 cell infected with HSV-1. (A) HEp-2 cells were mock infected and infected with HSV-1 at MOI 10 and collected at 3h, 6h, 9h, 24h post infection. The protein extracts were separated by polyacrylamide gel electrophoresis and the p-PKR, PKR, US3 and VHS expression levels were detected. GAPDH was used as a housekeeping control. (B-C) Band density was determined with the T.I.N.A. program, and was expressed as fold change over the appropriate housekeeping genes

The findings reported above on US3 and VHS collaboration on the phospho-PKR accumulation highlight the need to verify the accumulation of both proteins during HSV-1 infection in HEp-2 cells. Based on this, a time course was performed and HEp-2 cells infected or mock infected with HSV-1 at MOI 10 were collected at 3h, 6h, 9h, and 24h. The results, shown in figure 19, demonstrate that: i) the activation of phospho-PKR increases during viral infection and peaks at 9h post infection (Fig 19A lanes 2, 4, 6). ii) Clear reduction of phospho-PKR appears 24h post infection (Fig 19A lane 8). iii) the US3 and VHS proteins accumulate in the late stage of viral replicative cycle, (6h, 9h, 24h for US3, Fig 19A lanes 4,6,8) (9h and 24h for VHS, Fig 19A lanes 6 and 8). The data demonstrated that HSV-1 strictly controls phospho-PKR accumulation when high levels of US3 and VHS are simultaneously detected, as graphically reported in figure 19 B and C.

4.2.5. The accumulation of viral mRNA is responsible for the PKR activation in R7041 and R7356 virus infections.

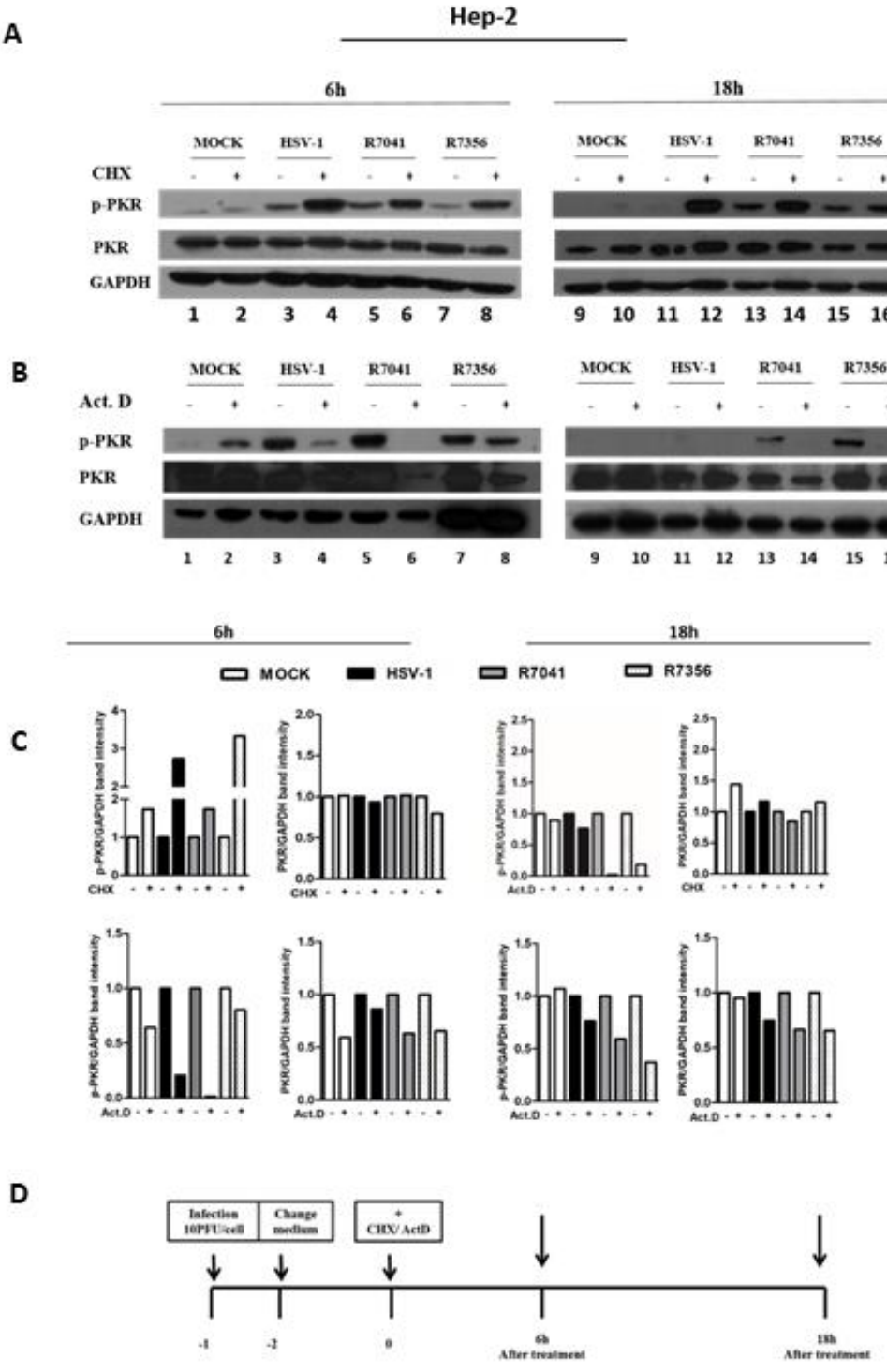

Figure 20: Detection of phosphorylated PKR and total PKR during viral replication in cells treated with protein or mRNA inhibitors. (A-B) HEp-2 cells were mock infected and infected with HSV-1 (F) and R7041 and R7356 viruses. Three hours post infection, the cells were untreated and treated with cycloheximide (CHX) (50μg/ml) and with actinomycin D (Act.D) (10μg/ml) and collected at 6h and 18h of treatment. Western Blot analysis was performed to p-PKR, PKR and GAPDH expression. (C) Band density was determined with the T.I.N.A. program, and was expressed as fold change over the appropriate housekeeping genes. (D) Graphical representation of experiment.

Based on previous results demonstrating that the regulation of PKR mediated by HSV-1 involves the mRNAs accumulation, the similar experiment was performed to evaluate whether mutant viruses, deleted in US3 or UL13, use the same mechanism. Therefore, HEp-2 cells were infected at MOI 10 with HSV-1 (F) wild-type virus or R7041 and R7356 mutant virus. Three hours after infection cells were treated with cycloheximide (CHX) (50µg/ml) and/or with actinomycin D (Act.D) (10µg/ml), then cells were harvested 6h and 18h after treatment (Fig. 20 D). Equal amount of total proteins was electrophoretically separated, transferred and probed with antibodies directed to phospho-PKR (thr446), total PKR and GAPDH.

The key features of the results presented in figure 20A are as follow: i) The accumulation of mRNAs, inducted by CHX, increases the accumulation of phospho-PKR in infected cells with HSV-1, R7041 and R7356 at 6h and 18h (Fig.20 A lanes 4, 6, 8, 12, 14, 16). ii) HSV-1 highly controls phospho-PKR accumulation at late stage of viral infection (Fig. 20 A lane 11 vs 3). iii) R7041 infection fails to control the phospho-PKR accumulation (Fig. 20 A lane 13 vs 11) confirming a regulatory role of US3 in the phospho-PKR activation. In addition, R7356 fails to control the phospho-PKR accumulation. The Act.D treatment blocks the transcriptional process and therefore the failure in the mRNAs accumulation affects to phospho-PKR activation, in all considered virus and at 6h and 18 of post treatment (Fig. 20 B lanes 4, 6, 8, 12, 14, 16). Further studies are necessary to better understand the regulatory mechanism mediated by UL13.

4.2.6. Transcriptional control mediated by HSV-1 on PKR mRNA expression

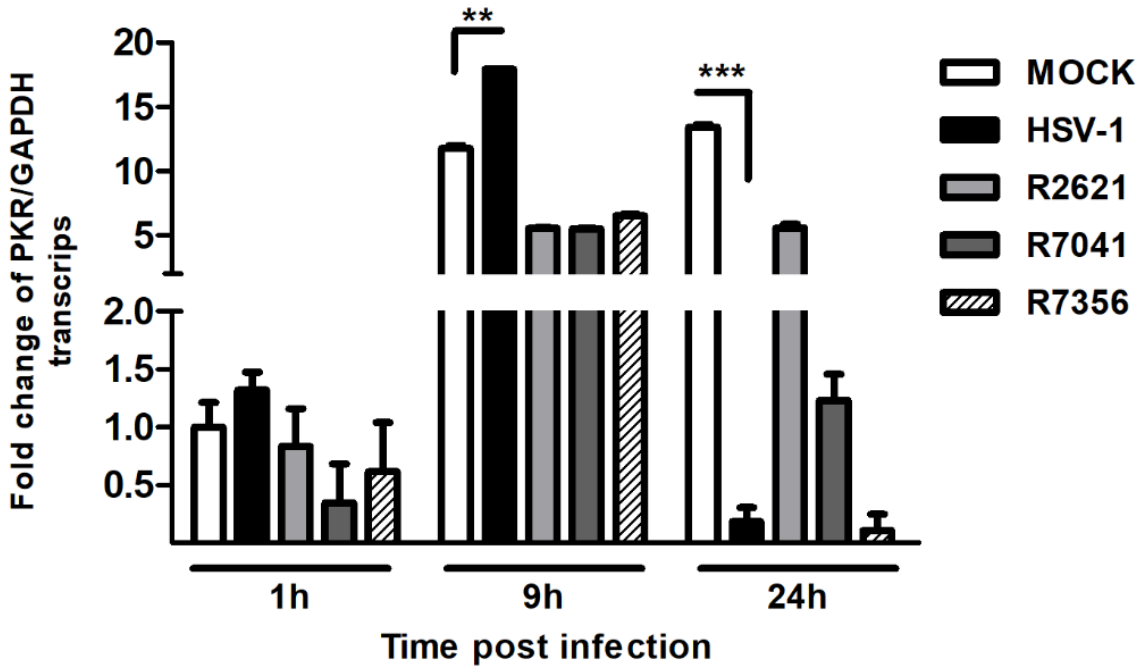

Figure 21: Detection of PKR transcripts following HSV-1 infection. HEp-2 cells were mock infected or infected with HSV-1, R2621, R7041 and R7356 viruses at MOI 10, collected at 1h, 9h, and 24h and subjected to RNA extraction by Trizol reagent, according to manufacturer's instructions. Quantitative Real-time PCR was used to detect the levels of PKR transcripts during HSV-1 infection. The expression levels of PKR and GAPDH, used as an endogenous control, were evaluated by using the comparative CT Method (ΔΔCT Method) as described in Materials and Methods. Statistical analyses were performed with one-way ANOVA analysis assay in triplicate and *** P<0.001 and **P<0.01 indicates significant changes.

Having established that HSV-1 is able to control accumulation of phospho-PKR during viral replication and that VHS, US3 and UL13 tegument proteins are involved in its regulation, the next step was determinate whether the viral control on PKR is limited at protein synthesis levels or whether also affects the levels of mRNAs transcripts. Therefore, HEp-2 cells were mock infected and infected with HSV-1, R2621, R7041 and R7356 viruses at MOI 10 and collected at 1h, 9h and 24h post infection. Total RNA was extracted by using Trizol reagent according to manufacturer's instructions. Quantitative Real-time PCR was performed as reported in Materials and Methods, by using following specific primers for PKR: fw: 5'-ggccgctaaacttgcatatc-3' and rev: 5'-gcgagtgtgctggtcactaa-'3.

The results, showed in figure 21, demonstrated the incapacity of the HSV-1 to block the accumulation of PKR transcripts compared to the uninfected cells in the first 9h of viral replication. Nevertheless, the accumulation of PKR-transcripts does not correspond to the accumulation of total PKR protein that remains mostly constant in the infected samples if compared to mock-infected (Fig. 19). At 24h post infection, HSV-1 was capable to shut down PKR transcripts synthesis if compared to the mock. Instead, R2621 show an opposite tendency compared to HSV-1 at 24h. Indeed, the R2621 more than R7041 mutant viruses, was incapable to shut down PKR transcription compared to HSV-1 infected cells.

Therefore, it is possible hypothesize that the virus is able to control the PKR response when the late viral proteins are accumulating at late stage of viral replication (Fig.19). Taken together, HSV-1 control the accumulation of PKR transcripts at late stage of viral replication. In addition, considering only the lack of accumulation of PKR transcripts, seems that, the HEp-2 cells were unable to sense at early stage of viral replication of the deleted viruses enrolled in this study.

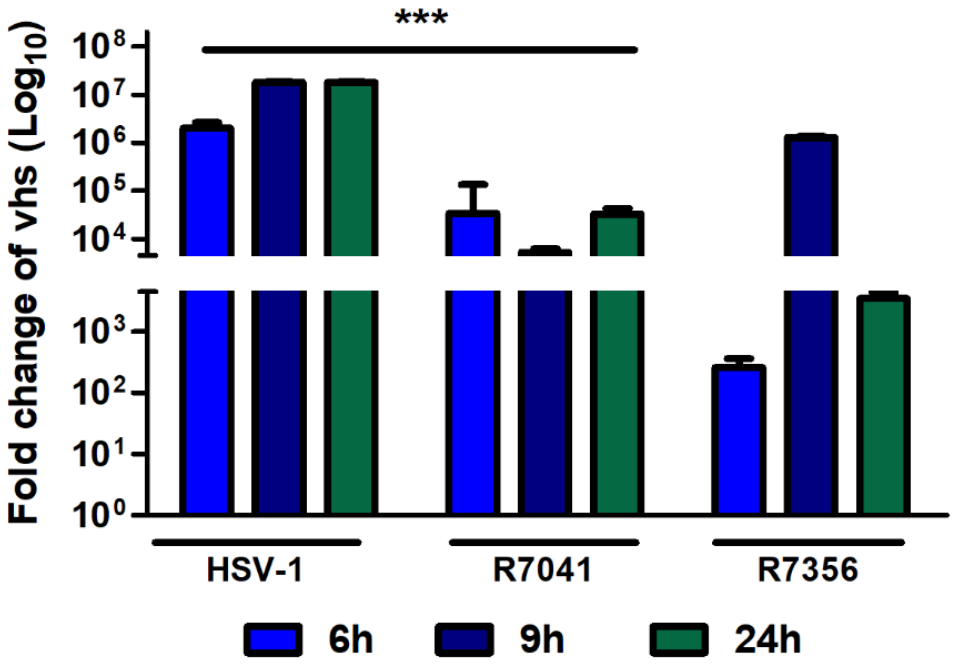

Figure 22: Evaluation of VHS transcripts levels in HEp-2 infected with HSV-1, R7041 and R7356 during viral cycle. HEp-2 cells were infected with HSV-1, R7041 and R7356 viruses at MOI 10, collected at different time point (6h, 9h, and 24h) and subjected to RNA extraction by Trizol reagent, according to manufacturer's instructions. Quantitative Real-time PCR was used to detect the VHS transcripts. The expression levels of VHS and GAPDH, used as an endogenous control, were evaluated by using the comparative CT Method (ΔΔCT Method) as described in Materials and Methods.

A crucial point in the regulation mechanism that has emerged in this work was to understand how the viral proteins regulate with each other and how this interaction was involved in the PKR regulation. Therefore, HEp-2 cells were infected with HSV-1, R7041 and R7356 at MOI 10 and collected at different time point (3h, 6h, 9h, and 24h). Quantitative Real-time PCR was performed by using following specific primers for VHS: fw: 5'-acataactgcggtgctcttc-3'; rev: 3'-ccgaaattctaacccaacag-5 in order to quantify the expression of VHS in HSV-1 and in both mutant viruses, R7041 and R7356 and to verify if it was responsible for downstream signals.

The results, shown in figure 22, can be summarized as follow: i) the expression of VHS in HEp-2 infected with HSV-1 gradually increases, with a peak at 9h and remain unchanged up to 24h. ii) In HEp-2 infected with R7041, the transcriptional levels of VHS were lower at 6h, 9h and 24h compared to HSV-1 infection. iii) In HEp-2 infected with R7356, the transcriptional levels of VHS accumulate with a peak at 9h, probably dependent on different regulation of UL13 on VHS [112]. Taken together, these findings suggest that the loss of US3 and in part of UL13, negatively affects to accumulation of VHS transcripts.

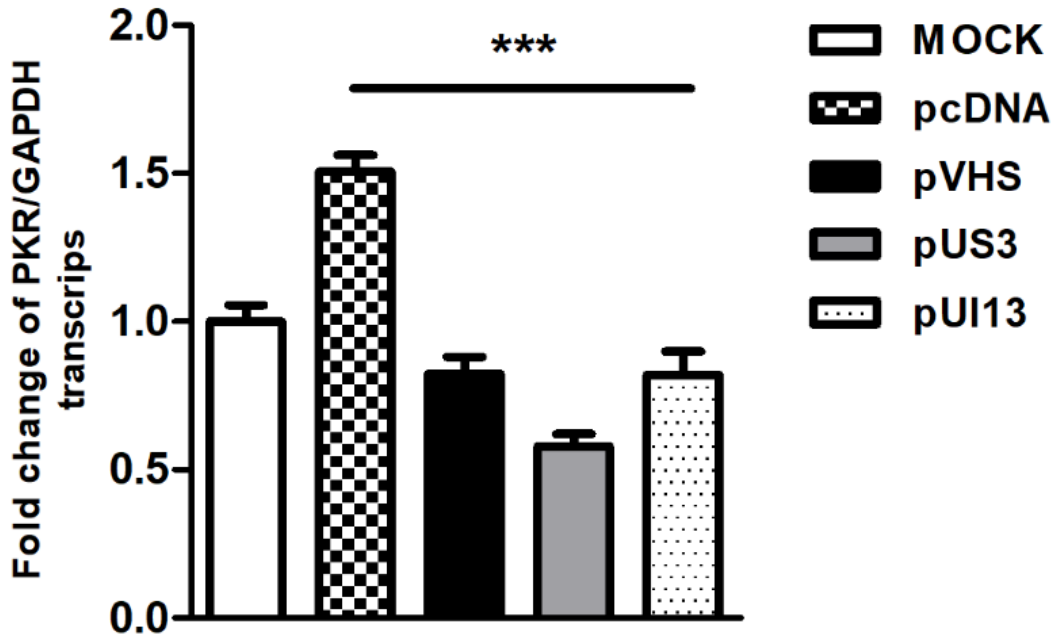

Figure 23: Detection of PKR transcripts following VHS, US3 and UL13 transfection. 293T cells were untrasfected and transfected with the plasmids designed as follow pVHS, pUS3, pUL13. pcDNA was used as a control vector. The cells were subjected to mRNAs extraction. Real-time PCR was used to detect the transcriptional levels of PKR and verify the involvement of specifics structural viral proteins in the regulation of PKR transcriptional levels. The levels of PKR and GAPDH, used as an endogenous control, were evaluated by using the comparative CT Method (ΔΔCT Method) as described in Materials and Methods. Statistical analyses were performed with one-way ANOVA analysis assay in triplicate and *** $P<0.001$ indicates significant changes.

In the viral infection, the expression of a protein is subjected to different type of regulation mediated by onset of viral proteins and by phosphorylation signals network, which influences the results. For this reason, *in vitro* transfection approach was used. Having pointed out this, 293T cells were transfected with the plasmids designed as follow pVHS, pUS3 and pUL13, as showed in figure 23, in order to verify the involvement of the considered tegument proteins in the regulation of PKR at transcriptional levels. 293T cells were transfected by mixture of Lipofectamine and plasmid encoding for VHS, US3 and U13 proteins, as described in material and methods.

The results show a significant reduction of PKR transcripts following pVHS transfection compared to pCDNA, used as control vector. According to the previous experiments and in line with the aim of this work, the involvement of US3 and UL13 structural viral proteins in the regulation of PKR at transcriptional levels was verified. The results clearly indicate that, the US3 and UL13 significantly affect PKR transcripts levels, negatively. It is clear that Us3 and UL13 use additional mechanisms in PKR regulation, not associates to RNAase activity of VHS.

4.2.7. Characterization of viral replication in PKR knocked out HEp-2 cell.

Due to the above results, the contribution of PKR to HSV replication remained unclear. To clarify the role of the PKR activation during HSV infection, it was sought to use a genetic approach. HEp-2 knocked out PKR-/- cells (kindly provided by prof. Bernard Roizman and Grace Guoying Zhou-Shenzhen International Institute for Biomedical Research, CHINA), were employed for the next step. Therefore, HEp-2- PKR knockedout (PKR-/-) and HEp-2 cell lines were infected with HSV-1 and collected at designed time post infection to evaluate: i) viral DNA quantification by absolute Real-time PCR (Fig. 24); ii) viral transcripts such as ICPO, UL42 and US11, by relative quantitation Real-time PCR (Fig. 25); iii) viral titers in HEp-2 compared to PKR-/- cells (Fig. 26).

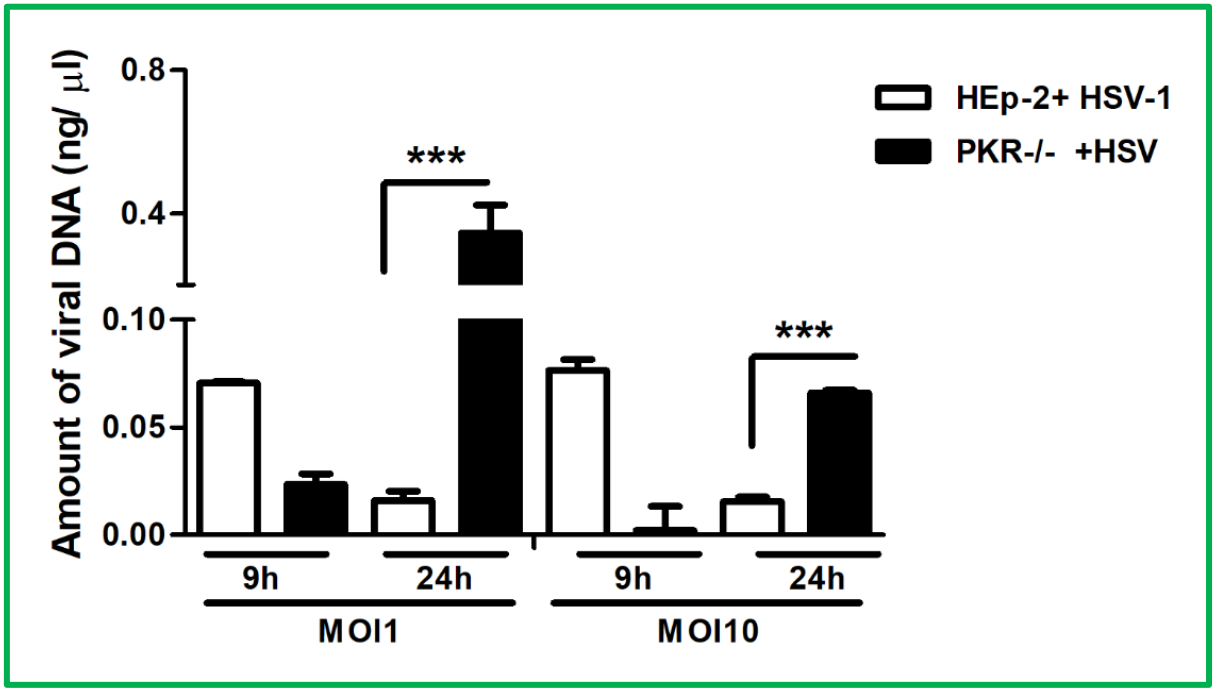

Figure 24: Evaluation of viral DNA in PKR-/- cell lines compared to HEp-2. PKR-/- and parental cell lines were infected with HSV-1 at MOI 1 and MOI 10 and collected at 9h and 24h post infection. The absolute quantification Real-time PCR was used to detect the amount of viral DNA in both cell lines by using specific TaqMan. Viral load was derived from the threshold cycle (CT) using the standard curve generated in parallel and the result is expressed as concentration in ng of DNA/µl. The procedures were published previously (Sciortino et al., 2013). Statistical analyses were performed with one-way ANOVA analysis assay in triplicate ± SD, ***P<0.001 indicates significant change.

The absolute quantification Real-time PCR was used to measure the amount of viral DNA in PKR-/- and HEp-2 cells. Both cells were infected with HSV-1 at lower and higher MOI, (MOI1 an MOI10, respectively) and collected at 9h and 24h post infection in TRIzol® for DNA extraction, as described in material and methods. As shown in Figure 24, the amount of viral DNA significantly (***P<0.001) increases in PKR-/- compared to HEp-2 cells at 24h post infection. In particular, lower MOI (MOI 1) shows an enhancement of viral DNA synthesis, correlated to the inactivation of PKR. Nevertheless, seems that in the PKR-/- a delay of viral DNA accumulation was shown at 9h post infection.

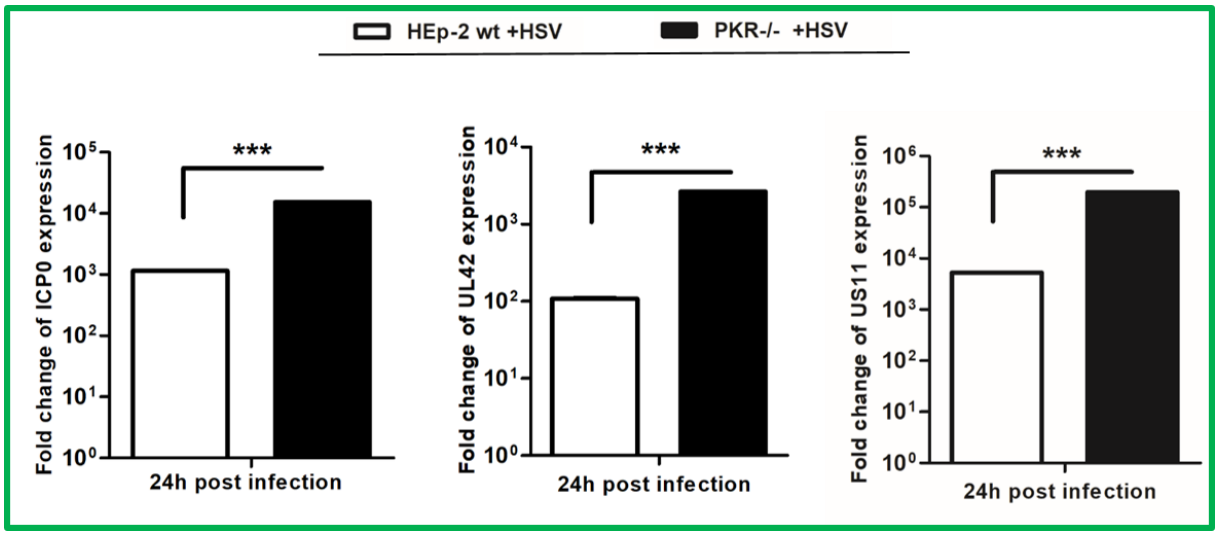

Figure 25: Expression of viral transcripts cascade in in HEp-2 and PKR-/- cell lines. HEp-2 and PKR-/- cells were infected MOI 10 with HSV-1 and harvested 24h post infection. The mRNA was purified with Trizol according to manufacturer's instructions. The measure of changes in the expression level of each considered gene was analyzed calculating the value of 2^-ΔΔCt. The assay was performed as means of triplicate ± SD and expressed as fold change over the housekeeping genes. *** indicate significant changes (P<0.0001).

To determine whether the higher accumulation of DNA correlated with the enhanced expression of the viral genes, we analyzed ICP0, UL42 and US11 viral transcripts accumulation as representative genes of sequential genetic cascade of HSV-1. Therefore, HEp-2 and PKR-/- cells were infected MOI 10 with HSV-1, harvested 24h post infection and processed to mRNA extraction and quantitative Real-time PCR. Figure 25 demonstrated a significantly (P<0.0001) higher levels of ICPO, UL42 and US11 in PKR-/- cells rather than in HEp-2 parental cell lines highlighting that the lack of viral control mediated by PKR allow to virus to improve its replicative capability.

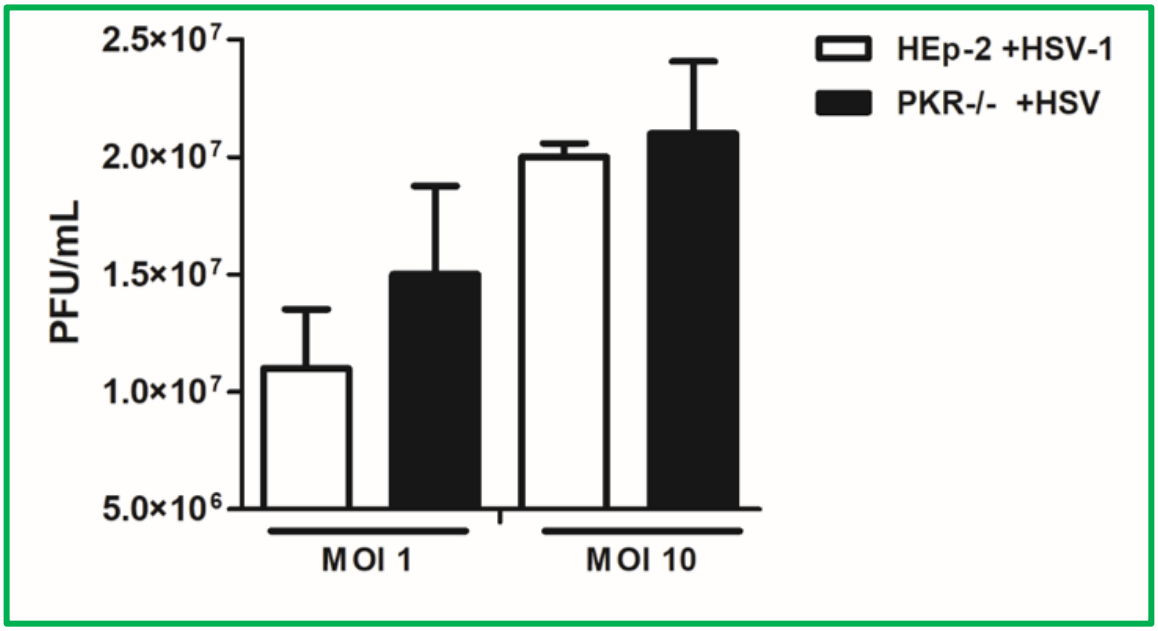

Figure 26: MOI-dependent virus yields of HSV-1 in HEp-2 and PKR-/- cell lines. HEp-2 and PKR-/- were infected with HSV-1 at MOI 1 and 10. The samples were harvested at 24h post infection and the virus yields were measured by standard plaque assay on Vero cells. The procedure was performed as follow: The samples were frozen and thawed for three times to obtain the total amount of virus (cell attached and unattached virus) and after were serially diluted 1:10 and used to infect Vero cells monolayers as described in Material and Methods.. The procedure was performed in triplicate ± SD.

Lastly, it has been evaluated the effect of loss of PKR on the replication of HSV-1 by standard plaque assay. As showed in figure 26, HEp-2 and PKR-/- cell lines were infected at two different MOIs (MOI 1 an MOI 10, respectively) with HSV-1, collected at 24h post infection and used to perform a plaques assay on Vero cells monolayers. The viral yields, obtained as described in material and methods, indicate the amount of total viral particles produced in PKR-/- and parental cell lines and the value of permissiveness of both cell lines. The results match with the findings obtained by Smilley's group [98] in other cell system, and show that, inactivating PKR does not fully rescue viral replication in all condition tested (Fig. 26).

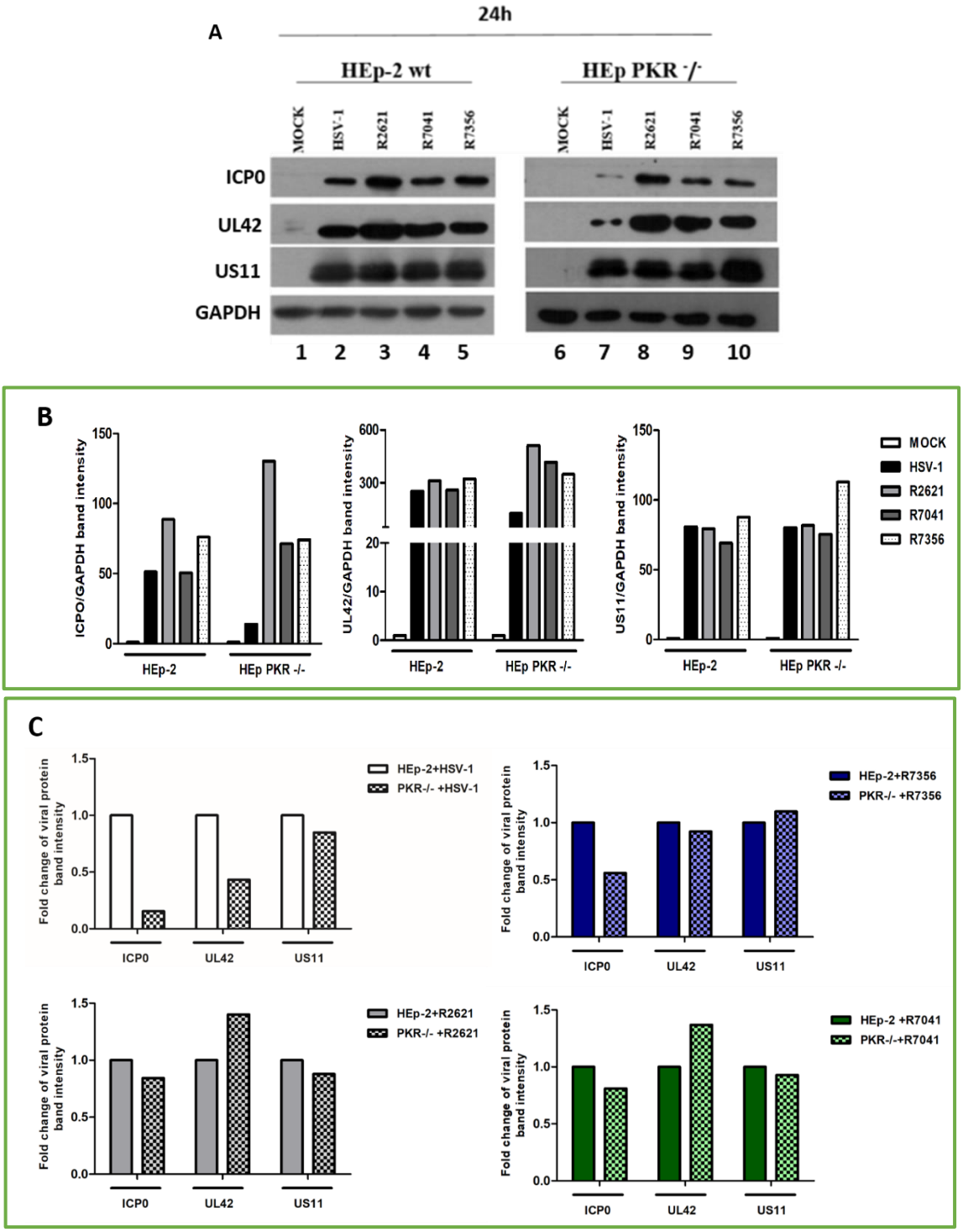

Figure 27: Expression of viral proteins cascade in HEp-2 and PKR-/- cell lines. (A) HEp-2 and PKR-/- were infected with HSV-1, R2621, R7041 and R7356 at MOI 10 and collected at 24h post infection. The protein extracts were separated by polyacrylamide gel electrophoresis and the ICP0, UL42 and US11 expression levels were detected. GAPDH was used as a housekeeping control. (B-C) Band density of was determined with the T.I.N.A. program, and was expressed as fold change over the appropriate housekeeping genes. Panel B graphically compares the expression levels of α (ICPO), β (UL42) and γ (US11) genes in HSV-1 and mutant viruses infected HEp-2 and PKR-/- cell lines. Panel C represents the fold change of viral proteins in PKR-/- compared to parental cells upon HSV-1 and mutant viruses infection.

Besides, western blot analysis was performed on HEP-2 compared to PKR-/- cell lines to detect: i) the expression levels of viral immediate-early (α), early (β), and late (γ) proteins; ii) the different expression of viral proteins cascade following infection with HSV-1 and considered all mutant viruses employed in this study. Therefore, HEp-2 and PKR-/- were infected with HSV-1, R2621, R7041 and R7356 at MOI 10 and collected at 24h post infection. Based on previous results showed in figure 25, we expected to find a rescue in the expression of viral proteins cascade.

The expression levels of viral immediate-early (α), early (β), and late (γ) protein following HSV-1 infection were showed in figure 27A and graphically reported in figure 27B and C. The results show a low amount of ICPO and UL42 proteins_in PKR-/- infected with HSV-1 compared to HEp-2 (Fig. 27, lane 7 vs 2). Any difference between both cell lines was detected in US11 protein expression following HSV-1 infection as reported in the quantification of band intensity in figure 27B. In addition, higher amount of immediate-early ICPO protein was detected in PKR-/- following R2621 infection compared to HSV-1, R7041 and R7356 infection more (Fig.27 lanes 8 vs 7,9 and 10) than HEp-2 cells (Fig.27 lanes 3 vs 2,4 and 5). Early protein UL42 is highly expressed following infection with R2621 and less with R7041 in PKR-/- (Fig.27 lanes 8 and 9 and 27C). Any differences in the expression levels of late protein US11 were detected in both HEp-2 and PKR-/- cells. The fold change of viral proteins in PKR-/- compared to parental cells upon HSV-1 and mutant viruses infection is showed in figure 27C.

These finding suggest that the inactivation of PKR not fully rescue the HSV-1 replication and it was limited at the transcriptional levels and viral DNA synthesis rather than accumulation of viral proteins and production of virus particles.

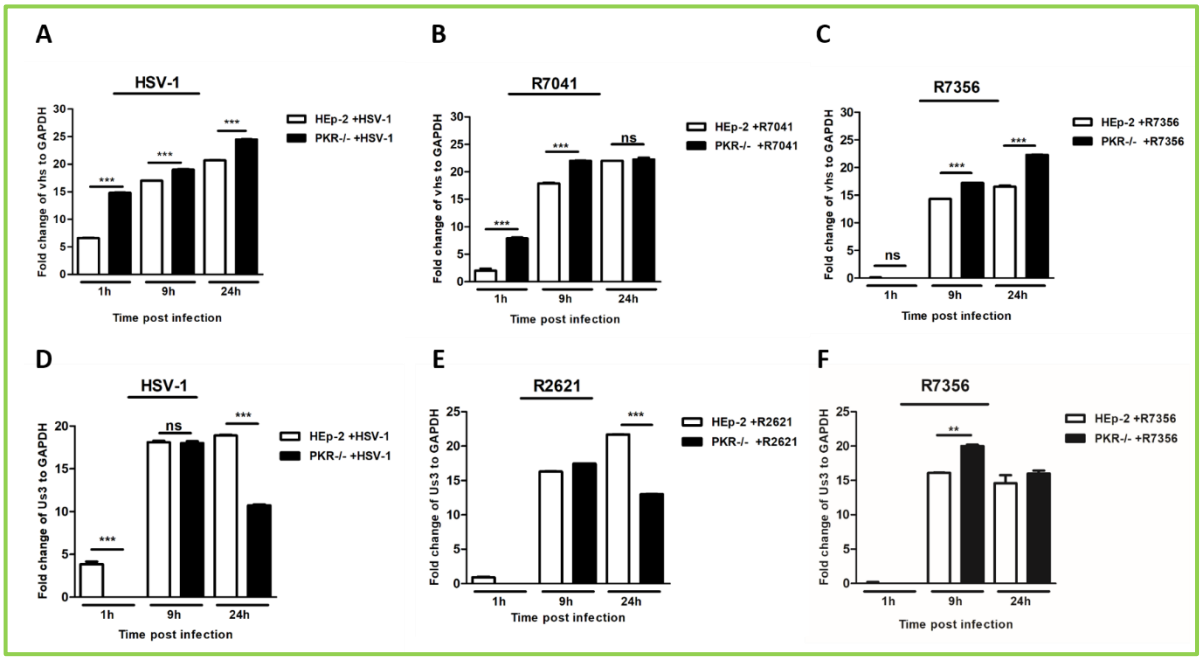

Figure 28: Expression of VHS and US3 transcripts in HEp-2 and PKR-/- cells infected with wild type and mutant viruses. HEp-2 and PKR-/- cells were infected MOI 10 with HSV-1, R2621, R7041 and R7356 and collected at 1h, 9h and 24h post infection. The mRNA was purified with Trizol according to manufacturer's instructions. The measure of changes in the expression level of each considered gene was analyzed calculating the value of 2^-ΔΔCt. The assay was performed as means of triplicate ± SD and expressed as fold change over the housekeeping genes. *** indicate significant changes (P<0.0001).

Previous results, shown in figure 22, have demonstrated that the accumulation of VHS transcripts can depends on the presences of US3 and UL13 proteins. Therefore, in the Figure 28, quantitative Real-time PCR was performed to evaluate whether the temporal regulation of VHS and US3 transcripts in R2621, R7041 and R7356 mutant viruses compared to HSV-1, occurs or not with a PKR-dependent mechanism. The results show that: i) The VHS transcripts progressively increase in both cell lines even if a significant accumulation (P<0.0001), were detected in PKR-/- cells infected with HSV-1 (Fig. 28 A). ii) The VHS transcripts progressively increase in both cell lines, up to 9h in PKR-/- more than HEp-2 cells infected with R7041(Fig. 28 B). iii) Significant increase (P<0.0001) of VHS transcripts was detected 24h post R7356 infection in PKR-/- (Fig.28C). iv) The US3 transcripts were significantly decreased (P<0.0001) following HSV-1 and R2621 infection at 24h (Fig. 28 D and E).

Anysignificant results were obtained following R7356 infection at 1h and 24h, with the exception of 9h (Fig. 28 F). These findings suggest that the accumulation of VHS transcripts was affected by PKR. Surprisingly, the loss of PKR allows both HSV-1 and R2621 viruses to not accumulate US3 transcripts at late time or viral replication.

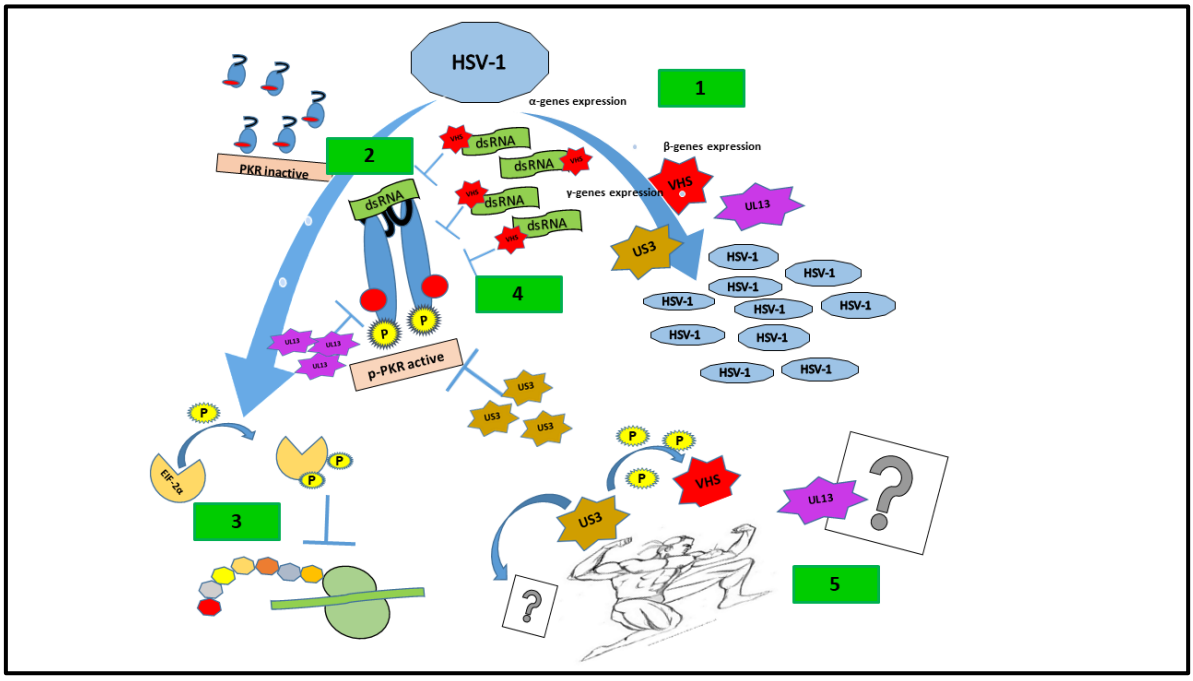

Figure 29: Graphical model of PKR regulation mediated by VHS, US3 and UL13. 1) The HSV-1 productive cycle represents a multifactorial event drove by a strictly regulated temporal cascade of gene expression divided in: immediate-early (α), early (β), and late (γ) which terminate with the production of new virions. 2) The virus-host interaction triggers the innate immune response mediated by PKR protein that interacting with the overlapped mRNA transcripts, produced during HSV-1 replication mimic dsRNA responsible for its activation. 3) The PKR activation induces phosphorylation of the alpha subunit of eukaryotic initiation factor-2 (eIF2α) and inhibits protein synthesis. 4) At the same time of the stimulation of cellular response, HSV-1 accumulates viral proteins involved in the immunological escape and in the inhibition of innate immune response PKR-mediated. VHS tegument protein probably degrades dsRNAs, which are responsible of PKR activation; 5) US3 and UL13 tegument protein control the activation of PKR with a unclear mechanism for UL13 and that seems to involve phosphorylation events mediated by Us3 on VHS linked to the modulation of PKR expression.

Taken together, the results showed above demonstrate that during replication, HSV-1 controls the PKR activation through the viral tegument proteins, VHS, US3 and UL13. The accumulation of viral proteins US3 and VHS, during HSV-1 replication, coincides temporally with the shutdown of the phospho-PKR expression. It is most probably that the endonuclease activity of VHS has an important regulatory role to limit the PKR activation and that US3 induces posttranslational modifications on VHS, which improve its activity. To date, it is possible to sustain that US3 and UL13, control the accumulation of phospho-PKR and regulate the PKR transcripts with a mechanism not yet understood (Fig. 29).

4.2.8. Regulation of transcriptional levels of p53 gene in infected parental and PKR-/- cell lines.

PKR protein has been shown to be an important element in the transcriptional signal transduction pathways activated by specific cytokines, growth factors, double-stranded (ds) RNA, and extracellular stresses. Indeed, PKR has been shown to be required for activation of other protein kinases such as p38, JNK, and IKK [74,153,154] and transcription factors such as NF-κB, IRF-1, p53 and AP-1 [72,73,79,153,155,156]. Based on these data, preliminary experiments were performed to analyze the recruitment of p53 following HSV-1 infection and in presence or not of PKR.

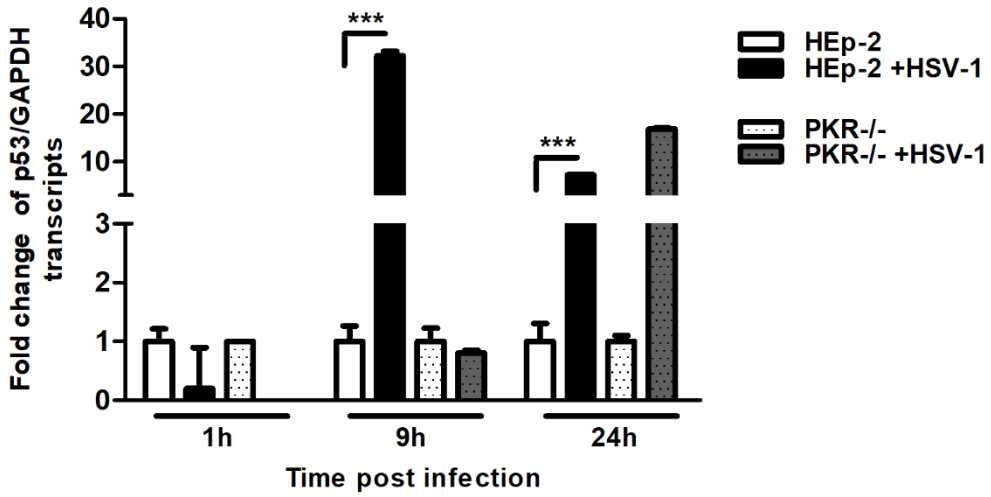

Figure 30: Evaluation of p53 transcripts following HSV-1 infection. HEp-2 and PKR-/- cell lines were mock infected or infected with HSV-1 at MOI 10, collected at 1h, 9h, and 24h and subjected to RNA extraction by Trizol reagent, according to manufacturer's instructions. Quantitative Real-time PCR was used to detect the transcriptional levels of p53 during HSV-1 infection. The expression levels of p53 and GAPDH, used as an endogenous control, were evaluated by using the comparative CT Method (ΔΔCT Method) as described in Materials and Methods. The experiment was performed in triplicate ± SD and *** indicates significant changes ($P<0.0001$).

HEp-2 and PKR-/- cell lines were mock infected or infected with HSV-1 at MOI 10, collected at 1h, 9h, and 24h and subjected to RNA extraction to quantitative Real-time PCR. The results, shown in figure 30, demonstrate: i) significantly high p53 transcriptional levels ($P<0.0001$) in infected HEp-2 and not in PKR-/- at 9h post infection. ii). Accumulation of p53 transcripts in infected PKR-/- cells and HEp-2 at 24h post infection. iii) The accumulation of p53 transcripts depends on viral infection in both cell lines. These findings suggest that during HSV-1 infection, p53 transcriptional levels increase up to 9h and decrease at 24h in HEp-2 cell lines, according to the literature data [139]. In PKR-/- cells the accumulation of p53 transcripts

during HSV-1 infection occurs only at 24h suggesting a delayed cellular response in absence of PKR which probably involves other cellular proteins, mediators of p53 pathway.

Further studies are necessary to analyze the signaling network linking HSV-1 to p53 and PKR and the associated molecular mechanisms.

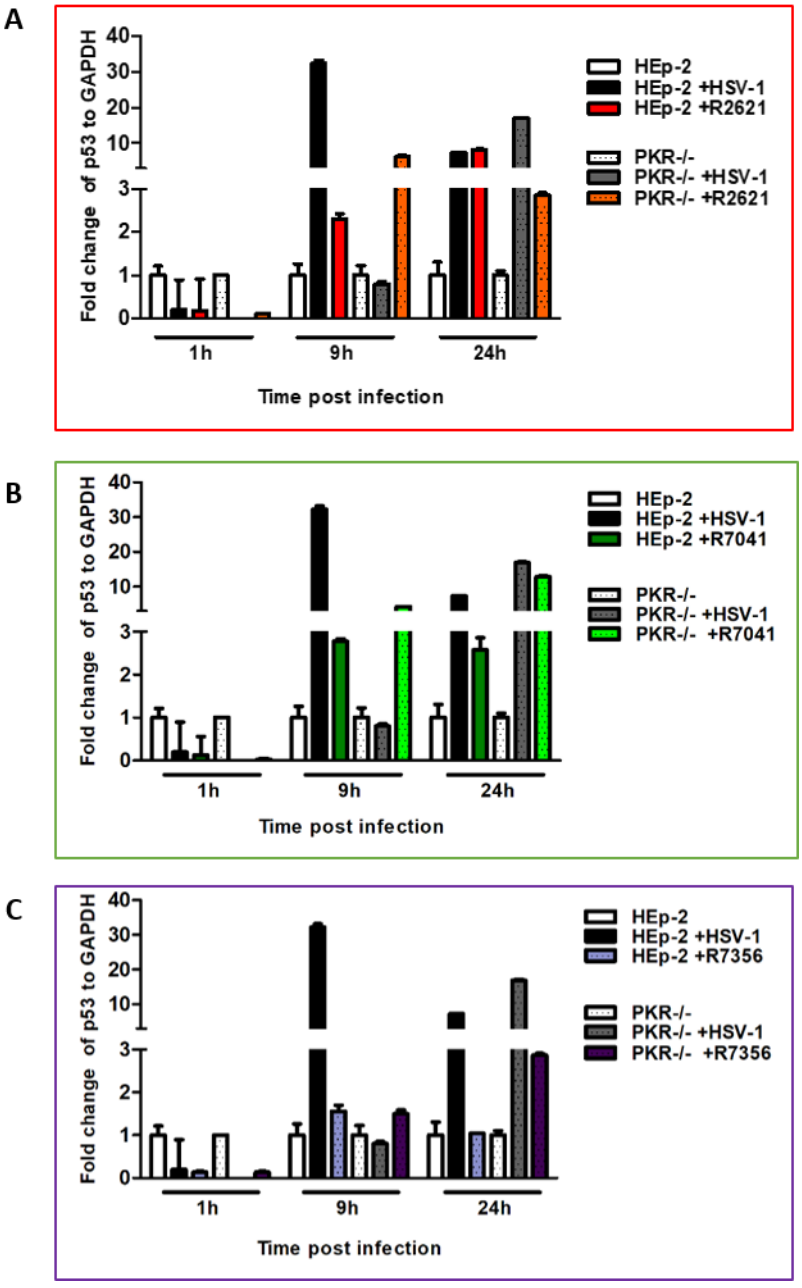

Figure 31: Evaluation of p53 transcripts following R2621, R7041 and R7356 infection and compares to HSV-1 in HEp-2 and PKR-/- cell lines. Cells were mock infected or infected with R2621, R7041 and R7356 at MOI 10, collected at 1h, 9h, and 24h and subjected to RNA extraction by Trizol reagent, according to manufacturer's instructions. Quantitative Real-time PCR was used to detect the transcriptional levels of p53 during viral infection. The expression levels of p53 and GAPDH, used as an endogenous control, were evaluated by using the comparative CT Method (ΔΔCT Method) as described in Materials and Methods. The experiment was performed in triplicate ± SD.

Based on the previous result reporting that p53 transcripts accumulate following HSV-1 infection, the next experiment explains the involvement of VHS, US3 and UL13 in this regulatory mechanism. HEp-2 and PKR-/- cell lines were mock infected or infected with R2621, R7041 and R7356 at MOI 10, and collected at 1h, 9h, and 24h. Samples were subjected to RNA extraction to quantify the transcriptional levels of p53 by Real-time PCR. Previous results have demonstrated that, at 9h post infection, HSV-1 increases the transcriptional levels of p53 in HEp-2 cell lines but not in PKR-/- cells. The results shown in Fig. 31 show a potential control of p53 mediate by considered viral proteins. In particular, in HEp-2 cells: i) at 9h post infection, lower amount of p53 transcripts are detected following infection with R2621, R7041 and R7356 and compared to HSV-1 infection (Fig. 31. A, B, C). ii) At 24h post infection, equal amount of p53 transcriptional levels were detected in R2621 (Fig. 31 A), R7041 (Fig. 31 B) and HSV-1. iii) At 24h post infection, low levels of p53 were detected following R7356 infection (Fig. 31 C). These findings demonstrate that UL13, more than VHS and US3, stimulates the accumulation of p53 transcripts during viral replication. Besides, in PKR-/-: i) at 9h post infection, higher p53 transcripts were detected following infection with R2621 (Fig. 31A) and R7041 (Fig. 31 B) compared to HSV-1 infection. ii) Lower p53 transcripts were detected at 9h following infection with R7356 compared to HSV-1 infection (Fig. 31 C). These findings demonstrate that R2621 and R7041 mutant viruses in absence of PKR tend to increase the transcriptional levels of p53 unlike of R7356. Therefore, HSV-1 stimulates the transcription of p53 with a PKR-dependent and UL13 seems to be involved in this mechanism.

DISCUSSION

The fundamental mission of all viruses is to replicate and spread to persist in the host environment. In order to perform these functions, is essential to confiscate the protein synthetic machinery and reduce the host immune response. Many viruses, including HSV-1, have developed many complex mechanisms to inhibit the innate immune response mediated by PKR. Literature data have demonstrated that HSV-1 contains a late gene, Us11, which, expressed early, binds to PKR and blocks its activation[85,86,]. Instead of blocking its activation, HSV encodes ICP34.5 protein, which recruits the phosphatase alpha to dephosphorylate eIF-2α, preserve the viral protein translation and indirectly block the PKR activity downstream its activation [87]. Several years ago, it has been proposed a new mechanism based on VHS tegument protein. Sciortino et al., 2013[1] showed the accumulation of p-PKR on HT1080 cell lines infected with deleted virus for VHS protein. The key findings reported here complement and extend the studies reported by Sciortino and collaborators. The modulation of PKR was analyzed after infection with HSV-1 and mutant HSV-1-viruses, deleted in tegument proteins closely connected with immunological escape. In particular, in this study it was shown for the first time, that during HSV-I replication, UL13 and US3 collaborate with VHS to regulate PKR activation.

Based on results reported in this work, is possible to divide the following discussions in 3 major tasks: I) The viral protein VHS controls the PKR-phosphorylation levels in different cell lines: HSV-1 controls the accumulation of p-PKR in cell lines-independent manner and with a VHS-dependent mechanism (Fig.13). Infection experiments by using deleted viruses in VHS showed that HSV-1 fails to block p-PKR activation when the RNase activity of VHS is compromised. Transient transfection experiments have been demonstrated also that mutation in the *vhs* gene sequence rather than a block on VHS, mediated by viral regulatory system involving UL48 and UL49, allow to the incapability to repress p-PKR accumulation (Fig. 14).

II) Involvement of viral proteins Us3 and UL13 in the regulation of p-PKR expression levels: About half of the HSV-1 encoding tegument proteins play essential roles in viral transport and maturation. Us3 and ul13 viral protein are involved in these processes but in the same time their kinases enzymatic nature makes them multifunctional viral proteins able to modulate the host metabolism and shutting down the host antiviral mechanism. For this reason, it has been investigated the role of US3 and UL13 tegument viral proteins in the regulation of p-PKR expression levels. US3 and UL13 are serine / threonine kinases involved in the viral and cellular regulation. Their structural role makes them the first viral proteins interacting with the cell instead their kinase activity makes them potential regulators of intracellular pathways.

Therefore, their involvement in the regulation of p-PKR was evaluated by using deleted virus for *us3* and *ul13* genes (Fig.16) and through transient transfection with plasmid DNA expressing US3 and UL13 proteins (Fig. 17). The results demonstrate for the first time that the US3 and UL13 tegument protein control the activation of phospho-PKR and that the signaling network between US3 and VHS is responsible for this control (Fig.18). HSV-1 activates the p-PKR accumulation during viral infection and controls it belatedly when high levels of US3 and VHS are simultaneously detected (Fig 19). In addition, experiments performed by using inhibitors of protein synthesis, have showed that the regulation of PKR mediated by HSV-1 involves the mRNAs accumulation and that an overload of mRNAs and the lack of VHS activity make the virus incapable to control the accumulation of p-PKR (Fig.15). Having established that HSV-1 is able to block the accumulation of p-PKR at late stage of viral infection and that some tegument proteins are involved in this regulatory mechanism, the successive step was to determinate whether the viral control on p-PKR is limited to protein synthesis or whether also affects to the levels of mRNAs expression. This is the aim of the series of experiments, shown in Figures. 21 and 23. At late stage of viral replication, HSV-1 shuts down PKR transcriptional levels compared to temporal accumulation of these in mock cells (Fig.21). In addition, US3 and UL13 negatively affect PKR transcriptional levels (Fig.23), and probably their role in this process depends on the presence of VHS.

III) Analyses of gene and protein expression and HSV-1 Replication in PKR Knocked-Out and parental cell lines: The aim of this series of experiments showed in Fig. 24, 25, 26, 27 and 28, was to examine whether the loss of PKR protein, involved in the innate immune response, rescues the viral replication and viral protein expression. Therefore, PKR-/- and HEp-2 cells were infected with HSV-1 and collected at designed time post infection to evaluate: I) viral DNA quantification by absolute Real-time PCR; II) viral transcripts such as ICPO, UL42 and US11, by relative quantitation Real-time PCR; III) viral titers in HEp-2 compared to PKR-/- cells. Enhancement of viral replication has been correlated to the absence of PKR, highlighting the capability of HSV-1 to better replicate in absence of PKR protein (Fig.24). The HSV-1 replication is normally controlled by host immunological escape mechanism and in particular, PKR represents an important protein involved in this process. The HSV-1 productive cycle represents a multifactorial event drove by a strictly regulated temporal cascade of gene expression divided in three type: immediate-early (α), early (β), and late (γ). To define weather PKR affects to the cascade of the viral genes, the expression levels of ICP0 immediate early, UL42 early and US11 late viral genes, representative of sequential genetic cascade of HSV-1, were detected.

The total absence of PKR produces an uncontrolled viral replication in the viral cycle tardive phases correlated to more increased synthesis of viral DNA wit consequent accumulation of viral transcripts (Fig.25). Otherwise, the loss in PKR function had no any effect on the production of mature viral particles as showed in Fig.26, as well as in the expression of viral proteins cascade(Fig.27). The viral rescue in PKR-/- cells was limited to transcriptional and viral DNA synthesis levels rather than the accumulation of viral proteins and the virus particles production, indicating additional epigenetic regulation to be discovered. Lastly, additionally to its translation regulation function, the PKR protein is also involved in differentiation and in control of cell growth, apoptosis, deletion of the tumor, and RNA-interference. In particular, it has been demonstrated that PKR interacts directly with the C-terminal part of p53 and phosphorylate p53 on the Ser392 residue [73]. The p53 protein responds to a wide range of stress factors through regulation of a variety of cellular pathways, such as apoptosis, cell cycle, cellular senescence, DNA repair, autophagy, and innate immune control [138]. Viral infection represents a type of cellular stress and in the context of HSV-1 infection, it has been demonstrated that p53 plays as positive and negative regulator in HSV-1 replication.

Previous studies have demonstrated that p53 promotes the HSV-1 replication and that, at the same time, downregulates the ICP0 expression[139]. It seems that viruses had developed regulatory mechanisms to utilize one or more of p53's functions to regulate some cell components for efficient viral replication. Based on these data, the transcripts levels of p53 have been analyzed during HSV-1 infection in PKR-/- and parental cell lines and infection with mutant viruses for VHS, US3 and UL13, have been performed to determinate the tegument viral proteins contribution in this cellular pathway. It has been found an accumulation of p53 transcripts during HSV-1 infection according to the literature data. Interestingly, low levels of p53 transcripts have been detected in PKR-/- cells (Fig.30) compared to parental cell lines, suggesting that HSV-1 stimulates the transcription of p53 with a PKR-dependent and that probably, the lack of PKR could stabilize p53 transcripts levels during HSV-1 infection. Lastly, to evaluate whether some of the examined tegument proteins are involved in the accumulation of p53 transcripts during HSV-1 infection, real-time PCR was performed following infection of HEp-2 and PKR-/- cells with R2621, R7041 and R7356 mutant viruses. Low levels of p53 transcripts were detected by R7356 infection in both cell lines, suggesting that the accumulation of p53 transcripts, during HSV-1 infection, could depends on UL13 rather than US3 and VHS viral proteins (Fig. 31). Further studies are necessary to analyze the signaling network linking HSV-1 to p53 and PKR and the associated molecular mechanisms.

CHAPTER V

5.1. Materials and Methods

5.1.1. Synthesis of MWCNT-CD-PEI-Rhod and G-CD@Ada-Rhod and preparation of assemblies based on MWCNTs and G-CD derivatives.

A new multiwalled carbon nanotube-β-cyclodextrin platform (MWCNT-CD) modified with branched polyethylenimine (PEI) and doped with Rhodamine (Rhod), designed as MWCNT-CD-PEI-Rhod, was synthesized as reported in Mazzaglia *et al.*, 2018[2]. To investigate the drug and gene delivery, the MWCNT-CD-PEI-Rhod platform was assembled with Cidofovir, with or without pCMS-EGFP (Clontech) plasmid. Covalent surface modifications of Graphene-based materials (G) with functional cationic cyclodextrin (CD) has been designed for the synthesis of multifunctional G-CD nanoplatform. The fluorescent dye ADA-Rhod was synthesized and used to form stable complex with G-CD and the obtained G-CD@ADA-Rhod complex was used to investigate the cellular uptake. G-CD/Doxo complex was synthetized from G-CD platform assembled with anticancer drug Doxorubicin (Doxo). G-CD@ADA-Rhod/pCMS-EGFP was assembled from CD@ADA-Rhod combined with the pCMS-EGFP plasmid (Clontech) and was used for gene delivery studies.

5.1.2. Cell cultures and virus.

Cell lines were originally obtained from the American Type Culture Collection (ATCC). Kidney epithelial cells from African green monkey, (Vero), were propagated in EMEM (Lonza, Belgium), supplemented with 6% fetal bovine serum (FBS, Euroclone), 100 U/ml penicillin and 100µg/ml streptomycin mixture (Lonza, Belgium). Human epithelial type 2 cells from laryngeal carcinoma, (HEp-2), were grown in RPMI 1640 medium (Lonza, Belgium) supplemented with 10% FBS, 100 U/ml penicillin and 100µg/ml streptomycin mixture. Wild type acute monocytic leukemia (THP-1) cells, kindly provided by Prof. Bernad Roizman (Kovler Laborators, University of Chicago, USA), were maintained in RPMI-1640 medium (Lonza, Belgium) supplemented with 10% FBS (Euroclone), 100 U/mL penicillin and 100 U/mL streptomycin, 1mM Sodium Piruvate, 10 mM Hepes Buffer. Human monocyte from histiocytic lymphoma (U937) cells were propagated in RPMI 1640 medium (Lonza, Belgium) supplemented with 2 mM L-glutamine, 100 U/ml penicillin, 100 µg/ml streptomycin, and 10% FBS (Euroclone).

Human epithelial cells from cervix carcinoma (HeLa) were growth in RPMI 1640 medium supplemented with (Lonza, Belgium) 10% FBS, 100 U/ml penicillin and 100µg/ml streptomycin mixture. All cell lines were cultured at 37°C in a 5% CO_2 incubator. The prototype HSV-1 (F) strain was a generous gift from Professor Bernard Roizman (University of Chicago, IL, USA). Viral stocks were propagated and then titered in Vero cells.

5.1.3. Antiviral activity of MWCNT-CD-PEI-Rhod/Cid and MWCNT-CD-PEI Rhod/Cid/pCMS-EGFP complexes.

The antiviral effects of nanoplatform complexes was evaluated through plaque reduction assay on Vero cells by using three different concentrations of the cyclodextrin modified carbon nanotubes (0.05 mg/mL; 0.025 mg/mL; 0.0125 mg/mL) with related Cidofovir (Cid) concentrations [(Cid)= 6.2µM; (Cid)=3.1µM and (Cid)= 1.5 µM]. For the assay procedure, the virus inoculum was diluted to yield 60 plaques/100 µL. Confluent monolayers of Vero cells were cultured in 24 multiwall plates and were infected with 100µl of each dilution. The plates were incubated for 1 h at 37 °C with gently shaking. Then, the viral inoculum was removed and monolayers were covered with Dulbecco's modified Eagle's medium containing 0.8% methylcellulose in the presence of tested samples at different concentrations. After 3 days, the medium was removed and the cells were fixed, stained with crystal violet, and visualized at 10x magnification with an inverted microscope (Leica DMIL) for plaque detection. The data were analysed as means of triplicate± SD for each dilution.

5.1.4. Studies of cellular uptake and co-localization of MWCNT-CD-PEI-Rhod.

Vero cells were pre-incubated for 1h at 37°C with a caveolae-mediated and a clathrin-mediated endocytosis inhibitor, filipin (2.5µg/mL) and sucrose (0.45M), respectively. Cells were then treated for additional 24h with MWCNT-CD-PEI-Rhod (0.05 mg/mL) in presence or absence of the inhibitors. The intracellular fluorescence of MWCNT-CD-PEI-Rhod was evaluated thought fluorescence microscope observation. After the incubation time, cells were layered on polylysinated slides and analyzed with standard DAPI/FITC/TRITC filter sets in a Biomed Fluorescence microscope (Letiz, Wetzlar, Germany). The nuclei were stained with Hoechst 33342 fluorescent DNA-binding dye.

5.1.5. Study of endocytic compartmentation of MWCNT-CD-PEI-Rhod.

Vero cells were simultaneously transduced with 100 µL of CellLight® Lysosomes-GFP (Cat. No. C10596) in presence of MWCNT-CD-PEI-Rhod (0.05 mg/mL). Twenty-four hours later, cells were collected and layered on sterile polylysinated slides for fluorescence microscope analysis (Biomed, Letiz, Wetzlar, Germany). Nuclei were visualized by staining with Hoechst 33342. Live-cell imaging was analysed using standard DAPI/FITC/TRITC filter sets.

5.1.6. Cell viability assay.

The cell viability of Vero and HEp-2 cells treated with MWCNT-CD-PEI-Rhod complex or Graphene-based vector (G-CD@ADA-Rhod and G-CD/Doxo) was determined on the basis of ATP levels using ViaLight™ plus cell proliferation and cytotoxicity bioassay kit according to the manufacturer's instructions (Lonza Group Ltd., Basel, Switzerland). Cells were grown in wells of 96-well plates and treated with different concentrations of indicated carbon-based nanoplatform complex and their conjugates. After the indicated incubation time the cells were harvested and the emitted light intensity related to ATP degradation was quantified with the GloMax Multi Microplate Luminometer (Promega Corporation, 2800 Woods Hollow Road Madison, WI, USA). The luminescence value was converted to the cell proliferation index (%) according to the following equation:

Cell viability % = [(A-B)/(C-B)] %

Where A denotes the average of treated sample, B represents background luminescence and C represents the average of untreated samples.

5.1.7. Inhibitors employed in cellular uptake evaluation.

HEp-2, THP-1, U937 and Vero cell lines were treated or untreated with 100µg/mL, 50 µg/mL and 25 µg/mL for 24 hours to investigate the intracellular uptake. HEp-2 cells were used to investigate the meccanism of internalization of G-CD@ADA-Rhod. Cells were pre-treated for 1h with endocitosisi inhibitors: Cytocalasin D (1µM) Chlorpromazine (10µM), Genistein (50µM or 5 µM), Simvastatin (5µM) and Wortmannin (10µM), followed by incubation for 24h with G-CD@ADA-Rhod (50µg/mL) in the presence of endocytosis inhibitors. After the indicated incubation time, the intracellular fluorescence of MWCNT-CD-PEI-Rhod was evaluated thought fluorescence microscope observation. Cells were layered on poly-lysinated slides and analysed with standard DAPI/FITC/TRITC filter sets in a Biomed Fluorescence microscope (Letiz, Wetzlar, Germany). The nuclei were stained with Hoechst 33342 fluorescent DNA-binding dye.

5.1.8. Intracellular uptake of G-CD/Doxo.

HEp-2 cells were untreated or treated with G-CD/Doxo (25 μg/mL) for 24h. Doxorubicin was used as a control. The sample were collected and washed with warm PBS for twice, fixed with PFA 4% for 30 minutes at room temperature and permeabilized with Triton 0, 1% for 1h, covered with a drop of mounting solution (ProLong™ Diamond Antifade Mountant with DAPI-Invitrogen p36971) for 30 minutes in a dark room and analyzed by a Confocal laser scanning microscopy Leica TCS SP8.

5.1.9. Intracellular signalling pathway of graphene-based nanosystem G-CD/Doxo complex.

HEp-2 and Vero cells line were untreated or untreated with 25μg/mL of G-CD/Doxo for different time. Doxorubicin was used as a control. Different conditions are indicated in the relative figures legend. After the indicated incubation time the cells were harvested and processer for immunoblot analysis or Real-time PCR.

5.1.10. Protein extractions and immunoblot analysis.

To obtain total proteins extraction cells were lysed in 62.5 mM Tris-HCl pH 6.8; DTT 1 M; 10% glycerol; 2% SDS; 0.01% Bromophenol Blue and held at 100 °C for 5 min. Nuclear and cytoplasmic fractions were isolated as reported elsewhere[157] and analysed for protein determination using a Qubit™ Protein Assay Kit (Invitrogen™). An equal amounts of protein extracts was subjected to Sodium dodecyl sulfate-polyacrylamide gel electrophoresis (SDS-PAGE) and transferred to nitrocellulose membranes (Bio-Rad Life Science Research, Hercules, CA). After incubation in blocking buffer, membranes were probed overnight at 4°C with the specific primary antibody, and then probed for 1h at RT with secondary antibodies, followed by chemioluminescent detection, according to the manufacturer's instructions. Protein bands were visualized by using Immobilon Classico Western HRP substrate (Merk, Millipore) and Super Signal West Pico (Thermo Scientific, Rockford, IL) as a chemiluminescent substrates. The expression levels of GAPDH or LAMIN B1 were used as loading controls. Quantitative densitometry analysis of immunoblot band intensities was performed by using the TINA software (version 2.10, Raytest, Straubenhardt, Germany) or ImageJ software.

5.1.11. Antibodies and Inhibitors.

Antibodies to the phosphorylated form of CDK-2 (T14-Y15; sc-101656) and to Wee-1 (B11; sc-5885) were purchased from Santa Cruz Biotechnology (Santa Cruz, CA). Antibodies to E2F-1 (#3742), phospho-p53 (Ser15; #9284), phosho-MDM2 (ser166; #3521), p21 Waf1/Cip1 (12D1; #2947), LC3B (D11; #3868), SQSTM 1-p62 (D5L7G; #88588), and BCL-2 (D17C4; #3498) were provided from Cell Signaling Technology®. Monoclonal antibody to MDM2 (ab38618) was purchased from Abcam. Polyclonal antibodies against the housekeeping gene GAPDH and LAMIN B1 (D9V6H) (#13435) were purchased from Abcam and Cell Signaling Technology®, respectively. Secondary antibodies anti-rabbit and anti-mouse IgG conjugated to peroxidase were also from Merck Millipore. Cytocalasin D (C8273) Chlorpromazine (C8138), Genistein (G6649), Simvastatin (S6196) and Wortmannin (W1628) were purchased from Sigma Aldrich.

5.1.12. RNA extraction, Reverse Transcription and Real-time PCR.

Total RNA was extracted using TRIzol® (Life Technologies) according to the manufacturer's instructions and reverse transcription was performed using ReverTra Ace® qPCR RT Master Mix (FSQ-201 Toyobo). The RT reaction was carried out in under the following conditions: at 37°C for 15 min, followed by 50°C for 5 min and 98°C for 5 min. The cDNA was stored at -80 °C and used for quantitative Real-time PCR. Quantitative Real-time PCR was carried out on a Cepheid Smart Cycler II System (Cepheid Europe, France) using Maxima SYBR Green (Thermo fisher Scientific). Shortly, the PCR reaction was carried out under the following conditions: initial denaturation at 95 °C for 10 min, 35 cycles at 95 °C for 15 sec/ 60 °C for 30 sec/72 °C for 45 sec, followed by generation of melting curve from 72 °C to 95 °C. The cDNA copy numbers were normalized to 18S[144,145]. The analytic primers for Real-time PCR are following:

E2F-1: Fw 5'-ACCTGGAAACTGACCATCAG-3' and Rev:3'-GTTCAGGTCGACGACACCGT-5'

18S: FW 5'-CTCAACACGGGAAACCTCAC-3' and Rev 3' CGCTCCACCAACTAAGAACG-5'

Each quantitative Real-time PCR experiments include a minus-reverse transcriptase control.

5.1.13. Evaluation of Autophagic flux by using the tandem mRFP-GFP-LC3 and by LC3I, LC3II/ SQSTM-p62 autophagy-related proteins.

HEp-2 were grown in multiwell culture slides and transiently transfected for 48h with mRFP-GFPLC3 plasmid [158] and 24h post transfection were untreated and treated with 25 µg/mL of Doxo and G-CD/Doxo and collected to be observed by Confocal laser scanning microscopy Leica TCS SP8. For the expression analysis of LC3I, LC3II and SQSTM-p62 proteins, HEp-2 cells were treated or untreated with G-CD/Doxo (25 µg/mL) for 24h, 48h and 72h. The cells were then collected and processed for protein extraction and immunoblot analysis.

5.1.14. Intracellular signalling pathway triggered by G-CD/miRNA-15a.

HEp-2 cell lines were treated with 25µg/mL of G-CD, G-CD@ADA-Rhod and G-CD/miRNA-15a for 24h. The G-CD/miRNA-15a was used with different N/P ratio and non-target (NT) miRNA was used as a negative control. After the incubation time cells were collected and processed for total protein extraction and immunoblot analysis in order to investigate expression of anti-apoptotic protein Bcl-2.

5.1.15. Statistical analysis.

The statistical studies were performed with One-way analysis of variance (ANOVA) and Student's t-test in order to compare different conditions. Quantitative densitometry analysis of immunoblot bands intensity was performed using T.I.N.A. software (version 2.10, Raytest, Straubenhardt, Germany) or ImageJ. For the data analysis and graphical representations, the GraphPad Prism 6 software (GraphPad Software, San Diego, CA, USA) was used. Each experiment was repeated for at least three times. The results are reported as means ±SD and asterisks (*, ** and ***) indicate the significance of *p*-values less than 0.05, 0.01 and 0.001, respectively.

5.2. RESULTS

5.2.1. Intracellular trafficking of multiwalled carbon nanotubes

The aim of this work was to analyze intracellular pathways and biological response stimulated by two potential engineered non-viral vectors in order to better design an engineered vector useful to: I) internalize into the cells II) deliver and release the cargo iii) stimulate a cellular response. Therefore, in the second part of this work thesis, two representative carbon-based nanomaterials, carbon nanotubes (CNTs) and graphene (G) have been evaluated as nanoplatforms to delivery anticancer and antiviral drugs, plasmid DNA and miRNA. CNTs can be described as rolled-up sheets of graphene forming single or multiwalled seam-less cylinders (SW- and MWCNTs, respectively). In our experiment, we use MWCNTs chemically modified with β-cyclodextrins (CDs) and branched polyethylenimine (PEI). The hybrid ternary materials were conjugated with Rhodamine (Rhod) to track in vitro the nanocarrier and to elucidate the uptake cellular mechanisms. The first investigated carbon-based nanovector is the nanoplatform namely MWCNT-CD-PEI-Rhod, the biological evaluation includes: I) the intracellular uptake and the associated mechanisms, II) the capability to delivery antiviral drug and the related response, III) the lysosomal compartment localization. The results, shown in this section, have been published by Mazzaglia A. et al., 2018[2].

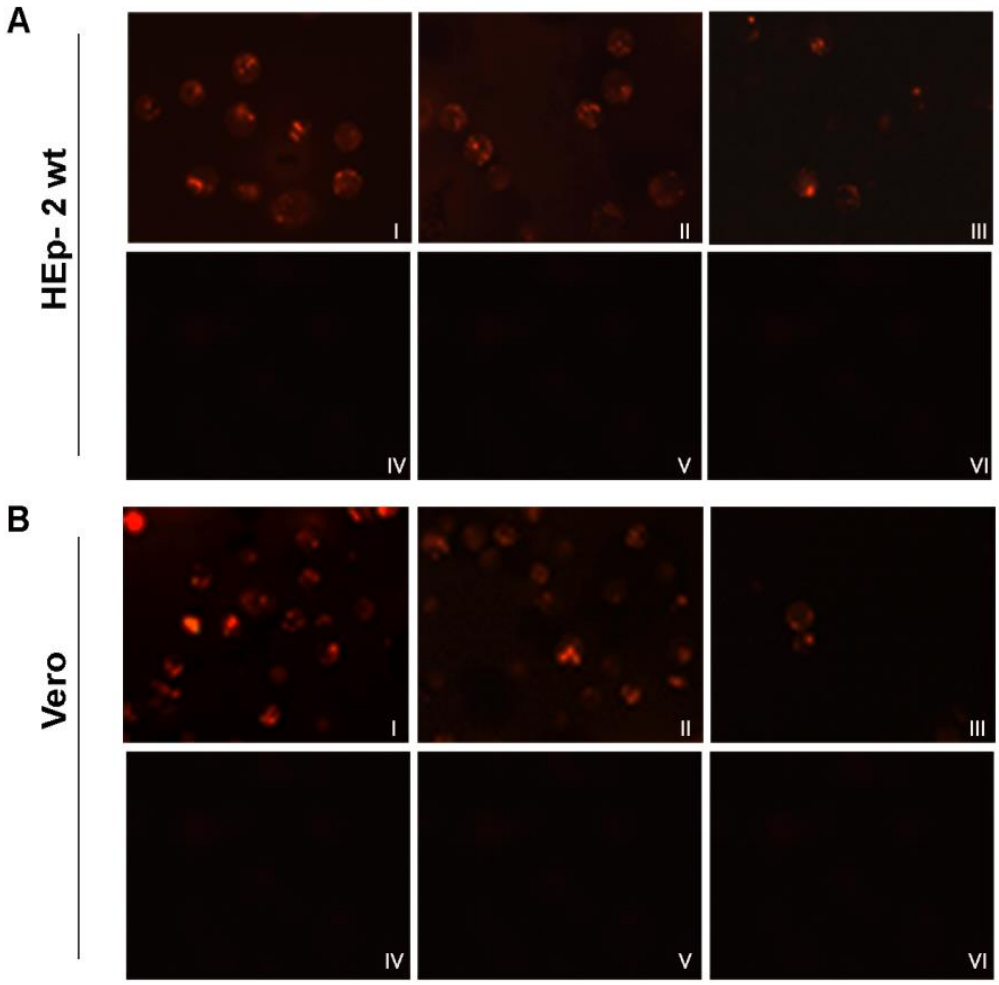

Mazzaglia A. et al.,2018

Figure 32: Cellular Uptake of MWCNT-CD-PEI-Rhod. HEp-2 cells and Vero cells were treated with MWCNT-CD-PEI-Rhod for 24h, collected and observed with fluorescence microscopy. (A) Fluorescence images of HEp-2 cells treated with MWCNT-CD-PEI-Rhod at concentration of 0.1 mg/mL (I), 0.05 mg/mL (II), and 0,025mg/mL (III). (B) Fluorescence images of Vero cells treated with MWCNT-CD-PEI-Rhod at concentration of 0.1 mg/mL (I), 0.05 mg/mL (II), and 0.025mg/mL (III). The cells were also treated with control platform without Rhodamine at concentration of 0.1 mg/mL and untreated as shown in IV, V and VI, respectively, for both panel A and B. Nanotubes internalization coincides with red fluorescent dots

The success of an engineered vector is the capability to internalize into the cells without or with a low cytotoxicity effect. For this reason, cytotoxicity assay (data not show) and cellular uptake experiments were performed. The figure shows the intracellular internalization of MWCNT-CD-PEI-Rhod nanoplatform. The assay was performed in non-tumor-animal and tumor-human cell lines. HEp-2 and Vero were treated with MWCNT-CD-PEI-Rhod at different concentrations [0.1mg/mL (I), 0.05mg/mL (II), 0,025mg/mL, (III)] for 24h and processed to auto-fluorescence analysis.

Fluorescence microscope analysis showed red dots corresponding to the internalized nanotubes in both cell lines (Fig 32. panel A I, II, III and panel B I, II and III) compared to the cells exposed to control platform without Rhodamine, as shown in IV, V and VI, respectively, for both panel A and B.

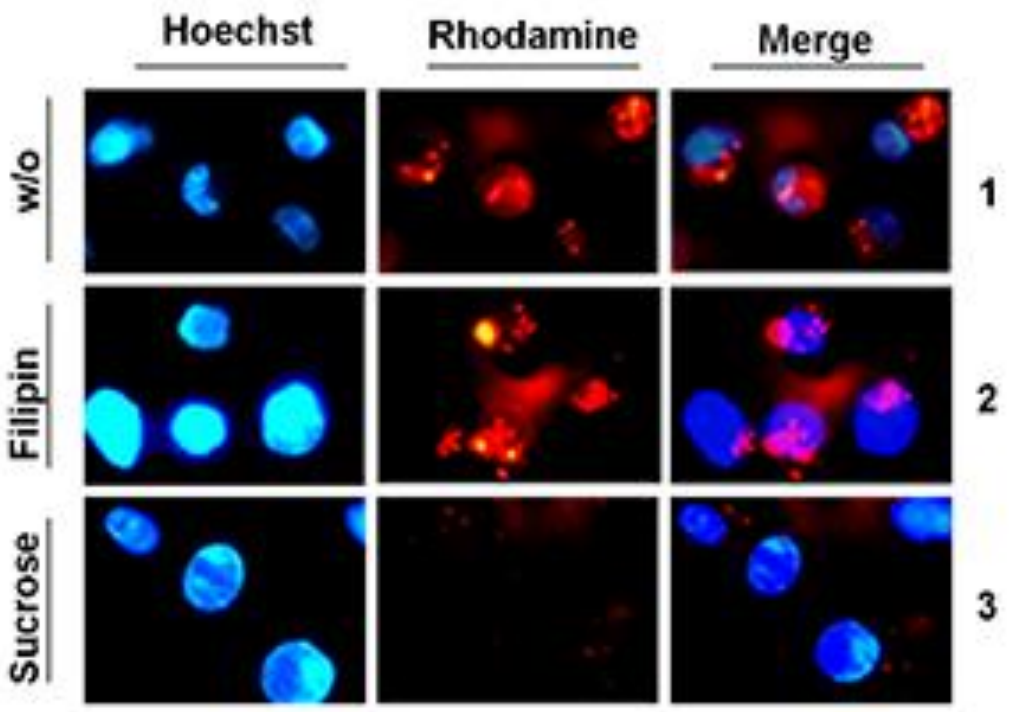

Mazzaglia A. et al.,2018

Figure 33: **Cellular uptake of MWCNT-CD-PEI-Rhod in the presence of two endocytosis inhibitors.** Vero cells were pre-incubated with filipin (2.5µg/mL) and sucrose (0.45M), caveolae-mediated and clathrin-mediated endocytosis inhibitors, respectively. After 1h incubation at 37°C the cells were then treated for additional 24h with MWCNT-CD-PEI-Rhod (0.05 mg/mL) in presence of the inhibitors and relative untreated controls. Standard DAPI/FITC/TRITC filter set was used to detect the intracellular fluorescence of MWCNT-CD-PEI-Rhod. Lane 1 shows Vero cells treated with MWCNT-CD-PEI-Rhod. Lanes 2 and 3 show Vero cells treated with MWCNT-CD-PEI-Rhod in the presence of filipin and sucrose, respectively. The nucleus was stained with Hoechst 33342 fluorescent DNA-binding dye. The merged images were reported in the last column. Nanoplatform internalization coincides with red fluorescent dots.

The uptake of MWCNTs or their conjugates by the cells was suggested to occur by different pathways such as phagocytosis, endocytosis or by an insertion and diffusion mechanism in which MWCNTs act as nanoneedles. To elucidate the cellular uptake, Vero and HEp-2 cell lines were incubated with to MWCNT-CD-PEI-Rhod in presence and treating with specific endocytosis inhibitor (sucrose and filipin). Sucrose treatment is known to deactivate the clathrin-dependent mechanism for cell internalization and filipin is able to block caveole-dependent endocytosis[132].

The results showed that, compared to the untreated cells (Fig. 33 lane 1), the sucrose treatment inhibits the nanotube internalization instead the filipin treatment no affects it. This finding demonstrated that the block of clathrin-dependent pathway affects to MWCNT-CD-PEI-Rhod internalization suggesting that MWCNT-CD-PEI-Rhod prefers clathrin-mediated endocytosis mechanism to entry inside the cells.

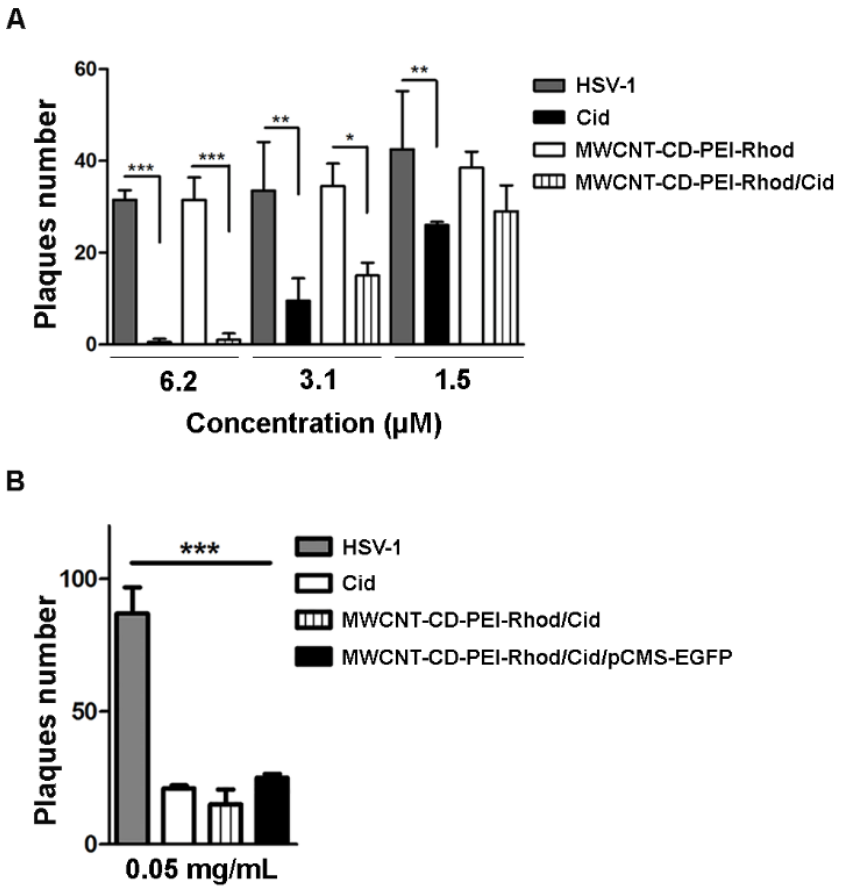

Mazzaglia A. et al.,2018

Figure 34: Plaque reduction assay of MWCNT-CD-PEI-Rhod/Cid and MWCNT-CD-PEI-Rhod/Cid/pCMS-EGFP complexes. Vero cells were infected with 100µL of the viral inoculum diluted to yield 60 plaques of HSV-1 and incubated for 1h at 37 °C. After the incubation time, the monolayers were overlaid with DMEM containing 0.8% methylcellulose in the presence of different concentrations of the cyclodextrin modified carbon nanotubes (0.05 mg/mL; 0.025 mg/mL; 0.0125 mg/mL) with related Cidofovir (Cid) concentrations [(Cid)=6.2µM; (Cid)=3.1µM and (Cid)= 1.5µM]. A) Antiviral activity at different Cid concentrations (6.2µM; 3.1µM and 1.5 µM). B) Antiviral activity of MWCNT-CD-PEI-Rhod/Cid and MWCNT-CD-PEI-Rhod/Cid/pCMS-EGFP complexes at 0.05mg/mL ([Cid] = 3.1 µM). The data were analysed as means of triplicate± SD for each dilution and asterisks (*, **, and ***) indicate the significance of p-values less than 0.05, 0.01, and 0.001, respectively. HSV-1 means infected and untreated cells; Cid means infected and Cidofovir treated cells.

Having estabilished that the designed platform is able to intracellular uptake, the next step was to verify the capability to deliver the antiviral drug, Cidofovir (Cid) into the cells. Therefore, the antiviral activity was performed through plaque reduction assay, as described in Material and methods. Vero cells were infected with HSV-1 and, after the incubation time, the monolayers were covered with Dulbecco's Modified Eagle's Medium containing 0.8% methylcellulose in the presence or not of Cid complexed with MWCNT-CD-PEI-Rhod at different concentrations (0.05mg/mL; 0.025 mg/mL; 0.0125 mg/mL). After 3 days, the cells were fixed, stained with crystal violet and visualized with an inverted microscope for plaque detection.

The antiviral effect of MWCNT-CD-PEI-Rhod/Cid complex was evaluated by analyzing the capability to inhibit plaque formation (Fig.34). In fact, the number of plaques in infected Vero cells exposed to MWCNT-CD-PEI-Rhod/Cid significantly decreases compared to HSV-1 and MWCNT-CD-PEI-Rhod controls, suggesting that the antiviral activity was due to the action of released drug into the cells (Fig.34 A). The drug and gene delivery ability of MWCNT-CD-PEI-Rhod nanoplatform was studied by performing parallel experiments of reduction plaque assay and auto fluorescence imaging. The platform was complexed with DNA plasmid encoding enhanced green fluorescence (pCMS-EGFP) to form MWCNT-CD-PEI-Rhod/pCMS-EGFP and the fluorescence microscope analysis showed red dots corresponding to internalized nanotubes but no green dots related to the expression of the green fluorescent protein (data not shown). Instead, the platform complexed with Cid and pCMS-EGFP (MWCNT-CD-PEI-Rhod/Cid/pCMS-EGFP) and used to reduction plaques assay, showed a significantly reduction of the number of plaques compared to HSV-1 control and similar to the reduction produced by Cid (Fig.34 B). This finding suggested that the antiviral effect was preserved also in the case of dual drug loading. These results suggested that the functionalized platform binding nucleic acid has a good tolerability and did not interfere with release of antiviral agent. However, the expression of entrapped nucleic acid failed, probably due to the slow escape from lysosome of nucleic acid tightly connected to the platform and consequently the lysosomal environment pH could trigger the nucleic acid degradation. For this reason, further studies were performed on another type of carbon-based materials to improve the design of non-viral vector able to gene delivery.

5.2.2. Characterization of new graphene-based platform internalization mechanism

In the framework of Research & Mobility project "Signalosome Complex Activation by New Nanotherapeutic Agents in Viral and Cancer Treatment" the GCD graphene based nanoplatform has been investigated. The pattern of multifunctional GCD nanoplatform has been designed to contain different sites of interactions for the molecular recognition: i) CD cavities for the entrapment of hydrophobic drugs or fluorescent probes; ii) cationic external CD rims for the electrostatic interactions with oligonucleotides; iii) G surfaces for the loading of drugs by π-π interactions (Doxorubicin, Dox) (Fig. 35). With the aim to study the physico-chemical characteristics of cationic GCD platform and its ability to cross the cell membrane, the fluorescent dye Ada-Rhod was synthesized and used to form stable complex with GCD. Taking advantage of high affinity of adamantane for CD cavities the complex Ada-Rhod@CD was used to investigate the cellular uptake.

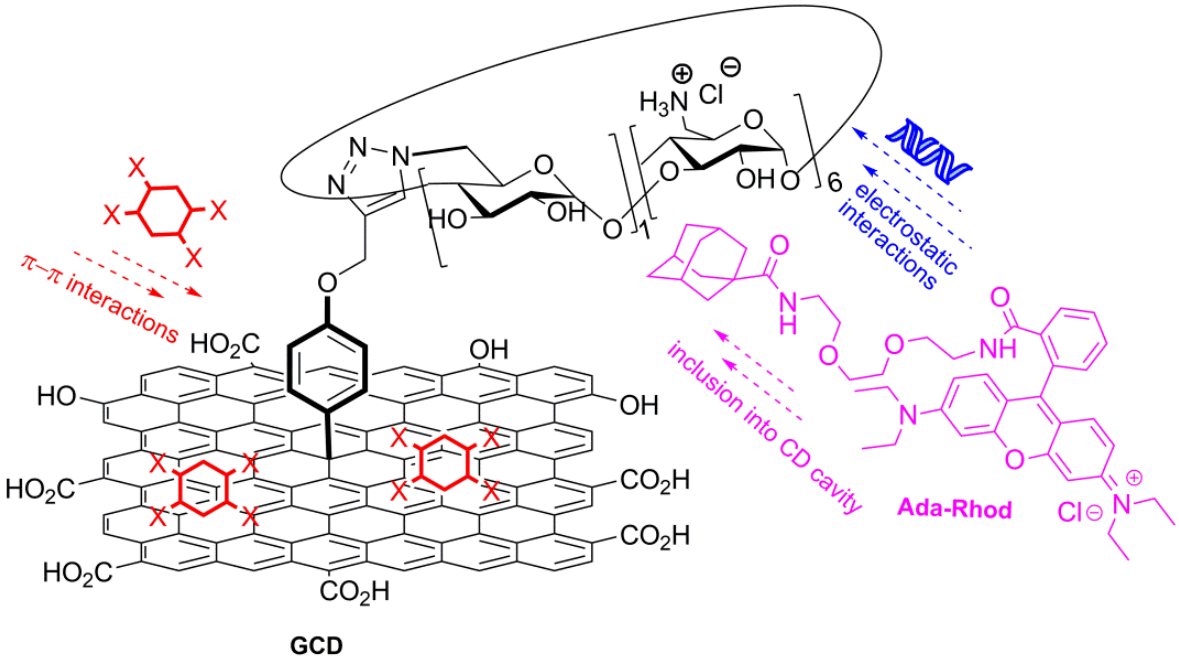

Figure 35: Schematic sketched of Functional Cationic Cyclodextrin Graphene Platform (GCD) with its pattern of potential interactions sites

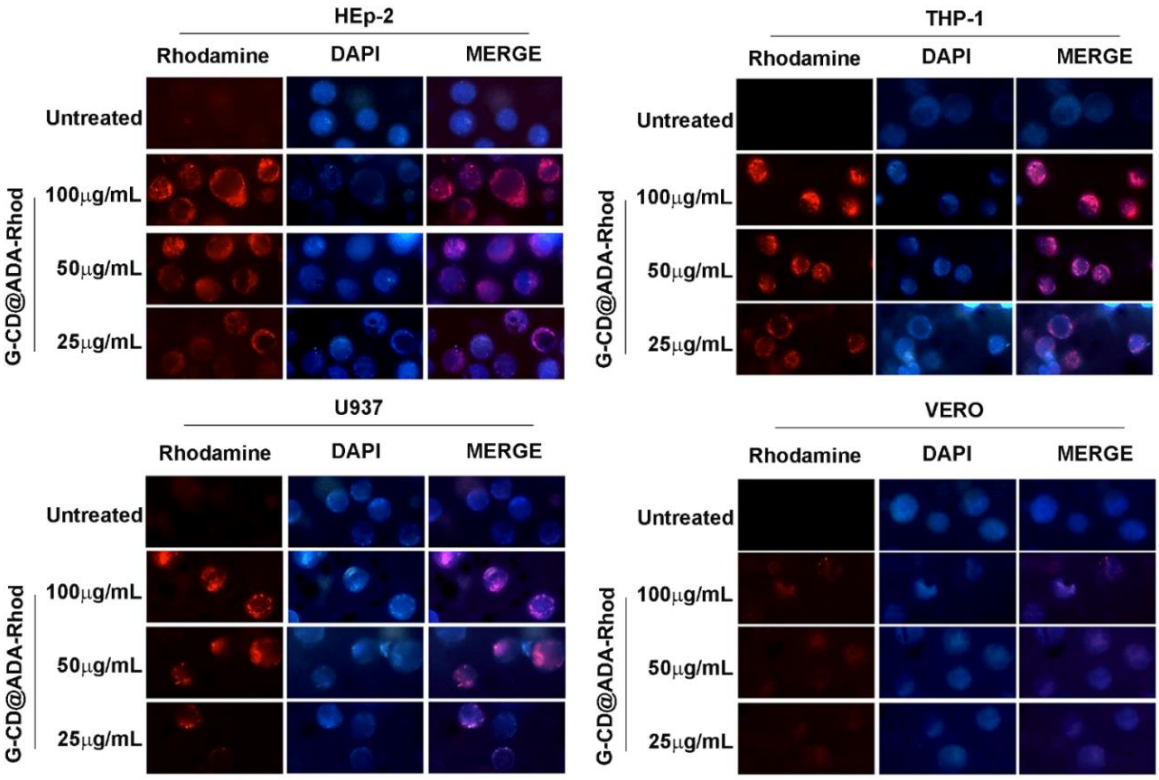

Figure 36: Cellular uptake of graphene-based nanosystem on different cell lines. HEp-2, THP-1, U937 and Vero cell lines were treated with different concentrations of G-CD@ADA-Rhod (100µg/mL, 50 µg/mL and 25µg/mL). Twenty-four hours later, the intracellular uptake of G-CD@ADA-Rhod was analysed by fluorescence analysis observation. In all panels the Rhodamine filter captures the G-CD@ADA-Rhod autofluorescence. The nuclei were stained with Hoechst 33342 fluorescent DNA-binding dye.

The cellular uptake of graphene-based nanosystem (G-CD@ADA-Rhod) was performed on several cell lines. HEp-2, Vero, THP-1 and U937 were treated with three different concentrations of G-CD@ADA-Rhod (100µg/mL, 50µg/mL and 25 µg/mL). The G-CD@ADA-Rhod internalization was proved by red fluorescent dots visualization localized into the cells after 24 h of treatment. The results show that graphene-based nanocarriers uptake in HEp-2, THP-1 and U937 tumoral cell lines in concentration-independent manner (Fig.36) and localize in perinuclear position. In Vero non tumoral cell line the red autofluorescence of nanosystem is lightly visualized by treatment with higher concentration of nanocarrier, exclusively (Fig 36). At lower concentrations (50µg/mL and 25 µg/mL) of graphene-based nanosystem none visualization of red fluorescent dots is detected suggesting that in non tumoral cell lines, the G-CD@ADA-Rhod uptake occurs in concentration-dependent manner.

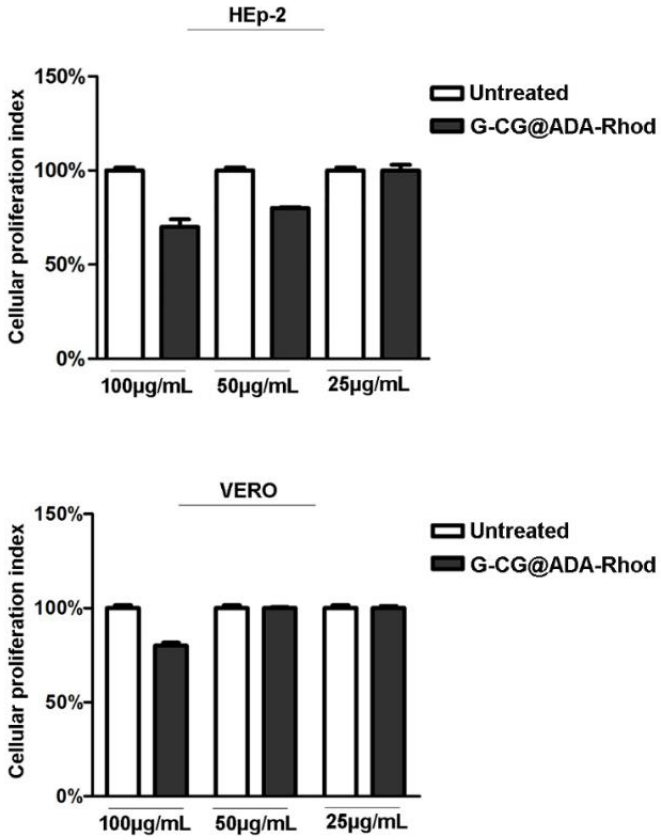

Figure 37: Viability assay in HEp-2 and Vero cells treated with G-CD@ADA-Rhod. The cell viability was determined on the basis of ATP levels using ViaLight™ plus cell proliferation and cytotoxicity bioassay kit (Lonza Group Ltd., Basel, Switzerland) in combination with GloMax® Multi Microplate Luminometer. HEp-2 and Vero cells were treated with three different concentrations of G-CD@ADA-Rhod (100 µg/mL, 50 µg/mL and 25 µg/mL). Twenty-four hours oftreatment the samples were collected and the luminescence value was converted in cellular proliferation index (%) as described in Materials and Methods. The assay was performed as means of triplicate ± SD.

Having establish that G-CD@ADA-Rhod internalizes in all considered tumor cell lines, HEp-2 were chosen to perform the next experiments related to cytotoxicity effect and biological response. The results, showed in Fig. 37, demonstrate a slight cytotoxicity effect in HEp-2 cell lines following exposition to G-CD@ADA-Rhod at 100 µg/mL and 50µg/mL. At low concentrations (25 µg/mL) none cytotoxicity effect was detected. Small variations in cellular toxicity levels result in Vero cell lines treated with high concentration of G-CD@ADA-Rhod according to effective uptake, shown in Fig. 37

On the contrary, the treatment with 50µg/mL and 25 µg/mL of G-CD@ADA-Rhod no revealed a cytotoxicity effect probably due to internalization failure. These findings suggest that the cells viability, following G-CD@ADA-Rhod exposition, slightly decreases when the G-CD@ADA-Rhod concentrations increase.

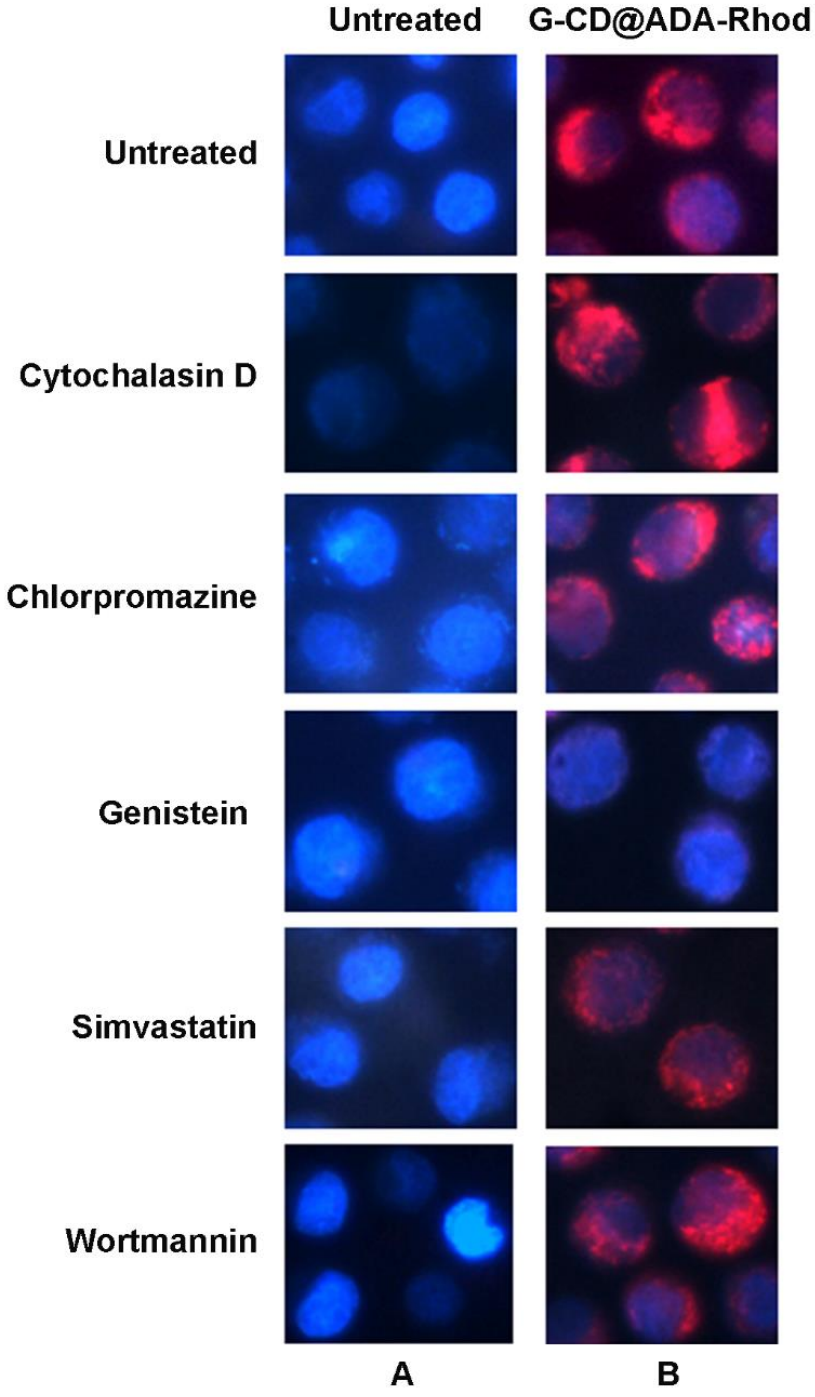

Figure 38: Effect of endocytosis inhibitors on cellular uptake of G-CD@ADA-Rhod. HEp-2 cells were pre-treated for 1h with Cytocalasin D (1µM) or Chlorpromazine (10µM), or Genistein (50µM), or Simvastatin (5µM) or Wortmannin (10µM). Then, the samples were incubated for 24 h in the presence of G-CD@ADA-Rhod (50 µg/mL). The intracellular fluorescence was observed using standard DAPI/FITC/TRITC filter sets in the fluorescence microscopy. The nuclei were stained with Hoechst 33342 fluorescent DNA-binding dye. The column A represents samples treated with different endocytosis inhibitors and untreated with CD@ADA-Rhod. The column B represent the CD@ADA-Rhod treated cells exposed to different endocytosis inhibitors. B column represent the merged images.

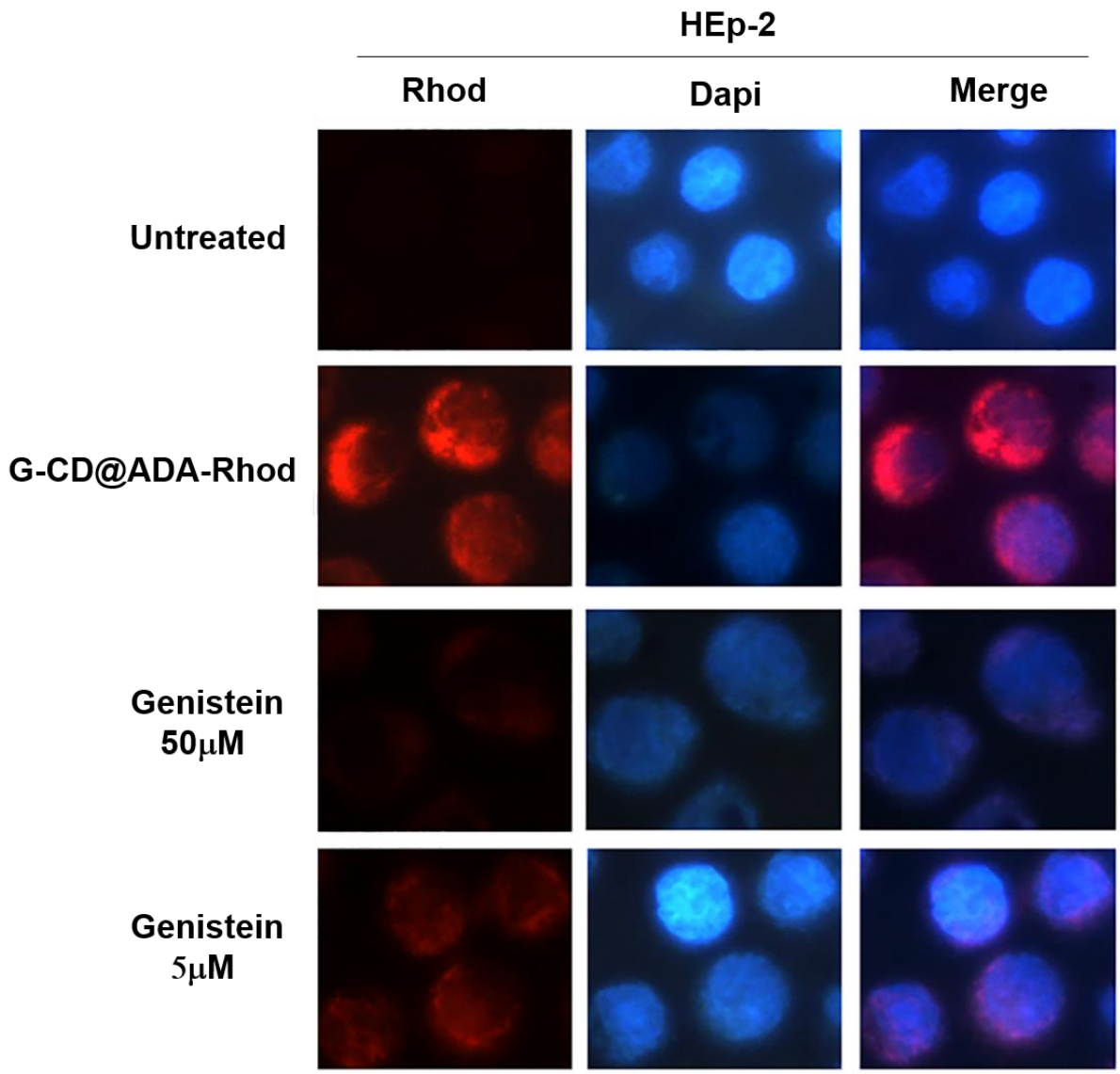

Figure 39: Effect of Genistein on internalization of G-CD@ADA-Rhod. HEp-2 cells were pre-treated for 1h with different concentration of Gynestein (50 µM and 5 µM) and untreated or treated with G-CD@ADA-Rhod (50µ g/mL) for 24h. The intracellular fluorescence was observed using standard DAPI/FITC/TRITC filter sets in the fluorescence microscopy. The nuclei were stained with Hoechst 33342 fluorescent DNA-binding dye, Right column represent the merged images.

In order to analyze the endocytosis mechanism used to promote the G-CD@ADA-Rhod uptake, pharmacological inhibitors of the major endocytic pathways were used: i) Chlorpromazine induces the irreversible membrane translocation of clathrins and other adapters proteins to endocytic vesicles; ii) Cytochalasin D inhibits the actin polymerization; iii) Genistein, is a specific inhibitor of protein tyrosine kinase involved in the translocation of actin and represents the most common inhibitor of caveolin-mediated endocytosis; iv) Wortmannin, it is an inhibitor of phosphoinositide 3-kinase implicated in vesicular trafficking; v) Simvastatin, reversible

inhibitors of the 3-hydroxy-3-methylglutaryl coenzyme A (HMG-CoA) reductase, it is involved in biosynthesis of cholesterol and precursors which regulate posttranslational modifications of intracellular proteins regulating vesicle trafficking [132]. HEp-2 cells were pre-treated for 1h with Cytochalasin D (1 µM), Chlorpromazine (10 µM), Genistein (50 µM), Simvastatin (5 µM), wortmannin (10 µM) and after were exposed to 50 µg/mL of G-CD@ADA-Rhod for 24h in presence of the inhibitor. The autofluorescence of G-CD@ADA-Rhod was observed in fluorescence microscopy by staining the nuclear compartment with Hoechst 33342 fluorescent DNA-binding dye (Fig. 38). The results demonstrate that Cytochalasin D, Chlorpromazine, Simvastatin and wortmannin have no affect on the intracellular uptake of G-CD@ADA-Rhod. Instead, the Genistein treatment inhibits the G-CD@ADA-Rhod internalization at high concentrations (50 µM) and slightly also at low concentrations (5 µM) (Fig.39). These finding suggest that G-CD@ADA-Rhod uptakes into the cells with a caveolin-mediated endocytosis mechanism.

5.2.3. Doxorubicin delivery by graphene-based nanovector and cellular response

Having establish that G-CD@ADA-Rhod efficiently crosses the cell membranes with a specific endocytosis mechanism, GCD platform was loaded with antineoplastic drug, Doxorubicin, to form G-CD/Doxo. Doxorubicin is known to bind to DNA-associated enzymes, intercalate with DNA base pairs, and activate specific intracellular antitumor signals. In this section will be explored: i) the auto fluorescence of GCD/Doxo, ii) concentration-dependent cytotoxicity effect of GCD/Doxo, iii) temporal expression of cytotoxicity effect of GCD/Doxo.

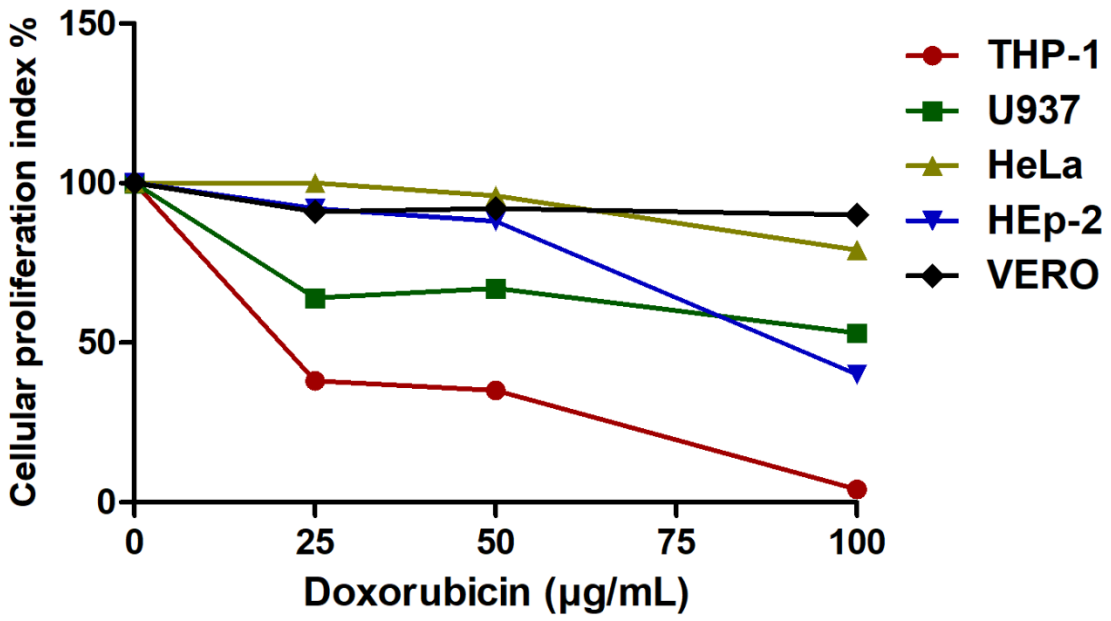

Figure 40: **Measurement of Doxorubicin sensitivity in different cell lines.** THP-1, U937, HeLa, HEp-2 and Vero cells were exposed to 100 µg/mL 50 µg/mL and 25 µg/mL of Doxo for 24h. The proliferation index (%) was determined on the basis of ATP level as described in Materials and Methods. The assay was performed as means of triplicates ±SD.

A cellular viability assay was performed in order to measure, on several cell lines, the Doxorubicin sensitivity at different concentrations. Therefore, THP-1, U937, HeLa, HEp-2 and Vero cells were exposed to 100 µg/mL, 50µg/mL and 25µg/mL of Doxo for 24h and the cellular proliferation index was detected. The results show that the doxorubicin sensitivity is higher in THP-1, HEp-2 and U937 cells in concentration-dependent manner (Fig. 40). In particular: i) in THP-1 cells about 60% of cytotoxicity effect was detected at 50µg/mL and 25µg/mL, 100% at 100 µg/mL. ii) in U937 cells about 40% of cytotoxicity effect was detected at 100µg/mL, 50µg/mL and 25µg/mL. iii) In HeLa cells a slight toxicity (15%) was detected at 100 µg/mL. iv) in Vero cells any cytotoxicity affect was detected. v) in HEp-2 cells about 60% of

cytotoxicity effect was detected at 100µg/mL and a slight toxicity (10%) at 50 µg/mL and 25 µg/mL. These findings highlight the sensibility and resistance degree to Doxorubicin in different cell lines.

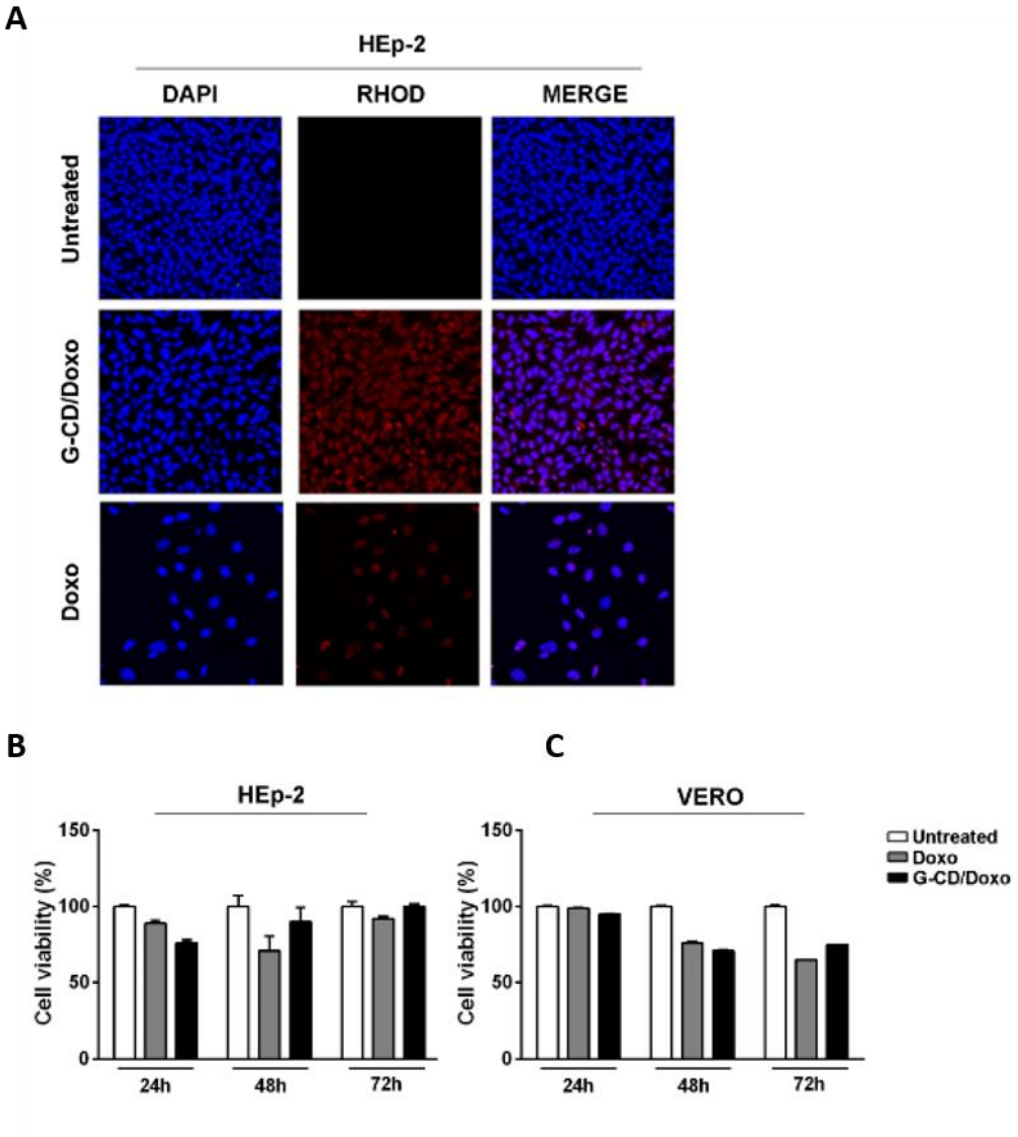

Figure 41: Cell viability of HEp-2 and Vero cells line treated with G-CD/Doxo and cellular uptake in HEp-2 cell line. A) Intracellular uptake of G-CD/Doxo in HEp-2 cell line. The cells were untreated or treated with G-CD/Doxo (0.025 mg/mL). Doxorubicin was used as a control. After 24h, the cells were harvested and the autofluorescence of CD/Doxo and Doxorubicin was evaluated by fluorescence analysis as described in Methods. The right column indicates merged images. B-C) HEp-2 and Vero cells were untreated and treated with 0.025 mg/mL of G-CD/Doxo for 24h, 48h and 72h. Doxorubicin was used as a control. At indicated time of treatment the cells were collected and the proliferation index (%) was determined on the basis of ATP level as described in Materials and Methods. The assay was performed as means of triplicates ±SD.

The next experiments were performed to investigate the capability of graphene-based nanocarrier to deliver Doxorubicin, a chemotherapeutic drug with a target-specific mechanism. The delivery and the release of doxorubicin were studied on tumoral cell lines at various time intervals and by treating with lower concentration of nanocarrier responsible for the induction

of an efficient intracellular uptake. The HEp-2 cells were exposed to low concentration of Doxo and G-CD/Doxo (25 µg/mL) for 24h and after were collected in polilysined slides as described in material and method.

Briefly, the sample were collected and washed with warm PBS for twice, fixed with PFA 4% for 30 minutes at room temperature and permeabilized with Triton 0,1% for 1h, covered with a drop of mounting solution (ProLong™ Diamond Antifade Mountant with DAPI-Invitrogen p36971) for 30 minutes in a dark room and analyzed by confocal microscopy. The column A represents HEp-2 cells untreated and treated with Doxo and G-CD/Doxo and visualized with DAPI filter to detect the nuclei. The column B represents HEp-2 cells untreated and treated with Doxo and G-CD/Doxo and visualized by Rhodamine filter to visualize the natural red color of free and entrapped Doxo. C column represents the merged images. Literatura data indicated for Doxorubicin both a nuclear or mitochondrial compartmentation. The image of our experiments shows that free Doxo and G-CD/Doxo localize in nuclear compartmentation suggesting that G-CD is able to deliver the drug (Figure 41A).

The next step was to determinate whether the concentration of G-CD/Doxo used to verify the drug delivery induces alterations in the cellular viability and whether the induced effect continues for a long time. Therefore, the cytotoxicity effect linked to ability of G-CD/Doxo to reduce the cellular proliferation was tested by cell viability assay in time-dependent kinetics (Fig. 41 B-C). In the panel, HEp-2 and Vero cells were exposed to 25 µg/mL of G-CD/Doxo for 24, 48 and 72 hours. Free Doxorubicin was used at the same concentration loaded in G-CD/Doxo as a control. The results show a reduced cellular viability in HEp-2 exposed for 24h to G-CD/Doxo compared to Doxo (Fig. 41 B). In addition, this cell viability alteration seems to finish following exposition to G-CD/Doxo for a long time. In Vero cells, although any variations in the cellular viability was detected at 24h of G-CD/Doxo treatment, at 48h and 72h cellular viability is reduced compared to the untreated control (Fig. 41 C). Further investigations will analyze whether the alterations of the cell viability correlate with a biological response mediated by Doxo.

5.2.4. **Signalosome pathways activated by GCD/Doxo nanoplatform**

A complex network of intracellular signals, composed of surface receptors, protein kinases, transcription factors and translational regulators, controls the activation of cellular processes and is called signalosome. Signalosome represents an important control system, which maintains a balance between positive and negative feedback connection of events and avoid an inappropriate cross talk between several pathways in the cells. The nuclear signalosome, for example, is important for the maintenance of genomic integrity and regulates the different phases of the cell cycle. The cell cycle is a succession of very well organized molecular events, which is regulated by checkpoint pathways. WEE-1 is kinase protein, which prevents mitotic entry via an inhibitory phosphorylation of cyclin-dependent kinases CDK1 and CDK2, activated during the S phase of cell cycle [159]. The WEE-1 kinetic expression was analyzed in Figure 42 after G-CD/Doxo exposition in tumor and non-tumor cell lines and the spatial localization of the WEE-1 and p-CDK2 T14/Y15 was showed in Figure 43.

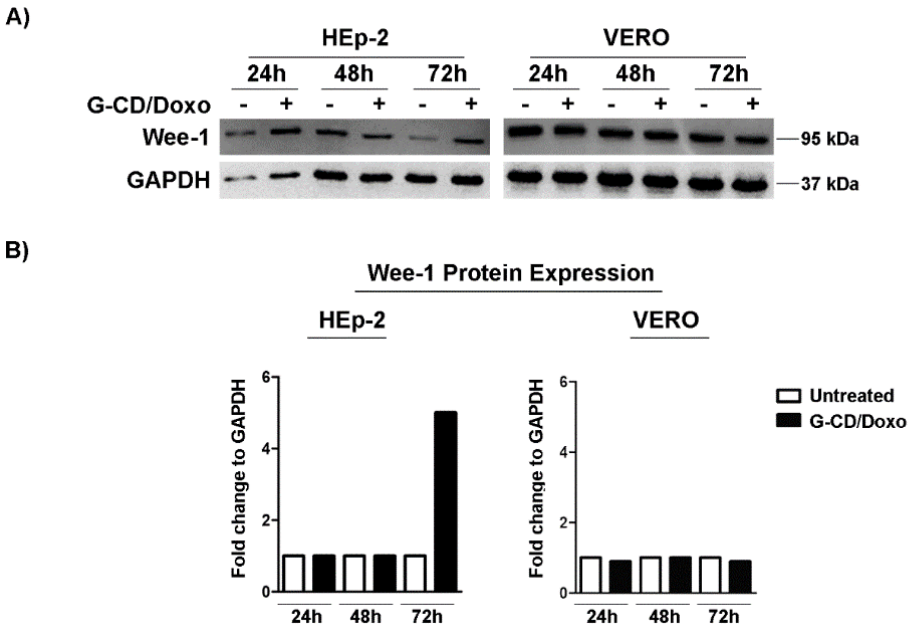

Figure 42: Wee-1 protein expression in HEp-2 and Vero cells line treated with GCD/Doxo. HEp-2 and Vero cell lines were untreated or untreated with 25 µg/mL of GCD/Doxo for indicate time (24h, 48h and 72h). A) Equal amount of proteins was separated by polyacrylamide gel electrophoresis and probed with specific antibody to Wee-1 protein. GAPDH was used as housekeeping gene. B) Band density was determined with the T.I.N.A. program, and was expressed as fold change over the housekeeping gene.

HEp-2 and Vero cells were exposed to 25 µg/mL of GCD/Doxo for 24h, 48h and 72h and collected to analyze the WEE-1 expression by western blot analysis. The results, graphically simplified in figure 42 panel B, show at 72h a clear accumulation of WEE-1 in HEp-2 exposed to GCD/Doxo compared to the basal levels. Instead, in Vero cells any variation in the WEE-1 expression levels was detected compared to the control. This finding suggests that the modulation of the WEE-1 mediated pathway occurs predominantly in tumor cell lines. In non-tumor system, the GCD/Doxo treatment not produces any biological response.

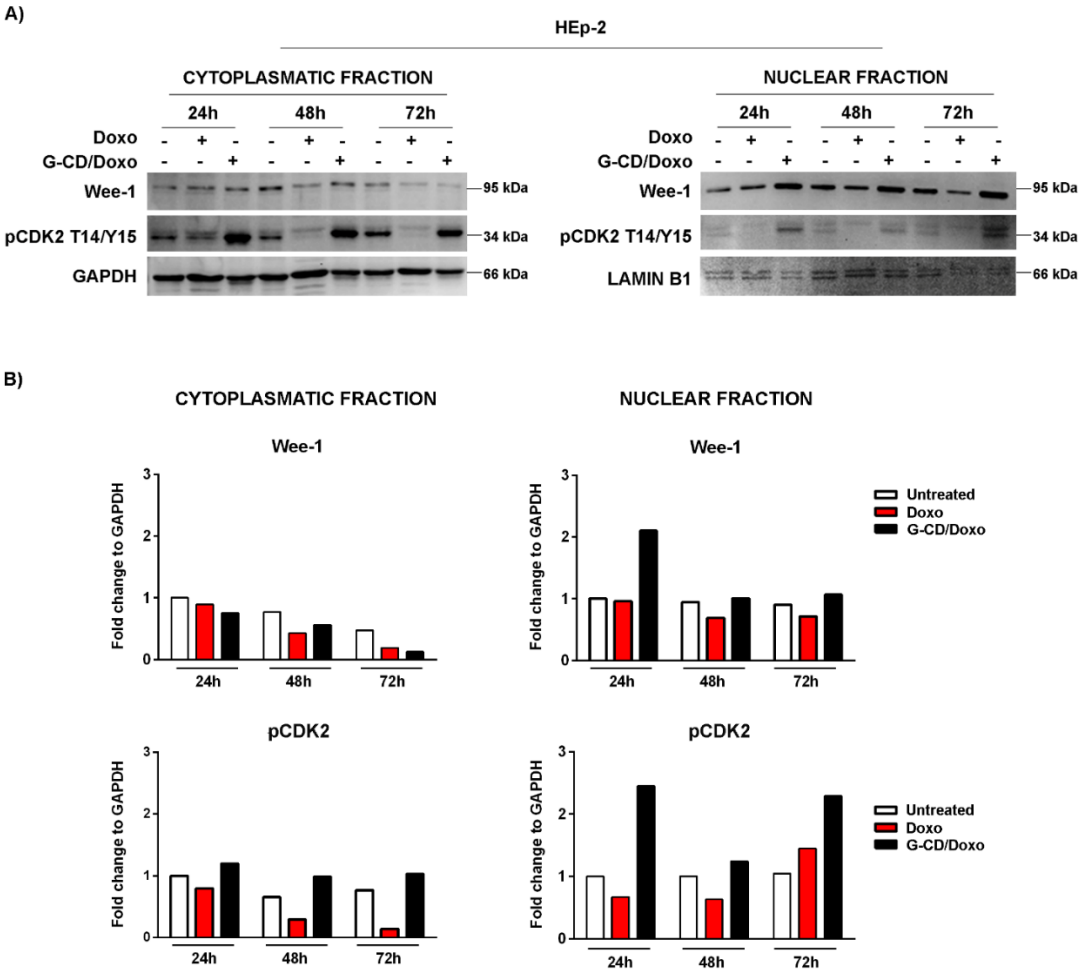

Figure 43: Wee-1 and phospho-CDK2 (pCDK2 T14/Y15) protein expression in HEp-2 cell line is triggered by GCD/Doxo. HEp-2 cells were untreated or untreated with 25 µg/mL of GCD/Doxo for 24h, 48h and 72h. Doxorubicin was used as a control. A) Equal amount of cytoplasmic and nuclear proteins were separated by polyacrylamide gel electrophoresis and probed with Wee-1 and phospho-CDK2 (pCDK2 T14/Y15) antibodies. GAPDH and LAMIN B1 were used as loading control for cytoplasmic and nuclear fraction, respectively. B) Band density was determined with the T.I.N.A. program, and was expressed as fold change over the appropriate housekeeping gene.

Having establish that WEE-1 activation in HEp-2 cells following GCD/Doxo exposition and according to the close connection with CDK2 proteins, the spatial distribution of both protein is showed in Fig 43. The HEp-2 cells were exposed to 25 µg/mL of GCD/Doxo and

Doxo for 24h, 48h and 72h, collected and subjected to cytoplasmic and nuclear protein extraction, as described in Materials and methods. The CDK2 inhibition mediated by phosphorylation at T14 and/or Y15 sites blocks the cell cycle progression from G1 to S phases. Therefore, WEE-1 normally controls the mitotic entry and CDK2 acts in the upstream phase. The results show a temporal reduction of the cytoplasmic expression of WEE-1 and pCDK2 and a progressive nuclear accumulation after G-CD/Doxo exposition compared to the Doxo exposition. This finding suggests that the exposition of G-CD/Doxo induces the nuclear accumulation of WEE-1 and pCDK2 more than Doxo treatment, suggesting that the G-CD is able to deliver the drug, protect it to develop a biological effect at low concentration. Therefore, probably the G-CD/Doxo induced cell cycle arrest in G1 checkpoint through phosphorylation of CDK2 and the accumulation of WEE-1.

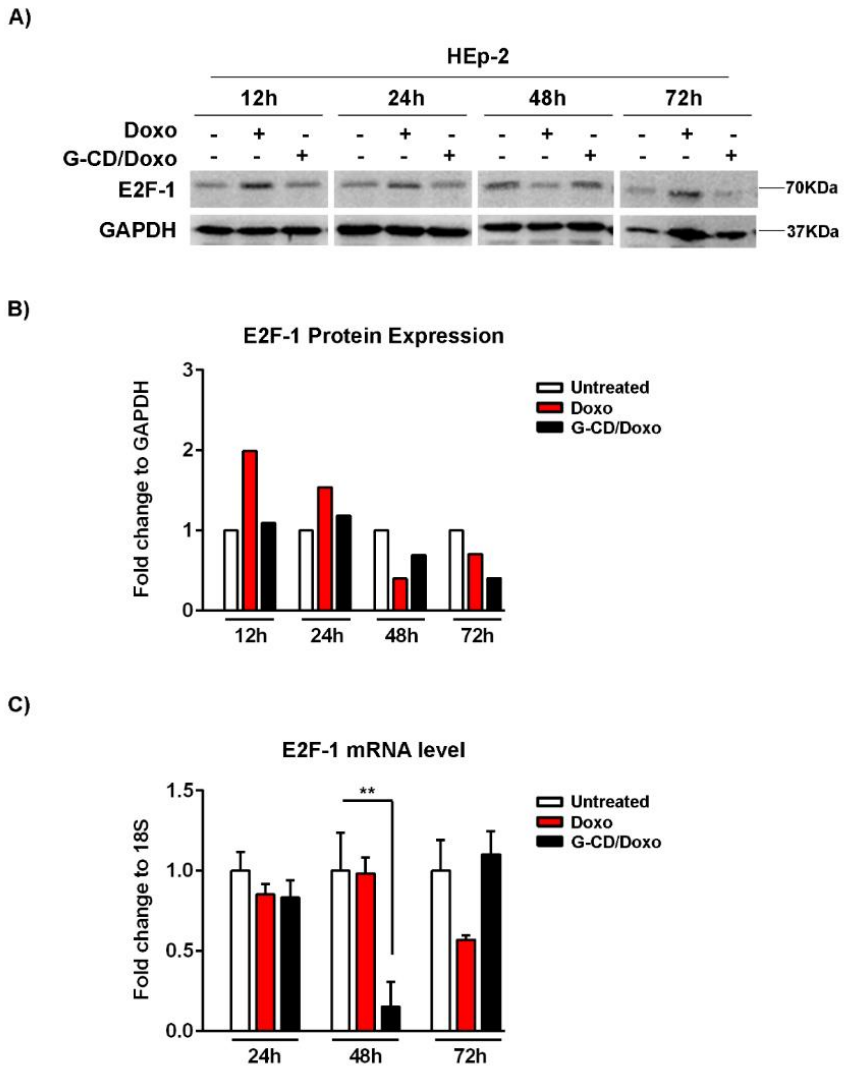

Figure 44: **E2F-1 protein expression and mRNA level in HEp-2 cell line treated with G-CD/Doxo.** A) HEp-2 cells were incubated with GCD/Doxo (25µg/mL) for indicated time. Doxorubicin was used as a control and Equal amount of cytoplasmic and nuclear proteins were separated by polyacrylamide gel electrophoresis and probed with anti-E2F-1 antibody. GAPDH was used as housekeeping gene. B) Band density was determined with the T.I.N.A. program, and was expressed as fold change over the housekeeping gene. C) Quantitative Real-Time PCR of E2F-1 mRNA levels in HEp-2 cells was evaluated at 24h, 48h, and 72h of treatment with G-CD/Doxo (0.025mg/mL). Transcripts were normalized as a fold change against the 18S copies number. Statistical analyses were performed with one-way ANOVA analysis assay in triplicate and **P < 0.01 indicates significant change.

Another factor involved in the S phase of the cell cycle progression is E2F-1 transcription factors [160]. The E2F family plays a crucial role in the control of cell cycle and action of tumor suppressor proteins. The function of E2F1 protein is regulated by retinoblastoma protein Rb. When Rb is not in its hyperphosphorylated form, it binds to E2F1 and block its action. On the contrary, upon phosphorylation of pRb, E2F1 is released from Rb/E2F1 inhibitory complex and acts by inducing the activation of the target gene transcription involved in the cell cycle progression.

Therefore, E2F1 down-regulation led to cell cycle arrest. The translational and transcriptional expression of E2F-1 levels were analyzed in figure 44 panel A, B, C. HEp-2 cell line were exposed to GCD/Doxo and Doxo for 24h, 48h and 72h and collected to western blot analysis and quantitative real-time PCR. The results show that: i) Doxo free treatment triggers an accumulation of E2F-1 protein expression at 12h and 24h of treatment (Fig. 44 panel A); i) G-CD/Doxo induces a reduction of the E2F-1 protein expression at 48h and 72h of treatment, compared to untreated cells (Fig. 44 panel A). iii) The transcriptional levels of E2F-1 in HEp-2 were not affected by Doxo exposition, instead significant reduction was detected 48h of G-CD/Doxo compared to Doxo and untreated control (Fig. 44 panel C). The results show that E2F-1 control mediated by G-CD/Doxo occurs belatedly and triggers a reduction of E2F-1 protein expression at 48h and 72h of treatment. The drug release mediated to GCD occurs as a late event and keep for a long time.

5.2.5. **p53 signaling pathway modulated by GCD/Doxo nanoplatform**

The transcription factor p53 is a tumor suppressor that is activated by several type of cellular stress and its dysregulation occurs in several cancer diseases, frequently[14]. The activation of the p53 and downstream proteins controls the cellular growth by inducing of cellular regulators involved in apoptosis, modulation of cell cycle and DNA repair processes. Briefly, upstream regulation of p53 is performed by Murine double minute 2 (MDM2) protein which tightly controls p53 through a negative feedback loop, influencing protein levels in the cell. MDM2 in the phosphorylated form binds to p53 at its transactivation domain and blocks its transcriptional factor activity. The E3 ubiquitin ligase activity of MDM2 induces the proteasomal degradation of p53 and serves to regulate the cellular levels. Following a DNA damage or stress conditions, the upstream activation of kinases enzyme triggers the downstream p53 phosphorylation, which interferes with binding to MDM2. The p53 upregulates p21 protein, which inactivates the cyclin/cyclin-dependent-kinase complex blocking the cell-cycle progression in the G1-S transition.

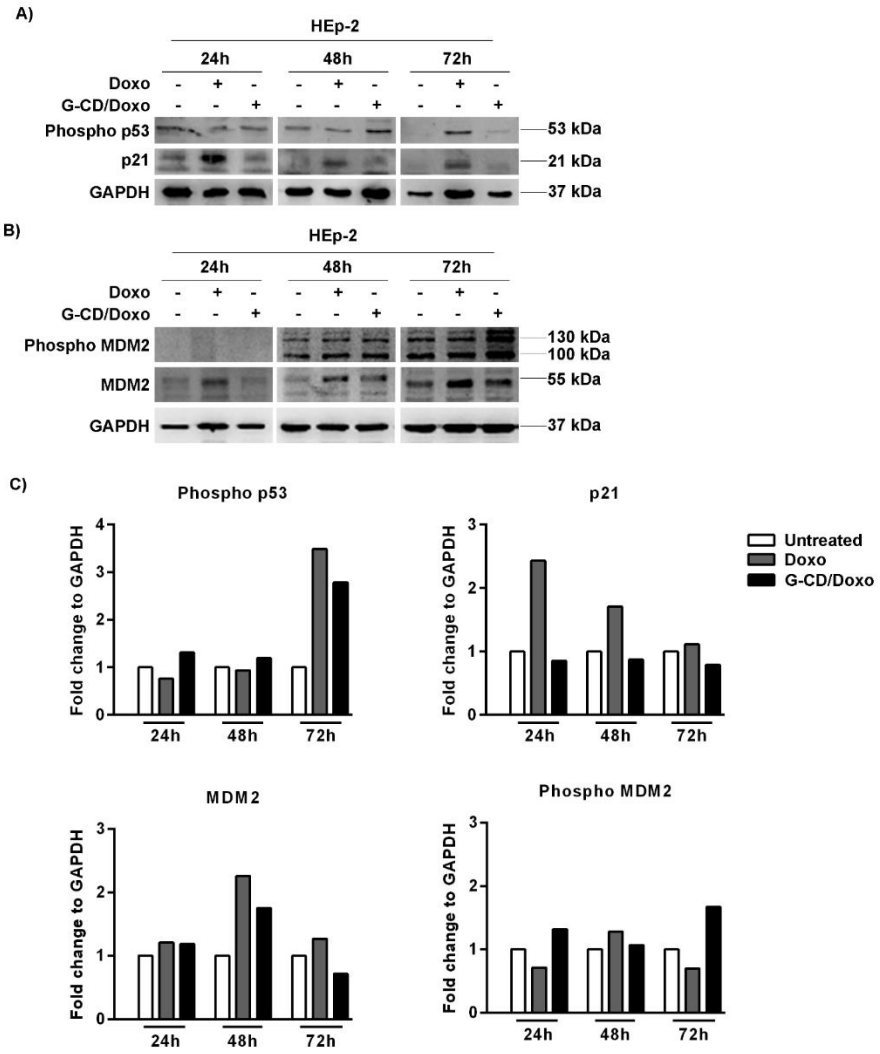

Figure 45: Detection of **phospho-p53, p21 and phospho-MDM2 proteins in HEp-2 cell after treatment with by G-CD/Doxo.** HEp-2 cells were untreated or untreated with 25 µg/mL of G-CD/Doxo for indicate time (24h, 48h and 72h). Doxorubicin was used as a control. A) and B) Equal amount of proteins was separated by polyacrylamide gel electrophoresis and probed with specific antibody to phospho-p53, p21, phospho-MDM2 and MDM2 proteins. GAPDH was used as housekeeping gene. C) Band density was determined with the T.I.N.A. program, and was expressed as fold change over the appropriate housekeeping gene.

Having establish the importance of p53 pathway regulation and that mutational inactivation of p53 is frequently observed in various human cancers[7,8], the figure 45 shows the temporal expression levels of phospho-p53, p21 and phospho-MDM2 protein in HEp-2 cell exposed to Doxo and G-CD/Doxo. Literature data have demonstrated that the chemotherapeutic agent doxorubicin induces the apoptosis processes by activating p53 [161]. Therefore, HEp-2 cells were untreated and treated with 25µg/mL of Doxo and G-CD/Doxo and collected 24h, 48, and 72h of treatment.

The results show that: i) p53 accumulates at 72h of treatment to Doxo and G-CD/Doxo; ii) p21 accumulates at 24h of Doxo treatment more than 72h suggesting that the activation occurs with an p53-mediated independent mechanism; iii) MDM2 levels peak were observed at 48h in Doxo and G-CD/Doxo treated cells; iv) a low variation is detected in p-MDM2 expression levels in particular at 72h of treatment. These findings suggest that p53 tend to accumulate following free Doxorubicin treatment, according to the literature data, and with G-CD/Doxo. The activation of p53 not involves the downstream signal p21-mediated but high levels of MDM2 at 48h indicate an upstream control in the p53 activation.

5.2.6. Autophagy pathway modulated by GCD/Doxo nanoplatform

To investigate the involvement of programmed cell death mediated by G-CD/Doxo exposition, the regulation of the autophagy process was evaluated. Autophagy is a mechanism that protects cells from several type of stress and maintain genomic integrity. It is a catabolic degradation essential to remove damaged cellular components and to recycle cellular organelles in order to support the cellular metabolic activities. Several methods were described to detect the autophagy induction or the autophagy flux [162]. Therefore, in this section, the regulation of the autophagy pathway, mediated by GCD/Doxo was analyzed by evaluating: i) The formation of autophagosomes through LC3II protein localization using plasmids expressing LC3II fused with fluorescente proteins (as described in Materials and Methods); ii) The protein quantification of LC3 and p62, which play a central role in autophagy.

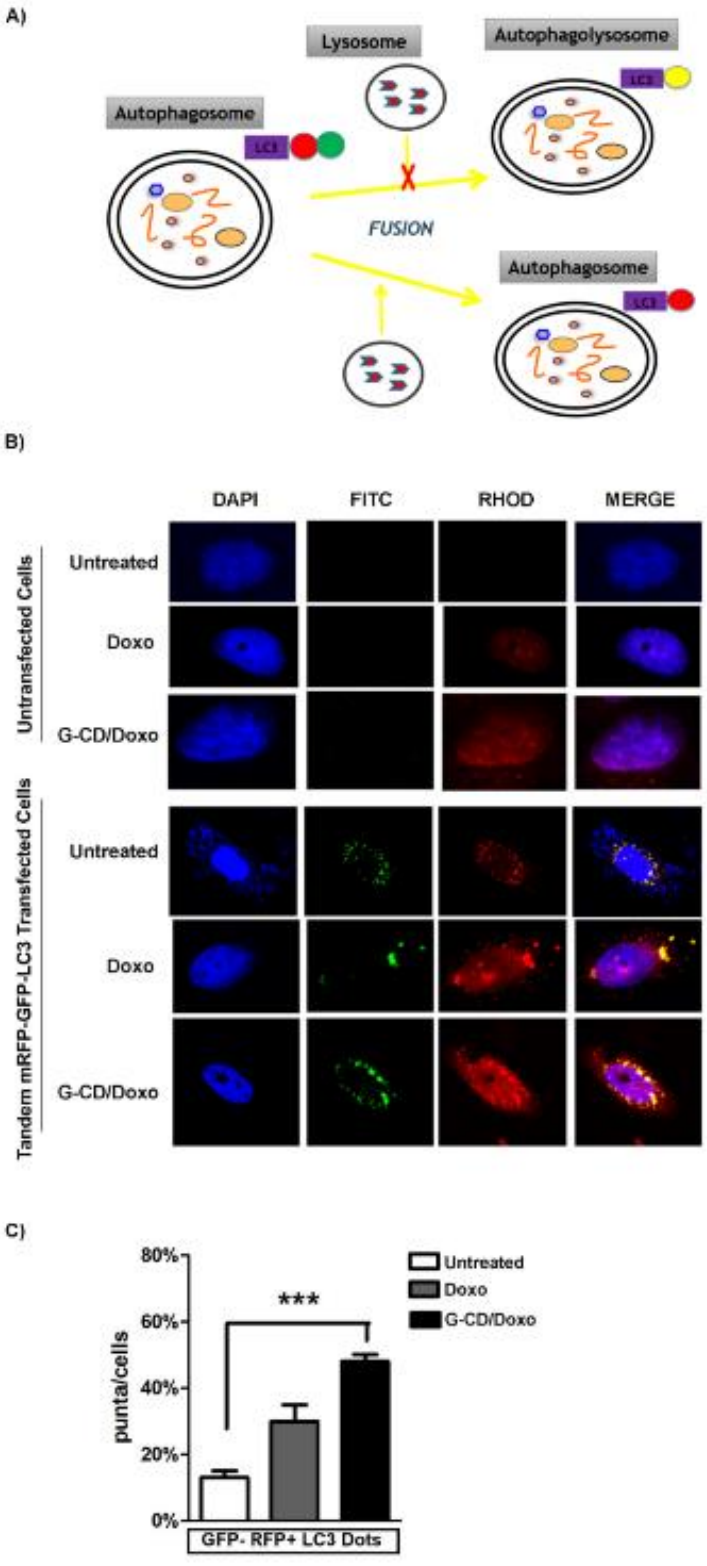

Figure 46: Monitoring of the autophagic flux by the tandem mRFP-GFPLC3 probe. A) Graphical representation of autophagic flux. B) Representative confocal images of HEp-2 cells transiently transfected with mRFP-GFP tandem fluorescent-tagged LC3 and untreated or treated with Doxo and GCD/Doxo (25 µg/mL) for 48h. C) Quantification of GFP-RFP+LC3 dots in HEp-2 untreated and treated with 25 µg/mL of Doxo and GCD/Doxo. Statistical analyses were performed with one-way ANOVA analysis assay in triplicate and ***P < 0.001 indicates significant change.

Autophagy is a dynamic multistep process that involves the formation of autophagosomes, fusion of the autophagosome with the lysosome to form the autolysosome, and finally the degradation of the contents in the autolysosome. The LC3II protein plays a critical role in autophagy, and the localization of this protein in the autophagosomes can be used as a general marker for formation of autophagosomes during stimulation of autophagy. An mRFP-GFP tandem fluorescent-tagged LC3 was used to monitor the autophagic flux. This method is based on differential quenching of the fluorescence emitted by the red and green probes in the lysosomal acidic compartment. The graphical representation of autophagy process, detected by mRFP-GFP-LC3, showed in figure 46 Panel A. Briefly, autophagosomes appear yellow (GFP+RFP+) and autolysosomes red (GFP-RFP +), because the GFP-LC3 is affected by the acidic environmental of lysosomes. Therefore, HEp-2 cells were grown in multiwell culture slides and transiently transfected for 48h with mRFP-GFPLC3 plasmid and 24h after transfection were untreated and treated with 25 µg/mL of Doxo and G-CD/Doxo and collected and analyzed with confocal microscopy. The results showed in Fig. 46 Panel B and C showed that: i) in untreated cells the number of green and red dots overlap and represents the basal autophagy level. ii) in Doxo treated cells about 30% of red dots were detected. iii) in G-CD/Doxo treated cells the 50 % of the red dots were detected. These finding suggest that the exposition to G-CD/Doxo significantly triggers the clear accumulation of autolysosomes, GFP-RFP + LC3, and indicates an activation of autophagy.

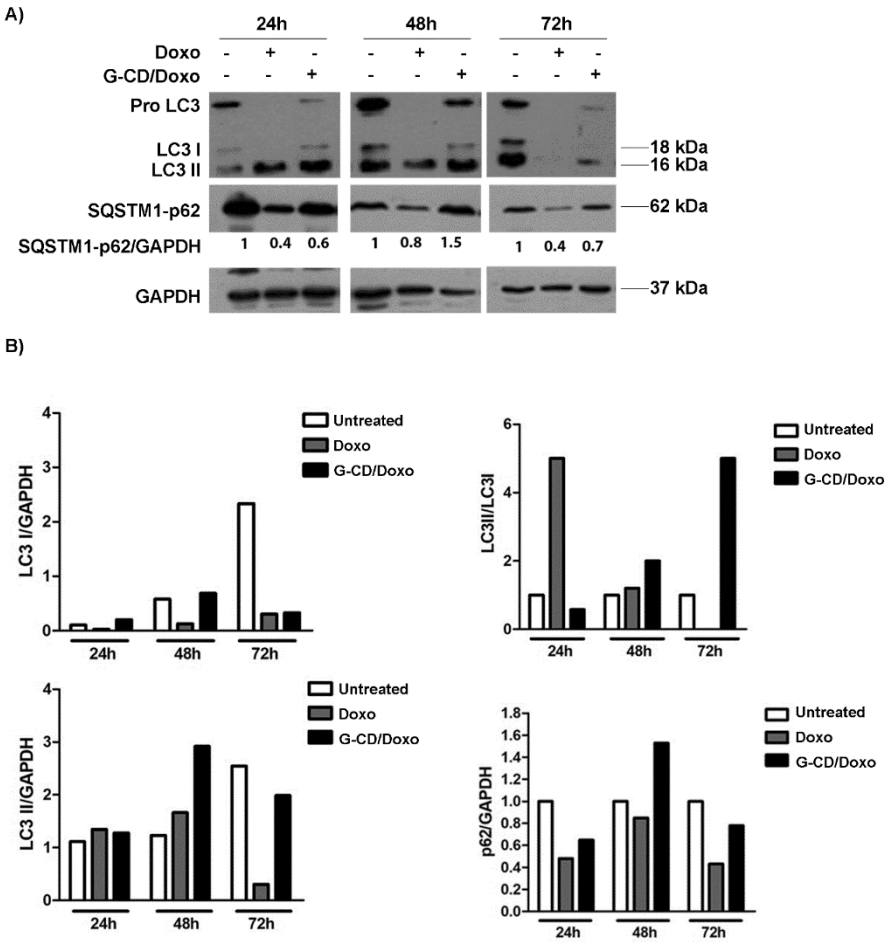

Figure 47: LC3I, LC3II and SQSTM-p62 autophagy-related protein expression in HEp-2 cell line treated with G-CD/Doxo. A) Immunoblotting of LC3I, LC3II and SQSTM-p62 in HEp-2 cells treated or untreated with G-CD/Doxo (0,025mg/mL) for the indicated times. B) The densitometric analysis of the LC3I/GAPDH, LC3II/GAPDH, LC3II/LC3I and SQSTM1-p62/GAPDH ratios is reported as a fold change.

An alternative method to monitor the autophagy is to detect the expression levels of LC3 protein by western blot analysis. During autophagy, cytosolic LC3-1 is conjugated to phosphatidylethanolamine to form LC3-II. LC3-II is recruited and incorporated into the autophagosomal membrane. The accumulation of LC3II correlates with the accumulation of autophagosomes and the ratio between the amount of LC3II and LC3I is an indicator of autophagic flux. The analysis of the expression levels of LC3II (Fi.47A) showed: i) in untreated cells the same quantitative expression of LC3I and LC3II; ii) a temporal accumulation of LC3II after exposition to G-CD/Doxo; iii) a limited accumulation of LC3II after exposition to Doxo at 24h. The graphical representation of LC3II/LC3I (Fig. 47B) showed that in HEp-2 cells exposed to Doxo, the activation of autophagy flux occurred at 24h and then decreased at 48h and 72h, totally. On the contrary, a temporal and graduated accumulation of L3II/LC3I occurred after G-CD/Doxo exposition.

An additional method to monitor autophagy is based on the quantification of p62 / SQSTM1 levels degraded by autophagosome following interaction with LC3 using western blot analysis. Therefore, the expression levels of p62 are inversely proportional to the intracellular autophagy levels. Therefore, the reduction of p62 protein expression correlates to activation of autophagy. Western blot analysis (Fig.47A-B) showed: i) low levels of p62 expression in HEp-2 exposed to Doxo compared to the untreated control at 24h, 48h and 72h; ii) low levels of p62 expression in HEp-2 exposed to G-CD/Doxo at 72h. The combined accumulation of LC3II/LC3I and reduction of p62 protein expressions were indicative of the induction of the autophagy process following G-CD/Doxo exposition.

5.2.7. Gene delivery by graphene-based nanovector

A key factor for gene therapy is to find efficient and safe vectors that protect DNA from nuclease degradation and facilitate its uptake with high transfection efficiency within the target cell. To explore the ability of G-CD platform as gene delivery vehicle, the DNA plasmid encoding enhanced green fluorescence protein (pCMS-EGFP) and miRNA-15a were used as a model system. The section 5.2.7 show the DNA plasmid delivery mediated by G-CD@ADA-Rhod (Fig. 48) and the intracellular molecular signal activated by miRNA15a delivered and released by G-CD (Fig. 49).

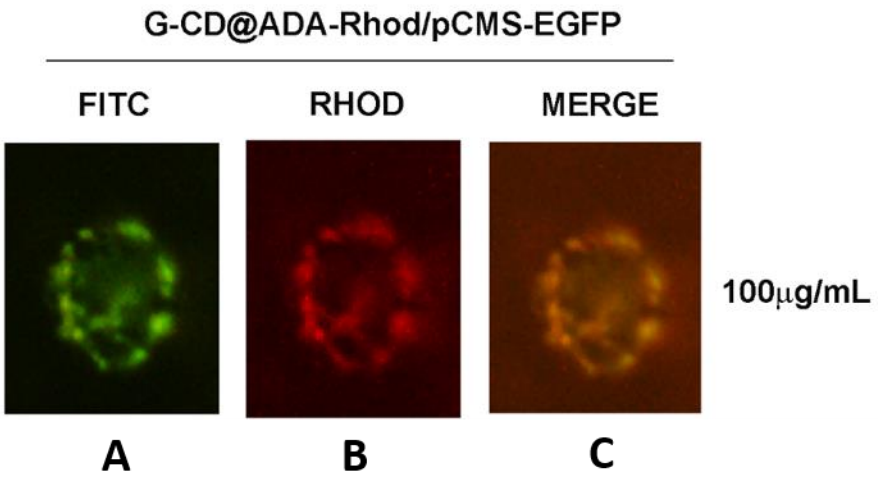

.

Figure 48: Gene delivery of G-CD@ADA-Rhod/pCMS-EGFP. HEp-2 cells were incubated with G-CD@ADA-Rhod/pCMS-EGFP at 100μg/mL. After 48h incubation time the cells were harvested and the intracellular fluorescence of pCMS-EGFP and Rhodamine was observed in the fluorescence microscopy. The columns A and B represent EGFP and Rhodamine fluorescence dots, respectively. The column C indicate merged image.

The G-CD@ADA-Rhod complex was treated with pCMS-EGFP, vortexed and set down for 10 minutes, to form G-CD@ADA-Rhod/pCMS-EGFP vector. HEp-2 cells were incubated for 48h with 100 μg/mL of G-CD@ADA-Rhod/pCMS-EGFP, collected and subjected to live autofluorescence by fluorescence microscopy. The red dots, corresponding to G-CD@ADA-Rhod/pCMS-EGFP internalized (Fig.48 B), and the green dots, indicating the EGFP expression (Fig.48 A), overlap (Fig. 48C). The colocalization of both dots suggest that the nanovector capability to gene delivery.

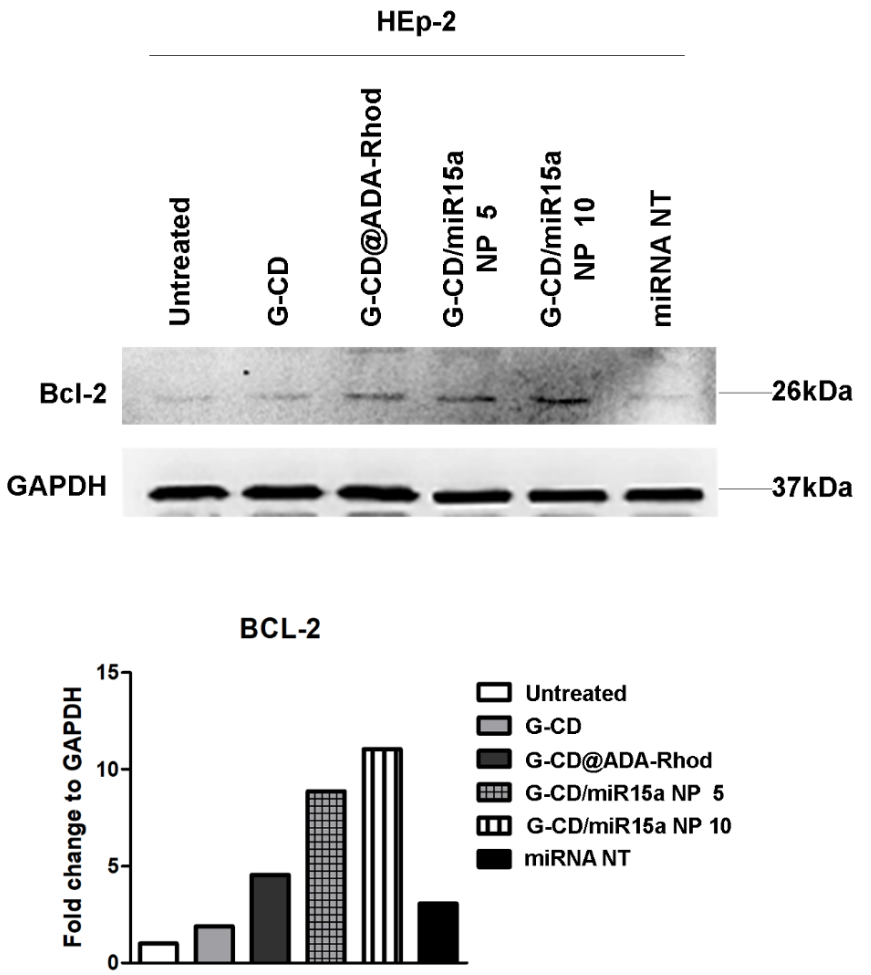

Figure 49: Intracellular signalling pathway triggered by G-CD/miRNA-15a. HEp-2 cells were treated with 25µg/mL of G-CD, G-CD@ADA-Rhod and G-CD@ADA-Rhod/miRNA-15a for 24h. The G-CD@ADA-Rhod /miRNA-15a was used with different N/P ratio and miRNA NT was used as a no target control. Equal amounts of proteins were separated by polyacrylamide gel electrophoresis, transferred and probed with specific antibody to anti-apoptotic protein Bcl-2. GAPDH was used as housekeeping gene. Band density was determined with the T.I.N.A. program and was expressed as the fold change over the appropriate housekeeping genes.

Lastly, GCD mediated gene delivery activity was verified by complexing the vector with miRNA-15a and with miRNA no target, used as a control. The miRNAs are small, noncoding RNAs that can act as an oncogene or a tumour suppressor and therefore, possess a strong diagnostic and therapeutic potential. However, the efficient delivery of therapeutic miRNA to the target tissue represents the challenge on which the construction of a non-viral vector is based. Therefore, the HEp-2 cells were untreated and treated for 24h with GCD, G-CD@ADA-Rhod, miRNA NT and GCD@ADA-Rhod/miRNA-15a. The miRNA-15a was linked to platform with a different nitrogen to phosphate ratio (i.e N/P=5 and N/P=10). Literature data were demonstrated that, miRNA15a exerts an anti-tumor effects by targeting several oncogenes that are associated with cancer and downregulates the BCL-2 expression levels inducing the apoptosis [163].

Therefore, in order to verify the effects of miRNA loaded on graphene platform, the expression of the its target, BCL-2, was detected by western blot. Surprisingly, the results showed an induction of BCL-2 expression levels following GCD@ADA-Rhod/miRNA-15a treatment in N/P dependent-manner (Fig.49) unlike to literature data. Low expression of the BCL-2 was detected in untreated sample and in the sample treated with GCD, G-CD@ADA-Rhod and miRNA NT, suggesting that the upregulation is clearly due to the miR-15a released. To date, it has been demonstrated that the upregulation of BCL-2 proteins is due to downregulation of miRNA15a [164].Therefore, it is possible that the mimic-miRNA delivery competes with the miRNA 15a endogenous allowing to failure of the BCL-2 downregulation. Ongoing studies will evaluate the miRNA15a transcripts in untreated and treated cells and molecular pathway activated by upregulation of BCL-2.

5.3. DISCUSSION

Gene transfer is the technique, which introduces new genetic materials inside the cells in order to study gene function and its regulation, to establish several diseases characterized by gene inactivation, to acquire DNA-based immunization, and finally, to explore potentials therapeutics applications. The size and the hydrophilic nature of the naked DNA limit their entry in cellular compartment. In addition, they are very susceptible to nuclease-mediated degradation. Therefore, the primary challenge for gene therapy is to develop carriers, characterized by low immunogenicity, low toxicity and tissue specificity, able to facilitate gene transfer to targeted cells without degradation of the delivered gene. In recent years, carbon-based nanoparticles have been plenty studied for their capability to drug and gene delivery. These materials, including fullerenes, one-dimensional carbon nanotubes, and two-dimensional graphene show carbon atoms with sp_2 hybridization forming a hexagonal arrangement. Their chemical structure, characterized by a small size and a large surface area, make them efficient platform for the loading of several drugs and/or ligands. Multiple methodologies have been developed to modify the carbon-based nanoparticles and make them soluble in an aqueous environment, biocompatible and able to internalize into the cells.

Therefore, in this work two potential non-viral vectors have been used as a platform to delivery anticancer and antiviral drugs, plasmid DNA and miRNA. Carbon nanotubes and graphene both engineered β- cyclodextrin were selected as a nanoplatform and their biological properties were investigated in this thesis work. The multiwalled carbon nanotube functionalized with cyclodextrin (MWCNT-CD), modified with branched polyethylenimine to form MWCNT-CD-PEI platform and consequently conjugated with Rhodamine (MWCNT-CD-PEI-Rhod) to track in vitro the nanocarrier and to elucidate the uptake cellular mechanisms. The results exposed in the section 5.2 and published in Mazzaglia A.et al., (2018)[2], demonstrated that the MWCNT-CD-PEI-Rhod is able to internalize with a specific clathrin-dependend endocytosis mechanism (Fig. 33), not affects the cellular viability and it is able to delivery antiviral drug resulting in the HSV-1 plaques number reduction (Fig. 34). At the high drug delivery efficiency, mediated by nanotube, corresponds an inefficient delivery of nucleic acids into the cells; the platform is not able to promote the delivery of DNA plasmid encoding enhanced green fluorescence protein (EGFP).

The second investigated platform (GCD) contains the cationic centres directly on cyclodestrin moieties for the linkage with nucleic acids and the cyclodextrin cavity was exploited for the complexation with ADA-Rhod (i.e fluorescent probe) in order to track the cellular internalization (Fig. 35). In addition, the graphene surfaces were exploited to load doxorubicin by π-π interactions. Therefore, three important tasks were studied: I. Internalization mechanisms; II. Anticancer drug delivery and induced molecular pathways; III. Gene delivery.

In *vitro* results demonstrated that the internalization of graphene-based platform occurs with a specific caveolin-mediated endocytosis mechanism (Fig. 36) and not induce any variations in the cellular viability (Fig. 37). The capability of graphene-based nanocarrier to deliver chemotherapeutic drug (Doxorubicin) has been investigated in tumor and non-tumor cell lines, by evaluating the differential temporal expression of target proteins involved in different molecular pathway. First of all, the expression levels of cell cycle check points regulators were analyzed (Fig. 42). WEE-1 is kinase protein, which prevents mitotic entry via an inhibitory phosphorylation of cyclin-dependent kinases CDK1 and CDK2, activated during the S phase of cell cycle[159]. The accumulation of WEE-1 was detected in tumor cell lines exposed up to 72h to low concentration of GCD/Doxo, rather than non-tumor cells (Fig. 42) A progressive temporal nuclear expression of WEE-1 and p-CDK2 T14/Y15 indicates the capability of the graphene-based platform to delivery Doxorubicin, release and produce a biological effect (Fig. 43).

In addition, manipulation of cell cycle involving E2F1 transcriptional factors was detected following GCD/Doxo treatment. It is note that E2F controls cell cycle and regulates the expression of tumor suppressor proteins[160]. The function of E2F1 protein is regulated by retinoblastoma protein Rb. When Rb is not in its hyperphosphorylated form, it binds to E2F1 and block its action. On the contrary, upon phosphorylation of pRb, E2F1 is released from Rb/E2F1 inhibitory complex and acts by inducing the activation of the target gene transcription involved in the cell cycle progression. Therefore, E2F1 downregulation led to cell cycle arrest. The reduction of E2F-1 protein expression has been observed at 48h and 72h of GCD/Doxo treatment suggesting that the drug release, mediated by G-CD, occurs as a late event and keep for a long time (Fig.44). Besides, regulatory signals involved in the cell cycle control, depend on p53 protein accumulation.

The transcription factor p53 is a tumor suppressor that is activated by several type of cellular stress and its dysregulation occurs in several cancer diseases, frequently[14]. The p53 phosphorylation interferes with binding to p53-inhibitor protein, MDM2. Activated p53 transcriptionally upregulates p21 protein which inactivates the cyclin/cyclin-dependent-kinase complex blocking the cell-cycle progression in the G1-S transition.

The accumulation of p53 was induced by graphene-based/doxo and not involves the downstream signal p21-mediated but high levels of MDM2 at 48h indicate an upstream control in the p53 activation (Fig. 45).

Further analysis will carry out to individuate the proteins involved in the regulation of the signals cascade activated by p53. Additionally, to p53 regulation, the autophagy processes was deeply examined by combining two different approaches: the quantification of autophagosomes by transient transfection with mRFP-GFP tandem fluorescent-tagged LC3 plasmid (Fig. 46), and the quantification of LC3 and p62 protein expressions (Fig. 47). Both approaches have highlighted that the Doxorubicin, released from platform, induces the activation of autophagy processes as a late event, probably to promote the elimination of the platform following the drug release. A key factor for gene therapy is to find efficient and safe vectors that protect DNA from nuclease degradation and facilitate its uptake with high transfection efficiency. The capability to gene delivery of graphene-based platform was performed by verifying the intracellular autofluorescence of DNA plasmid encoding enhanced green fluorescence protein (pCMS-EGFP) complexed with the platform and by evaluating a molecular pathway activated by miRNA15a delivered and released by graphene-based platform. The detection of green dots indicating the EGFP expression demonstrated that capability of nanovector to gene delivery (Fig. 48). In addition, the efficient delivery of miRNA15a was revealed by quantification of BCL-2 protein expression. In disagreement with several studies in which miRNA15a negatively regulate BCL-2 expression[165], in our cellular model, it has been demonstrated an induction of BCL-2 expression levels following GCD/miRNA-15a treatment in N/P dependent-manner (Fig.49). N/P indicates the ratio between amine groups of cationic cyclodextrin (N) to those of the phosphate ones (P) of nucleic acid. When the N/P increases, the number of positive charges increases and facilitates the binding to negative charges in the nucleic acid, resulting in a high transfection efficiency of the vector. In fact, high N/P (N/P 10) produces an accumulation of BCL-2 expression compared to law ratio (N/P 5). Taken together, these results suggest that the cyclodextrin- graphene platform is an efficient and safe nano-vector to promote drug and gene delivery.

Conclusions

The intracellular delivery needs of genetically engineered carriers, commonly called vectors, which facilitate gene transfer to targeted cells without degradation of the delivered gene. To date, it is possible to refer to two large families of vectors, viral and non-viral, used in clinical and research studies, responsible for the success of gene therapy in the treatment and prevention of several diseases. Many viruses such as retrovirus, adenovirus, herpes simplex virus, adeno-associated virus and poxvirus have been modified to eliminate their toxicity and maintain their high gene delivery capability[3]. The size of the viral genome is a limiting factor to gene delivery on the contrary, the capability to eliminate part of viral genome and to increase the space available to gene delivery, represents the major advantage to engine herpes simplex virus as an oncolytic vector[5].

The success of the oncolytic herpes simplex virus-based therapy requires deep knowledge about the interaction between virus and host. In particular, in this thesis work the immune evasion concept was extensively discussed as a mechanism to evade host anti-viral responses and promote virus replication. In this context, the PKR kinase protein tend to minimize the viral replication by interacting with dsRNA, phosphorylating and activating eIF2α and attenuating the translation of cellular proteins[80]. Most viruses, including HSV-1, create dsRNA as a product at some stage during viral genome replication and induce the PKR activation. HSV-1 contains a late gene, Us11, which, expressed early, binds to PKR and blocks its activation and ICP34.5, which recruits the phosphatase alpha to dephosphorylate eIF-2α[85,87]. To date, it has been demonstrated that VHS tegument protein blocks the accumulation of PKR probably via its endonuclease activity and then via the subtraction of mRNAs[1].

In this thesis work, the tegument viral proteins, closely connected to immunological escape, US3 and UL13 were widely investigated in their potential role against PKR. In particular, the results demonstrated for the first time that the US3 and UL13 tegument protein control the activation of phospho-PKR and that the signalling network between US3 and VHS is responsible for this control. The study of these proteins and of interplay between viral teguments proteins and host immune response could be useful to define new retargeting approaches in the HSV-1 oncolytic virus. Although the viruses mediate efficient gene delivery due to high ability to uptake and intake into the cells, several limitations were reported in *vitro* and in *vivo* such as low DNA/RNA loading capacity, immunogenicity, toxicity and difficulty in production. These negative factors have encouraged the development of non-viral vectors[4].

In recent years, carbon-based nanoparticles have been plenty studied for their capability to drug and gene delivery[62]. These materials, including fullerenes, one-dimensional carbon

nanotubes (CNTs), and two-dimensional graphene show carbon atoms with sp2 hybridization forming a hexagonal arrangement. Their chemical structure, characterized by a small size and a large surface area, make them efficient platform for the attachment of several drugs and/or ligands. Generally, nanocarriers interact with the cell membranes and enter into the cells by endocytosis mechanisms. The size, the charge and the shape of nanomaterials can be decisive to activate a specific endocytosis pathway. Carbon nanotubes (CNTs) and graphene are two representative carbon-based nanomaterials used as a platform in this work. The results exposed in this thesis work and published in Mazzaglia.*et al.,* 2018[2] ,have demonstrated that the nanotube carrier internalizes, deliveries and releases antiviral drug into the cells but not nucleic acids. For this reason, it has been designed a new graphene-based platform whose chemical functionalization on the surface and its shape made it an efficient drug and gene vector. Further studies will continue to investigate deeply the intracellular signaling network, which can be influence by viral and non-viral vectors, in order to improve the target delivery limiting the cytotoxicity effect.

References

1. Sciortino, M.T., Parisi, T., Siracusano, G., Mastino, A., Taddeo, B., Roizman, B. The virion host shutoff RNase plays a key role in blocking the activation of protein kinase R in cells infected with herpes simplex virus 1. *J. Virol.* 87 (6), 3271-3276; doi: 10.1128/JVI.03049-12 (2013).

2. Mazzaglia, A., Scala, A., Sortino, G., Zagami, R., Zhu, Y., Sciortino, M.T., Pennisi, R., Pizzo, M.M., Neri, G., Grassi, G., Piperno, A. Intracellular trafficking and therapeutic outcome of multiwalled carbon nanotubes modified with cyclodextrins and polyethylenimine. *Colloids Surf B Biointerfaces* 163, 55-63; doi:10.1016/j.colsurfb.2017.12.028 (2018).

3. Vannucci, L., Lai, M., Chiuppesi, F., Ceccherini-Nelli, L., Pistello, M. Viral vectors: a look back and ahead on gene transfer technology. *New Microbiol.* 36 (1), 1-22 (2013).

4. Thapa, B., Narain, R. Mechanism, current challenges and new approaches for non-viral gene delivery. *Polymers and Nanomaterials for Gene Therapy* 1, 1-27 (2016).

5. Peters, C., Rabkin, S.D. Designing herpes viruses as oncolytics. *Mol Ther Oncolytics.* 2, 15010; doi:10.1038/mto.2015.1015010 (2015).

6. Edelstein, M.L., Abedi, M.R., Wixon, J. Gene therapy clinical trials worldwide to 2007--an update. J Gene Med. 9 (10), 833-842; doi:10.1002/jgm.1100 (2007).

7. Kandoth, C., McLellan, M.D., Vandin, F., Ye, K., Niu, B., Lu, C., Xie, M., Zhang, Q., McMichael, J.F., Wyczalkowski, M.A., Leiserson, M.D.M., Miller, C.A., Welch, J.S., Walter, M.J., Wendl, M.C., Ley, T.J., Wilson, R.K., Raphael, B.J., Ding, L. Mutational landscape and significance across 12 major cancer types. *Nature* 502 (7471), 333-339; doi:10.1038/nature12634 (2013).

8. Kim, M.P., Zhang, Y., Lozano, G. Mutant p53: Multiple Mechanisms Define Biologic Activity in Cancer. *Frontiers in Oncology* 5, 249; doi:10.3389/fonc.2015.00249 (2015).

9. Dittmer, D., Pati, S., Zambetti, G., Chu, S., Teresky, A.K., Moore, M., Finlay, C., Levine, A.J. Gain of function mutations in p53. *Nat Genet.* 4 (1), 42-46; doi: 10.1038/ng0593-42 (1993).

10. Doyle, B., Morton, J.P., Delaney, D.W., Ridgway, R.A., Wilkins, J.A., Sansom, O.J. p53 mutation and loss have different effects on tumourigenesis in a novel mouse model of pleomorphic rhabdomyosarcoma. *J. Pathol.* 222, 129-137; doi: 10.1002/path.2748 (2010).

11. Lang, G.A., Iwakuma, T., Suh, Y.A., Liu, G., Rao, V.A., Parant, J.M., Valentin-Vega, Y.A., Terzian, T., Caldwell, L.C., Strong, L.C. Gain of function of a p53 hot spot mutation in a mouse model of Li-Fraumeni syndrome. *Cell*. 119, 861-872; doi: 10.1016/j.cell.2004.11.0062004 (2004).

12. Morton, J.P., Timpson, P., Karim, S.A., Ridgway, R.A., Athineos, D., Doyle, B., Jamieson, N.B., Oien, K.A., Lowy, A.M., Brunton, V.G. Mutant p53 drives metastasis and overcomes growth arrest/senescence in pancreatic cancer. Proc. *Natl. Acad. Sci. USA.* 107, 246-251; doi: 10.1073/pnas.0908428107 (2010).

13. Olive, K.P., Tuveson, D.A., Ruhe, Z.C., Yin, B., Willis, N.A., Bronson, R.T., Crowley, D., Jacks, T. Mutant p53 gain of function in two mouse models of Li-Fraumeni syndrome. *Cell.* 119, 847-860; doi:10.1016/j.cell.2004.11.004 (2004).

14. Muller, P.A. J., Vousden, K. H. Mutant p53 in Cancer: New Functions and Therapeutic Opportunities. *Cancer Cell*, 25 (3), 304-317; doi:10.1016/j.ccr.2014.01.021 (2014).

15. Esser, C., Scheffner, M., Höhfeld, J. The chaperone-associated ubiquitin ligase CHIP is able to target p53 for proteasomal degradation. *J. Biol. Chem.* 280, 27443-27448; doi:10.1074/jbc.M501574200 (2005).

16. Li, D., Marchenko, N.D., Moll, U.M. SAHA shows preferential cytotoxicity in mutant p53 cancer cells by destabilizing mutant p53 through inhibition of the HDAC6-Hsp90 chaperone axis. *Cell Death Differ.* 18, 1904-1913; doi:10.1038/cdd.2011.71 (2011).

17. Mizushima, N., Levine, B., Cuervo, A.M., Klionsky, D.J. Autophagy fights disease through cellular self-digestion. *Nature* 451, 1069-1075; doi:10.1038/nature06639 (2008).

18. Borst, J., Ahrends, T., Bąbała, N., Melief, C.J.M., Kastenmüller, W. $CD4^+$ T cell help in cancer immunology and immunotherapy. *Nat Rev Immunol.* 29; doi:10.1038/s41577-018-0044-0 (2018).

19. Palmieri, D.J., Carlino, M.S. Immune Checkpoint Inhibitor Toxicity. *Curr Oncol Rep.* 20 (9), 72; doi: 10.1007/s11912-018-0718-6 (2018).

20. Springer, J., Niculescu-Duvaz, I. Gene-directed enzyme prodrug therapy (GDEPT): choice of prodrugs. *Advanced Drug Delivery Reviews* 22(3), 351-364; doi:10.1016/S0169-409X(96)00449-8 (1999).

21. Zhang, J., Kale, V., Chen, M. Gene-Directed Enzyme Prodrug Therapy. *The AAPS Journal* 17 (1), 102-110; doi:10.1208/s12248-014-9675-7 (2015).

22. Scollay, R. Gene therapy: a brief overview of the past, present, and future. *Ann N Y Acad Sci.* 953, 26-30 (2001).

23. Chen, N.G., Szalay, A.A. Oncolytic Virotherapy of Cancer. In: *Minev B. (eds) Cancer Management in Man: Chemotherapy, Biological Therapy, Hyperthermia and Supporting Measures. Cancer Growth and Progression. Springer, Dordrecht*. 13, 295-316. doi:10.1007/978-90-481-9704-0_16 (2011).

24. Bolhassani, A., Safaiyan, S., Rafati, S. Improvement of different vaccine delivery systems for cancer therapy. *Mol Cancer.* 10, 3; doi: 10.1186/1476-4598-10-3 (2011).

25. Choi, A.H., O'Leary, M.P., Fong, Y., Chen, N.G. From Benchtop to Bedside: A Review of Oncolytic Virotherapy. *Biomedicines* 4 (3), 18; doi:10.3390/biomedicines4030018 (2016).

26. Cary, Z.D., Willingham, M.C., Lyles, D.S. Oncolytic Vesicular Stomatitis Virus Induces Apoptosis in U87 Glioblastoma Cells by a Type II Death Receptor Mechanism and Induces Cell Death and Tumor Clearance In Vivo. *Journal of Virology* 85 (12), 5708–5717; doi:10.1128/JVI.02393-10 (2011).

27. Elankumaran, S., Rockemann, D., Samal, S.K. Newcastle disease virus exerts oncolysis by both intrinsic and extrinsic caspase-dependent pathways of cell death. *J Virol.* 80 (15), 7522-7534; doi:10.1128/JVI.00241-06 (2006).

28. Hirvinen, M., Rajecki, M., Kapanen, M., Parviainen, S., Rouvinen-Lagerström, N., Diaconu, I., Nokisalmi, P., Tenhunen, M., Hemminki, A., Cerullo, V. Immunological effects of a tumor necrosis factor alpha-armed oncolytic adenovirus. *Hum Gene Ther.* 26 (3), 134-144; doi:10.1089/hum.2014.069 (2015).

29. Zhu, W., Zhang, H., Shi, Y., Song, M., Zhu, B., Wei, L. Oncolytic adenovirus encoding tumor necrosis factor-related apoptosis inducing ligand (TRAIL) inhibits the growth and metastasis of triple-negative breast cancer. *Cancer Biol Ther.* 14 (11), 1016-1023. doi:10.4161/cbt.26043 (2013).

30. McKee, T.D., Grandi, P., Mok, W., Alexandrakis, G., Insin, N., Zimmer, J.P., Bawendi, M.G., Boucher, Y., Breakefield, X.O., Jain, R.K. Degradation of fibrillar collagen in a human melanoma xenograft improves the efficacy of an oncolytic herpes simplex virus vector. *Cancer Res.* 66 (5), 2509-2513; doi:10.1158/0008-5472.CAN-05-2242 (2006).

31. Nishio, N., Dotti, G. Oncolytic virus expressing RANTES and IL-15 enhances function of CAR-modified T cells in solid tumors. *Oncoimmunology.* 4 (2), e988098; doi:10.4161/21505594.2014.988098 (2015).

32. Filley, A.C., Dey, M. Immune System, Friend or Foe of Oncolytic Virotherapy? *Frontiers in Oncology* 7, 106; doi:10.3389/fonc.2017.00106 (2017).

33. Wold, W.S., Toth, K. Adenovirus vectors for gene therapy, vaccination and cancer gene therapy. *Curr Gene Ther.* 13 (6), 421-433 (2013).

34. Bass-Stringer, S., Bernardo, B.C., May, C.N., Thomas, C.J., Weeks, K.L., McMullen, J.R. Adeno-Associated Virus Gene Therapy: Translational Progress and Future Prospects in the Treatment of Heart Failure. *Heart Lung Circ.* doi:10.1016/j.hlc.2018.03.005 (2018).

35. Zhong, L., Li, B., Mah, C.S., Govindasamy, L., Agbandje-McKenna, M., Cooper, M., Herzog, R.W., Zolotukhin, I., Warrington, K.H. Jr, Weigel-Van Aken, K.A., Hobbs, J.A., Zolotukhin, S., Muzyczka, N., Srivastava, A. Next generation of adeno-associated virus 2 vectors: point mutations in tyrosines lead to high-efficiency transduction at lower doses. *Proc Natl Acad Sci U S A.* 105 (22), 7827-7832; doi:10.1073/pnas.0802866105 (2008).

36. Santiago-Ortiz, J.L., Schaffer, D.V. Adeno-associated virus (AAV) vectors in cancer gene therapy. *J Control Release*. 240, 287-301; doi:10.1016/j.jconrel.2016.01.001 (2016).

37. Ertl, H.C. Viral vectors as vaccine carriers. *Curr Opin Virol.* 21, 1-8; doi: 10.1016/j.coviro.2016.06.001 (2016).

38. Greenberg, B. Gene therapy for heart failure. *Trends in Cardiovascular Medicine* 27 (3), 216-222; doi:10.1016/j.tcm.2016.11.001 (2017).

39. Kaufman, H.L., Kim, D.W., DeRaffele, G., Mitcham, J., Coffin, R.S., Kim-Schulze, S. Local and distant immunity induced by intralesional vaccination with an oncolytic herpes virus encoding GM-CSF in patients with stage IIIc and IV melanoma. *Ann Surg Oncol.* 17 (3), 718-730; doi:10.1245/s10434-009-0809-6 (2010).

40. Melchjorsen, J., Matikainen, S., Paludan, S.R. Activation and Evasion of Innate Antiviral Immunity by Herpes Simplex Virus. *Viruses* 1 (3), 737-759; doi:10.3390/v1030737 (2009).

41. Saha, D., Wakimoto, H., & Rabkin, S.D. Oncolytic herpes simplex virus interactions with the host immune system. *Current Opinion in Virology* 21, 26-34; doi:10.1016/j.coviro.2016.07.007 (2016).

42. Yang, Y., Wu, S., Wang, Y., Pan, S., Lan, B., Liu, Y., et al. The Us3 Protein of Herpes Simplex Virus 1 Inhibits T Cell Signaling by Confining Linker for Activation of T Cells (LAT) Activation via TRAF6 Protein. *The Journal of Biological Chemistry*, 290 (25), 15670-15678; doi:10.1074/jbc.M115.646422 (2015).

43. Van Lint, A.L., Murawski, M.R., Goodbody, R.E., Severa, M., Fitzgerald K.A., Finberg, R.W., Knipe, D.M., Kurt-Jones, E.A. Herpes simplex virus immediate-early ICP0 protein inhibits Toll-like receptor 2-dependent inflammatory responses and NF-kappaB signaling. *J Virol.* 84 (20), 10802-10811; doi:10.1128/JVI.00063-10 (2010).

44. Xing, J., Wang, S., Lin, R., Mossman, K.L., Zheng, C. Herpes simplex virus 1 tegument protein US11 downmodulates the RLR signaling pathway via direct interaction with RIG-I and MDA-5. *J Virol.* 86 (7), 3528-3540; doi:10.1128/JVI.06713-11 (2012).

45. Manservigi, R., Argnani, R., Marconi, P. HSV Recombinant Vectors for Gene Therapy.*The Open Virology Journal* 4, 123-156; doi:10.2174/1874357901004010123 (2010).

46. Li, H., Zhang, X. Oncolytic HSV as a vector in cancer immunotherapy. *Methods Mol Biol.* 651, 279-90; doi:10.1007/978-1-60761-786-0_16 (2010).

47. Martuza, R.L., Malick, A., Markert, J.M., Ruffner, K.L., Coen, D.M. Experimental therapy of human glioma by means of a genetically engineered virus mutant. *Science* 252 (5007), 854-856 (1991).

48. Goins, W.F., Hall, B., Cohen, J.B., Glorioso, J.C. Retargeting of Herpes Simplex Virus (HSV) Vectors. *Current Opinion in Virology* 21, 93-101; doi:10.1016/j.coviro.2016.08.007 (2016).

49. Campadelli-Fiume, G., Petrovic, B., Leoni, V., Gianni, T., Avitabile, E., Casiraghi, C., Gatta, V. Retargeting Strategies for Oncolytic Herpes Simplex Viruses. Viruses 8 (3), 63; doi:10.3390/v8030063 (2016).

50. Agelidis, A.M., Shukla, D. Cell entry mechanisms of HSV: what we have learned in recent years. *Future Virology* 10 (10), 1145-1154; doi:10.2217/fvl.15.85 (2015).

51. Oh, M.J., Akhtar, J., Desai, P., Shukla, D. A role for heparan sulfate in viral surfing. *Biochem Biophys Res Commun.* 391 (1), 176-181; doi:10.1016/j.bbrc.2009.11.027 (2010).

52. Montgomery, R.I., Warner, M.S., Lum, B.J., Spear, P.G. Herpes simplex virus-1 entry into cells mediated by a novel member of the TNF/NGF receptor family. *Cell.* 87 (3), 427-436 (1996).

53. Laquerre, S., Anderson, D.B., Stolz, D.B., Glorioso, J.C. Recombinant herpes simplex virus type 1 engineered for targeted binding to erythropoietin receptor-bearing cells. J Virol. 72 (12), 9683-9697 (1998).

54. Menotti, L., Cerretani, A., Hengel, H., Campadelli-Fiume, G. Construction of a Fully Retargeted Herpes Simplex Virus 1 Recombinant Capable of Entering Cells Solely via Human Epidermal Growth Factor Receptor 2. J Virol. 82 (20), 10153-10161; doi:10.1128/JVI.01133-08 (2008).

55. Gatta, V., Petrovic, B., Campadelli-Fiume, G. The Engineering of a Novel Ligand in gH Confers to HSV an Expanded Tropism Independent of gD Activation by Its Receptors. PLoS Pathogens 11 (5), e1004907; doi:10.1371/journal.ppat.1004907 (2015).

56. Petrovic, B., Gianni, T., Gatta, V., Campadelli-Fiume, G. Insertion of a ligand to HER2 in gB retargets HSV tropism and obviates the need for activation of the other entry glycoproteins. PLoS Pathogens 13 (4), e1006352; doi:10.1371/journal.ppat.1006352 (2017).

57. Zhou, G., Roizman, B. Characterization of a Recombinant Herpes Simplex Virus 1 Designed to Enter Cells via the IL13Rα2 Receptor of Malignant Glioma Cells. Journal of Virology 79 (9), 5272-5277 doi:10.1128/JVI.79.9.5272-5277.2005 (2005).

58. Al-Dosari, M.S., Gao, X. Nonviral Gene Delivery: Principle, Limitations, and Recent Progress. *The AAPS Journal* 11 (4), 671; doi:10.1208/s12248-009-9143-y (2009).

59. Davis, M.E. Non-viral gene delivery systems. *Curr Opin Biotechnol.* 13 (2), 128-131 (2002).

60. Ramamoorth, M., Narvekar, A. Non Viral Vectors in Gene Therapy- An Overview. *Journal of Clinical and Diagnostic Research* 9 (1), GE01-GE06; doi:10.7860/JCDR/2015/10443.5394 (2015).

61. Montellano, A., Da Ros, T., Bianco, A., Prato, M. Fullerene C_{60} as a multifunctional system for drug and gene delivery. *Nanoscale* 3 (10), 4035-4041; doi:10.1039/c1nr10783f (2011).

62. Mohajeri, M., Behnam, B., Sahebkar, A. Biomedical applications of carbon nanomaterials: Drug and gene delivery potentials. *J Cell Physiol.* doi:10.1002/jcp.26899 (2018).

63. Yang, K., Zhang, S., Zhang, G., Sun, X., Lee, S.T., Liu, Z. Graphene in mice: ultrahigh in vivo tumor uptake and efficient photothermal therapy. *Nano Lett.* 10 (9), 3318-3323; doi:10.1021/nl100996u (2010).

64. Li, R.Q., Ren, Y., Liu, W., Pan, W., Xu, F.J., Yang, M. MicroRNA-mediated silence of onco-lncRNA MALAT1 in different ESCC cells via ligand-functionalized hydroxyl-rich nanovectors. *Nanoscale.* 9 (7), 2521-2530; doi:10.1039/c6nr09668a (2017).

65. Thompson, M.R., Kaminski, J.J., Kurt-Jones, E.A., Fitzgerald, K.A. Pattern recognition receptors and the innate immune response to viral infection. *Viruses* 3 (6), 920-940; doi:10.3390/v3060920 (2011).

66. Christensen, J.E., Thomsen, A.R. Co-ordinating innate and adaptive immunity to viral infection: mobility is the key. *APMIS* 117 (5-6), 338-355. doi:10.1111/j.1600-0463.2009.02451.x (2009).

67. Alcami, A., Koszinowski, U.H. Viral mechanisms of immune evasion. *Immunol Today* 21 (9), 447-455 (2000).

68. Tortorella, D., Gewurz, B.E., Furman, M.H., Schust, D.J., Ploegh, H.L. Viral subversion of the immune system. *Annu Rev Immunol.* 18, 861-926; doi:10.1146/annurev.immunol.18.1.861 (2000).

69. Noda, S., Aguirre, S.A., Bitmansour, A., Brown, J. M., Sparer, T. E., Huang, J., Mocarski, E.S. Cytomegalovirus MCK-2 controls mobilization and recruitment of myeloid progenitor cells to facilitate dissemination. *Blood* 107 (1), 30-38; doi:10.1182/blood-2005-05-1833 (2006).

70. Vandevenne, P., Sadzot-Delvaux, C., Piette, J. Innate immune response and viral interference strategies developed by human herpesviruses. *Biochem Pharmacol.* 80 (12), 1955-1972; doi:10.1016/j.bcp.2010.07.001 (2010).

71. Goodbourn, S., Didcock, L., Randall, R.E. Interferons: cell signalling, immune modulation, antiviral response and virus countermeasures. *J Gen Virol.* 81 (10), 2341-2364; doi:10.1099/0022-1317-81-10-2341 (2000).

72. Kumar, A., Yang, Y.L., Flati, V., Der, S., Kadereit, S., Deb, A. *et al.* Deficient cytokine signaling in mouse embryo fibroblasts with a targeted deletion in the PKR gene: role of IRF-1 and NF-kappaB. *The EMBO Journal*, 16 (2), 406-416; doi:10.1093/emboj/16.2.406 (1997).

73. Cuddihy, A.R., Wong, A.H., Tam, N.W., Li, S., Koromilas, A.E. The double-stranded RNA activated protein kinase PKR physically associates with the tumor suppressor p53 protein and phosphorylates human p53 on serine 392 in vitro. *Oncogene* 18 (17), 2690-2702; doi:10.1038/sj.onc.1202620 (1999).

74. Zamanian-Daryoush, M., Mogensen, T.H., DiDonato, J.A., Williams, B.R. NF-kappaB activation by double-stranded-RNA-activated protein kinase (PKR) is mediated through NF-kappaB-inducing kinase and IkappaB kinase. *Mol Cell Biol.* 20(4):1278-90 (2000).

75. Oganesyan, G., Saha, S.K., Guo, B., He, J.Q., Shahangian, A., Zarnegar, B., Perry, A., Cheng, G. Critical role of TRAF3 in the Toll-like receptor-dependent and -independent antiviral response. *Nature* 439, 208-211 (2006).

76. Donzé O, Deng J, Curran J, Sladek R, Picard D, Sonenberg N. The protein kinase PKR: a molecular clock that sequentially activates survival and death programs. *The EMBO Journal*. 2004;23(3):564-571. doi:10.1038/sj.emboj.7600078.

77. Dey, M., Cao, C., Dar, A.C., Tamura, T., Ozato, K., Sicheri, F., Dever, T.E. Mechanistic link between PKR dimerization, autophosphorylation, and eIF2alpha substrate recognition. *Cell.* 122 (6), 901-913; doi:10.1016/j.cell.2005.06.041 (2005).

78. Cole, J.L. Activation of PKR: an open and shut case? *Trends Biochem Sci.* 32 (2), 57-62; doi:10.1016/j.tibs.2006.12.003 (2007).

79. Williams, B.R. PKR; a sentinel kinase for cellular stress. *Oncogene.* 18 (45), 6112-6120; doi:10.1038/sj.onc.1203127 (1999).

80. Dzananovic, E., McKenna, S.A., Patel, T.R. Viral proteins targeting host protein kinase R to evade an innate immune response: a mini review. *Biotechnol Genet Eng Rev.* 34 (1), 33-59; doi:10.1080/02648725.2018.1467151 (2018).

81. García, M.A., Gil, J., Ventoso, I., Guerra, S., Domingo, E., Rivas, C., Esteban, M. Impact of protein kinase PKR in cell biology: from antiviral to antiproliferative action. *Microbiol Mol Biol Rev.* 70 (4), 1032-1060; doi:10.1128/MMBR.00027-06 (2006).

82. Chang, Y.H., Lau, K.S., Kuo, R.L., Horng, J.T. dsRNA Binding Domain of PKR Is Proteolytically Released by Enterovirus A71 to Facilitate Viral Replication. *Front Cell Infect Microbiol.* 7, 284; doi:10.3389/fcimb.2017.00284 (2017).

83. Bergmann, M., Garcia-Sastre, A., Carnero, E., Pehamberger, H., Wolff, K., Palese, P., Muster, T. Influenza virus NS1 protein counteracts PKR-mediated inhibition of replication. *J Virol.* 74 (13), 6203-6206 (2000).

84. Pflugheber, J., Fredericksen, B., Sumpter, R.Jr, Wang, C., Ware, F., Sodora, D.L., Gale, M.Jr. Regulation of PKR and IRF-1 during hepatitis C virus RNA replication. *Proc Natl Acad Sci USA.* 99 (7), 4650-4655; doi:10.1073/pnas.062055699 (2002).

85. Cassady, K.A., Gross, M., Roizman, B. The herpes simplex virus US11 protein effectively compensates for the gamma1(34.5) gene if present before activation of protein kinase R by precluding its phosphorylation and that of the alpha subunit of eukaryotic translation initiation factor 2. *J Virol.* 72 (11), 8620-8626 (1998).

86. Peters, G.A., Khoo, D., Mohr, I., Sen, G.C. Inhibition of PACT-Mediated Activation of PKR by the Herpes Simplex Virus Type 1 Us11 Protein. *J Virol.* 76 (21), 11054-11064; doi:10.1128/JVI.76.21.11054-11064.2002 (2002).

87. He, B., Gross, M., Roizman, B. The gamma (1)34.5 protein of herpes simplex virus 1 complexes with protein phosphatase 1alpha to dephosphorylate the alpha subunit of the eukaryotic translation initiation factor 2 and preclude the shutoff of protein synthesis by double-stranded RNA-activated protein kinase. *Proc Natl Acad Sci U S A.* 94 (3), 843-848 (1997).

88. Lussignol, M., Queval, C., Bernet-Camard, M.F., Cotte-Laffitte, J., Beau, I., Codogno, P., Esclatine, A. The herpes simplex virus 1 Us11 protein inhibits autophagy through its interaction with the protein kinase PKR. *J Virol.* 87 (2), 859-871; doi:10.1128/JVI.01158-12 (2013).

89. Pak, A.S., Everly, D.N., Knight, K., Read, G.S. The virion host shutoff protein of herpes simplex virus inhibits reporter gene expression in the absence of other viral gene products. *Virology* 211 (2), 491-506; doi:10.1006/viro.1995.1431 (1995).

90. Honess, R.W., Roizman, B. Regulation of herpesvirus macromolecular synthesis. I. Cascade regulation of the synthesis of three groups of viral proteins. *J Virol.* 14 (1), 8-19 (1974).

91. Shu, M., Taddeo, B., Roizman, B. The nuclear-cytoplasmic shuttling of virion host shutoff RNase is enabled by pUL47 and an embedded nuclear export signal and defines the sites of degradation of AU-rich and stable cellular mRNAs. *J Virol.* 87 (24), 13569-13578; doi:10.1128/JVI.02603-13 (2013).

92. Esclatine, A., Taddeo, B., Evans, L., Roizman, B. The herpes simplex virus 1 UL41 gene-dependent destabilization of cellular RNAs is selective and may be sequence-specific. *Proc Natl Acad Sci U S A.* 101 (10), 3603-3608; doi:10.1073/pnas.0400354101 (2004).

93. Everly, Jr., D.N., Feng, P., Mian, I.S., Read, G.S. mRNA Degradation by the Virion Host Shutoff (Vhs) Protein of Herpes Simplex Virus: Genetic and Biochemical Evidence that Vhs Is a Nuclease. *J Virol* 76 (17), 8560-8571; doi:10.1128/JVI.76.17.8560-8571.2002 (2002).

94. Taddeo, B., Roizman, B. The Virion Host Shutoff Protein (UL41) of Herpes Simplex Virus 1 Is an Endoribonuclease with a Substrate Specificity Similar to That of RNase A. *J Virol* 80 (18), 9341-9345; doi:10.1128/JVI.01008-06 (2006).

95. Bannazadeh-Baghi, H., Bamdad, T., Soleimanjahi, H. The effect of herpes simplex virus virion host shutoff gene- a new suicide gene- on tumor cells. *Iran Biomed J.* 13 (3), 185-189 (2009).

96. Smith, K.D., Mezhir, J.J., Bickenbach, K., Veerapong, J., Charron, J., Posner, M.C., Roizman, B., Weichselbaum, R.R. Activated MEK suppresses activation of PKR and enables efficient replication and in vivo oncolysis by Deltagamma (1)34.5 mutants of herpes simplex virus 1. *J Virol.* 80 (3), 1110-1120; doi:10.1128/JVI.80.3.1110-1120.2006 (2006).

97. Pasieka, R.J., Lu, B., Crosby, S.D., Wylie, K.M., Morrison, L.A., Alexander, D.E., Menachery, V.D., Leib, D.A. Herpes simplex virus virion host shutoff attenuates establishment of the antiviral state. *J. Virol.* 82, 5527-5535; doi:10.1128/JVI.02047-07 (2008).

98. Dauber, B., Poon, D., Dos Santos, T., Duguay, B.A., Mehta, N., Saffran, H.A., Smiley, J.R. The Herpes Simplex Virus Virion Host Shutoff Protein Enhances Translation of Viral True Late mRNAs Independently of Suppressing Protein Kinase R and Stress Granule Formation. *J Virol.* 90 (13), 6049-6057; doi:10.1128/JVI.03180-15 (2016).

99. Feng, P., Everly, D.N., Read, G.S. mRNA Decay during Herpes Simplex Virus (HSV) Infections: Protein-Protein Interactions Involving the HSV Virion Host Shutoff Protein and Translation Factors eIF4H and eIF4A. *J Virol.* 79 (15), 9651-9664; doi:10.1128/JVI.79.15.9651-9664.2005 (2005).

100. Smiley J.R. Herpes Simplex Virus Virion Host Shutoff Protein: Immune Evasion Mediated by a Viral RNase? *J Virol.* 78 (3), 1063-1068; doi:10.1128/JVI.78.3.1063-1068 (2004).

101. Baines, J.D. Envelopment of herpes simplex virus nucleocapsids at the inner nuclear membrane. In: Arvin, A., Campadelli-Fiume, G., Mocarski, E., Moore P.S., Roizman, B., Whitley R., Yamanishi, K. *Human Herpesviruses Biology, Therapy, and Immunoprophylaxis.* Cambridge University Press; 11 (2007).

102. Xu, X., Che, Y., Li, Q. HSV-1 tegument protein and the development of its genome editing technology. *Virol J.* 13, 108; doi:10.1186/s12985-016-0563-x (2016).

103. Wang, X., Patenode, C., Roizman, B. US3 protein kinase of HSV-1 cycles between the cytoplasm and nucleus and interacts with programmed cell death protein 4 (PDCD4) to block apoptosis. *Proc Natl Acad Sci U S A* 108 (35), 14632-14636; doi:10.1073/pnas.1111942108 (2011).

104. Kato, A., Yamamoto, M., Ohno, T., Kodaira, H., Nishiyama, Y., Kawaguchi, Y. Identification of Proteins Phosphorylated Directly by the Us3 Protein Kinase Encoded by Herpes Simplex Virus 1. *J Virol.* 79 (14), 9325-9331. doi:10.1128/JVI.79.14.9325-9331.2005 (2005).

105. Kato, A., Tsuda, S., Liu, Z., Kozuka-Hata, H., Oyama, M., Kawaguchi, Y. Herpes Simplex Virus 1 Protein Kinase Us3 Phosphorylates Viral dUTPase and Regulates Its Catalytic Activity in Infected Cells. *J Virol.* 88 (1), 655-666; doi:10.1128/JVI.02710-13 (2014).

106. Imai, T., Koyanagi, N., Ogawa, R., Shindo, K., Suenaga, T., Sato, A. *et al.* Us3 Kinase Encoded by Herpes Simplex Virus 1 Mediates Downregulation of Cell Surface Major Histocompatibility Complex Class I and Evasion of CD8+ T Cells. *PLoS ONE*, 8 (8), e72050; doi:10.1371/journal.pone.0072050 (2013).

107. Wang, K., Ni, L., Wang, S., Zheng, C. Herpes Simplex Virus 1 Protein Kinase US3 Hyperphosphorylates p65/RelA and Dampens NF-κB Activation. *J Virol.* 88 (14), 7941-7951; doi:10.1128/JVI.03394-13 (2014).

108. Chuluunbaatar, U., Roller, R., Mohr, I. Suppression of Extracellular Signal-Regulated Kinase Activity in Herpes Simplex Virus 1-Infected Cells by the Us3 Protein Kinase. *J Virol* 86 (15), 7771-7776; doi: 10.1128/JVI.00622-12 (2012).

109. Sagou, K., Imai, T., Sagara, H., Uema, M., Kawaguchi, Y. Regulation of the Catalytic Activity of Herpes Simplex Virus 1 Protein Kinase Us3 by Autophosphorylation and Its Role in Pathogenesis. *J Virol* 83(11), 5773–5783; doi:10.1128/JVI.00103-09 (2009).

110. Long, M.C., Leong, V., Schaffer, P.A., Spencer, C.A., Rice, S.A. ICP22 and the UL13 Protein Kinase Are both Required for Herpes Simplex Virus-Induced Modification of the Large Subunit of RNA Polymerase II. *J Virol* 73 (7), 5593-5604 (1999).

111. Gershburg, S., Geltz, J., Peterson, K.E., Halford, W.P., Gershburg, E. The UL13 and US3 Protein Kinases of Herpes Simplex Virus 1 Cooperate to Promote the Assembly and Release of Mature, Infectious Virions. *PLoS ONE* 10 (6), e0131420; doi:10.1371/journal.pone.0131420 (2015).

112. Shibaki, T., Suzutani, T., Yoshida, I, Ogasawara, M., Azuma, M. Participation of type I interferon in the decreased virulence of the UL13 gene-deleted mutant of herpes simplex virus type 1. *J Interferon Cytokine Res.* 21 (5), 279-85; doi: 10.1089/107999001300177466 (2001).

113. Mailänder, V., Landfester, K. Interaction of Nanoparticles with Cells. *Biomacromolecules* 10, 2379-2400; doi:10.1021/bm900266r (2009).

114. Wang, A.Z., Langer, R., Farokhzad, O.C. Nanoparticle delivery of cancer drugs. *Annu Rev Med* 63, 185-198; doi:10.1146/annurev-med-040210-162544 (2012).

115. Liu, Z., Robinson, J.T., Sun, X.M., Dai, H.J. PEGylated Nanographene Oxide for Delivery of Water-Insoluble Cancer Drugs. *J Am Chem Soc*, 130, 10876-10877; doi:10.1021/ja803688x (2008).

116. Liu, K., Zhang, J., Yang, G., Wanga, C., Zhu, J.J. Direct electrochemistry and electrocatalysis of hemoglobin based on poly (diallyldimethylammonium chloride functionalized graphene sheets/room temperature ionic liquid composite film. *Electrochem Commun* 12, 402-405; doi:10.1016/j.elecom.2010.01.004 (2010).

117. Guo, C.X., Zheng, X.T., Lu, Z.S., Lou, X.W., Li, C.M. Biointerface by Cell Growth on Layered Graphene-Artificial Peroxidase-Protein Nanostructure for in Situ Quantitative Molecular Detection. *Adv Mater* 22, 5164-5167; doi:10.1002/adma.201001699 (2010).

118. Zan, X., Fang, Z., Wu, J., Xiao, F., Huo, F., Duan, H. Free-standing Graphene Paper Decorated with 2d-Assembly of Au@Pt Nanoparticles as Flexible Biosensors to Monitor Live Cell Secretion of Nitric Oxide. *Biosens Bioelectron* 49, 71-78; doi:10.1016/j.bioelechem.2016.02.002 (2013).

119. Cui, L., Zhu, B.W., Qu, S., He, X.P., Chen, G.R. "Clicked" Galactosyl Anthraquinone on Graphene Electrodes for the Label-Free Impedance Detection of Live Cancer Cells. *Dyes Pigm* 121, 312-315; doi:10.1016/j.dyepig.2015.05.034 (2015).

120. Wang, Y., Liu, K, Luo, Z., Duan,Y. Preparation and tumor cell model based biobehavioral evaluation of the nanocarrier system using partially reduced graphene oxide functionalized by surfactant. *Int J Nanomed* 10, 4605-4620; doi:10.2147/IJN.S82354 (2015).

121. Yang, X.Y., Niu, G.L., Cao, X.F., Wen, Y.K., Xiang, R., Duan, H.Q., Chen, Y.S.J. The preparation of functionalized graphene oxide for targeted intracellular delivery of siRNA. *Mater Chem* 22, 6649-6654; doi:10.1039/C2JM14718A (2012).

122. Qin, X.C., Guo, Z.Y., Liu, Z.M., Zhang, W., Wan, M.M., Yang, B.W. Folic acid-conjugated graphene oxide for cancer targeted chemo-photothermal therapy. *J Photochem Photobiol B Biology*, 120, 156-162; doi:10.1016/j.jphotobiol.2012.12.005 (2013).

123. Chatterjee, N., Eom, H-J., Choi, J. A systems toxicology approach to the surface functionality control of Graphene cell interactions. *Biomaterials*, 35, 1109-1127; doi:10.1016/j.biomaterials.2013.09.108 (2014).

124. Yin, T., Liu, J., Zhao, Z., Zhao, Y., Dong, L., Yang, M., Zhou, J., Huo, M. Redox Sensitive Hyaluronic Acid-Decorated Graphene Oxide for Photothermally Controlled Tumor-Cytoplasm- Selective Rapid Drug Delivery. *Adv Funct Mater* 27, 1604620-1604632; doi:10.1002/adfm.201604620 (2017).

125. Liu, Y., Han, W., Xu, Z., Fan, W., Peng, W., Luo, S. Comparative toxicity of pristine graphene oxide and its carboxylimidazole or polyethylene glycol functionalized products to Daphnia magna: A two generation study. *Environ Pollut* 237, 218-227; doi:10.1016/j.envpol.2018.02.021 (2018).

126. Sinha, A., Cha, B.G., Choi, Y., Nguyen, T.L., Yoo, P.J., Jeong, J.H., Kim, J. Carbohydrate-Functionalized rGO as an Effective Cancer Vaccine for Stimulating Antigen-Specific Cytotoxic T Cells and Inhibiting Tumor Growth. *Chem Mater* 29, 6883-6892; doi:10.1021/acs.chemmater.7b02197 (2017).

127. Zhou, H., Zhao, K., Li, W., Yang, N., Liu, Y., Chen, C., Wei, T. The interactions between pristine graphene and macrophages and the production of cytokines/chemokines via TLR- and NF-kB-related signaling pathways, *Biomaterials*, 33, 6933-6942; doi:10.1016/j.biomaterials.2012.06.064 (2012).

128. Tabish, T.A., Pranjol, M.Z.I., Hayat, H., Rahat, A.A.M., Abdullah, T.M., Whatmore, J.L., Zhang, S.W. In vitro toxic effects of reduced graphene oxide nanosheets on lung cancer cells. *Nanotechnology* 28, 504001; doi:10.1088/1361-6528/aa95a8 (2018).

129. Kang, Y., Liu, J., Wu, J., Yin, Q., Liang, H., Chen., A., Shao, L. Graphene oxide and reduced graphene oxide induced neural pheochromocytoma-derived PC12 cell lines apoptosis and cell cycle alterations via the ERK signaling pathways. *Int J Nanomedicine* 2, 5501-5510; doi:10.2147/IJN.S141032 (2017).

130. Li, Y., Yang, L., Ying, L., Yujian, F., Taotao, W., Le Guyader, L., Ge, G., Liu, R-S., Chang, Y-Z., Chen, C. The triggering of apoptosis in macrophages by pristine graphene through the MAPK and TGF-beta signaling pathways. *Biomaterials*, 33 402-411; doi:10.1016/j.biomaterials.2011.09.091 (2012).

131. Koua, L., Suna, J., Zhaib, Y., He, Z., The endocytosis and intracellular fate of nanomedicines: Implication for rational design. *Asian Journal of Pharmaceutical Sciences* 8(1), 1-10; doi:10.1016/j.ajps.2013.07.001 (2013).

132. Dutta, D., Donaldson, J.G. Search for inhibitors of endocytosis: Intended specificity and unintended consequences. *Cellular Logistics* 2 (4), 203-208; doi:10.4161/cl.23967 (2012).

133. Li, Y., Lu, Z., Li, Z., Nie, G., Fang, Y. Cellular uptake and distribution of graphene oxide coated with layer-by-layer assembled polyelectrolytes. *Journal of Nanoparticle Research* 16 (5), 2384; doi:10.1007/s11051-014-2384-4 (2014).

134. Jin, P., Wei, P., Zhang, Y., Lin, J., Sha, R., Hu, Y., Zhang, J., Zhou, W., Yao, H., Ren, L., Yang, J.Y., Liu, Y., Wen, L. Autophagy-mediated clearance of ubiquitinated mutant huntingtin by graphene oxide. *Nanoscale* 8 (44), 18740-18750; doi:10.1039/c6nr07255k (2016).

135. Ji, X., Xu, B., Yao, M., Mao, Z., Zhang, Y., Xu, G., Tang, Q., Wang, X., Xia, Y. Graphene oxide quantum dots disrupt autophagic flux by inhibiting lysosome activity in GC-2 and TM4 cell lines. *Toxicology* 374, 10-17; doi:10.1016/j.tox.2016.11.009 (2016).

136. Lin, K.C., Lin, M.W., Hsu, M.N., Yu-Chen, G., Chao, Y.C., Tuan, H.Y. *et al.* Graphene oxide sensitizes cancer cells to chemotherapeutics by inducing early autophagy events, promoting nuclear trafficking and necrosis. *Theranostics* 8 (9), 2477-2487; doi:10.7150/thno.24173 (2018).

137. Matis, J., Kúdelová, M. Early shutoff of host protein synthesis in cells infected with herpes simplex viruses. *Acta Virol* 45 (5-6), 269-277 (2001).

138. Beckerman, R., Prives, C. Transcriptional Regulation by P53. *Cold Spring Harbor Perspectives in Biology* 2 (8), a000935; doi:10.1101/cshperspect.a000935 (2010).

139. Maruzuru, Y., Fujii, H., Oyama, M., Kozuka-Hata, H., Kato, A., Kawaguchi, Y. Roles of p53 in Herpes Simplex Virus 1 Replication. *J Virol* 87 (16), 9323-9332; doi:10.1128/JVI.01581-13 (2013).

140. Poon, A.P., Roizman B. Differentiation of the shutoff of protein synthesis by virion host shutoff and mutant gamma (1)34.5 genes of herpes simplex virus 1. *Virology.* 229 (1), 98-105; doi:10.1006/viro.1996.8425 (1997).

141. Purves, F.C., Longnecker, R.M., Leader, D.P., Roizman, B. Herpes simplex virus 1 protein kinase is encoded by open reading frame US3 which is not essential for virus growth in cell culture. *J Virol.* 61 (9), 2896-2901 (1987).

142. Purves, F.C., Roizman, B. The UL13 gene of herpes simplex virus 1 encodes the functions for posttranslational processing associated with phosphorylation of the regulatory protein alpha 22. *Proc Natl Acad Sci U S A* 89 (16), 7310-7314 (1992).

143. Sciortino, M.T., Taddeo, B., Giuffrè-Cuculletto, M., Medici, M.A., Mastino, A., Roizman B. Replication-competent herpes simplex virus 1 isolates selected from cells transfected with a bacterial artificial chromosome DNA lacking only the UL49 gene vary with respect to the defect in the UL41 gene encoding host shutoff RNase. *J Virol.* 81 (20), 10924-10932; doi:10.1128/JVI.01239-07 (2007).

144. Taddeo, B., Sciortino, M.T., Zhang, W., Roizman B. Interaction of herpes simplex virus RNase with VP16 and VP22 is required for the accumulation of the protein but not for accumulation of mRNA. *Proc Natl Acad Sci U S A.* 104 (29), 12163-12168; doi:10.1073/pnas.0705245104 (2007).

145. Poon A.P., Roizman B. Mapping of key functions of the herpes simplex virus 1 U(S)3 protein kinase: the U(S)3 protein can form functional heteromultimeric structures derived from overlapping truncated polypeptides. *J Virol.* 81 (4), 1980-1989; doi:10.1128/JVI.02265-06 (2007).

146. Zhu, Z., Du, T., Zhou, G., Roizman, B. The Stability of Herpes Simplex Virus 1 ICP0 Early after Infection Is Defined by the RING Finger and the UL13 Protein Kinase. *J Virol.* 88 (10), 5437-5443; doi:10.1128/JVI.00542-14 (2014).

147. Paavilainen H., Lehtinen J., Romanovskaya, A., Nygårdas, M., Bamford, D.H., Poranen, M.M., Hukkanen, V. Inhibition of Clinical Pathogenic Herpes Simplex Virus 1 Strains With Enzymatically Created siRNA Pools. *J. Med. Virol.*; 88, 2196-2205; doi:10.1002/jmv.24578 (2016).

148. Hukkanen, V., Rehn, T., Kajander, R., Sjöroos, M., Waris, M. Time-resolved fluorometry PCR assay for rapid detection of herpes simplex virus in cerebrospinal fluid. *J. Clin. Microbiol.* 38, 3214-3218 (2000).

149. Kessler, H.H., Mühlbauer, G., Rinner, B., Stelzl, E., Berger, A., Dörr, H.W. *et al.* Detection of Herpes Simplex Virus DNA by Real-Time PCR. *Journal of Clinical Microbiology* 38 (7), 2638-2642 (2000).

150. Chacko, M.S., Adamo, M.L. Double-stranded RNA decreases IGF-I gene expression in a protein kinase R-dependent, but type I interferon-independent, mechanism in C6 rat glioma cells. *Endocrinology.* 143 (2), 25-34; doi:10.1210/endo.143.2.8628 (2002).

151. Nejepinska, J., Malik, R., Filkowski, J., Flemr, M., Filipowicz, W., Svoboda, P. dsRNA expression in the mouse elicits RNAi in oocytes and low adenosine deamination in somatic cells. Nucleic Acids Research, 40(1), 399-413; doi:10.1093/nar/gkr702 (2012).

152. Pall, M.L. Cycloheximide as inhibitor of protein synthesis doi:10.4148/1941-4765.2035 (1966).

153. Chu, W.M., Ostertag, D., Li Z.W., Chang L., Chen Y., Hu Y., Williams B., Perrault J., Karin, M. JNK2 and IKKβ are required for activating the innate response to viral infection. *Immunity* 11, 721-731 (1999).

154. Iordanov, M.S., Paranjape, J.M., Zhou, A., Wong, J., Williams, B.R.G., Meurs, E.F., *et al.* Activation of p38 Mitogen-Activated Protein Kinase and c-Jun NH2-Terminal Kinase by Double-Stranded RNA and Encephalomyocarditis Virus: Involvement of RNase L, Protein Kinase R, and Alternative Pathways. *Molecular and Cellular Biology*, 20 (2), 617-627 (2000).

155. Kumar, A., Haque, J., Lacoste, J., Hiscott, J., Williams, B.R. Double-stranded RNA-dependent protein kinase activates transcription factor NF-kappa B by phosphorylating I kappa B. *Proc Natl Acad Sci U S A.* 91 (14), 6288-6292 (1994)

156. Wong, A.H., Tam, N.W., Yang, Y.L., Cuddihy, A.R., Li, S., Kirchhoff, S. *et al.* Physical association between STAT1 and the interferon-inducible protein kinase PKR and implications for interferon and double-stranded RNA signaling pathways. *The EMBO Journal*, 16 (6), 1291-1304; doi:10.1093/emboj/16.6.1291 (1997).

157. Colao, I., Pennisi, R., Venuti, A., Nygårdas, M., Heikkilä, O., Hukkanen, V., Sciortino, M.T. The ERK-1 function is required for HSV-1-mediated G1/S progression in HEP-2 cells and contributes to virus growth. *Scientific Reports* 7, 9176; doi:10.1038/s41598-017-09529-y (2017).

158. Kimura, S., Noda, T., Yoshimori, T. Dissection of the autophagosome maturation process by a novel reporter protein, tandem fluorescent-tagged LC3. *Autophagy.* 3 (5), 452-60 (2007).

159. Sørensen, C.S., Syljuåsen, R.G. Safeguarding genome integrity: the checkpoint kinases ATR, CHK1 and WEE1 restrain CDK activity during normal DNA replication. *Nucleic Acids Research* 40 (2), 477-486; doi:10.1093/nar/gkr697 (2012).

160. Joseph R. Nevins. The Rb/E2F pathway and cancer. *Human Molecular Genetics*, Volume 10, Issue 7, 1 April 2001, Pages 699–703, https://doi.org/10.1093/hmg/10.7.699

161. Wang, S., Konorev, E.A., Kotamraju, S., Joseph, J., Kalivendi, S., Kalyanaraman, B. Doxorubicin induces apoptosis in normal and tumor cells via distinctly different mechanisms. intermediacy of $H_{(2)}O_{(2)}$- and p53-dependent pathways. *J Biol Chem.* 279 (24), 25535-25543 (2004).

162. Dupont, N., Orhon, I., Bauvy, C., Codogno, P. Autophagy and autophagic flux in tumor cells. *Methods Enzymol.* 543, 73-88; doi:10.1016/B978-0-12-801329-8.00004-0 (2014).

163. Chen, L., Tang, L., Calin, G., Croce, C.M., Kipps, T.J. Expression of MicroRNA (miR) miR-15a/miR-16-1 Downregulates Expression of BCL-2 Protein in Chronic Lymphocytic Leukemia. *Blood* 108, 2796 (2006).

164. Lungu G, Kuang X, Stoica G, Wong PK. Monosodium luminol upregulates the expression of Bcl-2 and VEGF in retrovirus-infected mice through downregulation of corresponding miRNAs. *Acta Virol.*; 54 (1):27-32 (2010)

165. Leng J, Song Q, Zhao Y, Wang Z. miR-15a represses cancer cell migration and invasion under conditions of hypoxia by targeting and downregulating Bcl-2 expression in human osteosarcoma cells. International Journal of Oncology; 52(4):1095-1104. doi:10.3892/ijo.2018.4285 (2018).

Aknowledgements

This study was supported by the grant from Italian Ministry of University and Research, Research Projects of National Interest 2010-2011 (2010PHT9NF_005) and by University of Messina Research & Mobility 2016 Project (Project Code: RES_AND_MOB_2016_Sciortino). Thanks to Professor Nicola Micale for the English revision of the whole manuscript, Professor Maria Teresa Sciortino for design experiments and revision of this thesis work and Professor Anna Piperno and Dr. Antonino Mazzaglia for the synthesis of the graphene-based nanomaterials. Special thanks to Maria Grazia Ceraolo, Maria Musarra Pizzo and Giusi Melita for technical support.

Aknowledgements

Firstly, I would like to express my sincere gratitude to my tutor and mentor Prof.ssa Maria Teresa Sciortino for the continuous support during my PhD period and for the scientific method and scientific thinking, which she transferred to me. I would like thanks her for putting hers trust in me and for the opportunities provided to me during my PhD period. Without hers precious support it would not have been possible for me to conduct this research.

Additionally, I am honored to have met the Professor Bernard Roizman during my mobility period in Shenzhen. Thanks for the exchange of knowledge and for supported me with new scientific ideas. I will never forget it!!!

Besides, thanks to Professor Grace Zhou, Director of Shenzhen International Institute of Biomedical Research, (China) for the hospitality and availability gave me during my mobility period in Shenzhen. Thank you for have been so nice and sweet to me and for our stimulating discussions.

Thanks to Professor Vejio Hukkanen of the Department of Virology at the University of Turku, (Finland) and thanks to Dr. Massimo Tommasino of the International Agency for Research on Cancer World Health Organization (IARC) at Lyon, (France) to have share with me their expertise during my mobility period in Finland and in Lyon.

Thanks to Professor Anna Piperno and Dr.Antonino Mazzaglia for gave me the possibility to expand my scientific knowledge to chemical field.

Thanks to my colleagues and friends, Giusy, Enrico, Assunta, Daniele e Maria for having helped me in these years and thanks to all the guys that I met during mobility periods.

A special thanks to Maria, a FRIEND before to be a colleague, for having encouraged me always. Thanks for the sleepless nights, for your positiveness and for having worked with me to edit this thesis work. Ours friendship have no and will not have spatio-temporal limitations.

Thanks to my family for the support that they provided me every day, thanks to my mom, my dad and my sister for having believed in me always.

Thanks to my lovely Antonio for having waited me and loved me every day for 9 years…and now for all life!

Thanks to me for giving up on the obstacles and for having continued to believe in my work and in my potentiality!

INDICE